UNIVERSITY *of the*
WESTERN CAPE

GEOLOGICAL MODELLING FOR CARBON STORAGE OPPORTUNITIES IN THE ORANGE BASIN SOUTH AFRICA

By
Jade Aiden Holtman
Student Number: 2802428

A thesis submitted in fulfilment of the requirements for the degree of Magister Scientiae in the Department of Earth Sciences, University of the Western Cape

Supervisor: Dr M. Opuwari
Co Supervisor: Prof S. Titinchi

Declaration

I declare that the thesis titled “Geological modelling for storage opportunities in the Orange basin South Africa” is my own work, that it has not been submitted before for any degree or examination in any other university, and that all sources I have used or quoted have been indicated and acknowledged by means of complete references.

Jade Aiden Holtman August 2019

Signature

Acknowledgements

I would like to thank my Supervisor Dr. M. Opuwari for is patience and support in guiding me through this process.

To my Co-Supervisor Professor S.Titinchi I would like to express my gratitude for your support and inputs on my thesis.

I would also like to thank Dr. Chris Samakinde for imparting his knowledge and guiding me on the practical aspects of my thesis.

This project was conducted under the sponsorship of South African National Energy Development Institute (SANEDI) South African Centre for Carbon Capture and Storage (SACCCS) thank you for giving me the financial peace of mind to complete my studies. Thank you so much Mr. Thabo Mosia and Ms. Evelyn Nyandoro for your administrative support and for your enthusiasm shown toward my project.

Lastly I dedicate this thesis to my family, my daughter and God for standing by me and pushing me to the completion of this thesis.

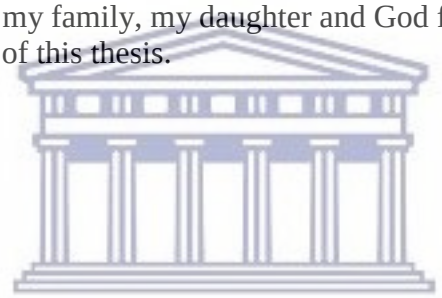

Abstract

This study investigates the viability of the sedimentary deposits in the Northern Orange basin for carbon storage and sequestration. A combination of geological modelling, petrographic and geochemical techniques are used to investigate this scenario after an initial seismic-well tie had been performed to match the formation tops in Well AF-1 with the 3D seismic volume acquired in this basin in 2009. Core description of well AF-1 assisted in identifying different facies and samples taken at specific depths for petrographic and geochemical analyses, while different geological formations were mapped from the calibrated positions of seismic-well tie throughout the seismic volume.

The well data and geophysical logs were utilized to generate petrophysical properties and used to calibrate observations made from seismic interpretations. The facies log used in this study was generated using the Python's script on Petrel 2014 Gamma Ray, while the density log was used to generate the porosity log. The generated facies and porosity logs were upscaled and used to populate a 3D grid using faults and surfaces identified in the seismic volume. The sedimentological properties of the subsurface were identified utilizing petrographic descriptions including measurements of sorting, colour and grain sizes. While the mineralogical properties of the record was verified through XRD analyses and thin section.

The facies and porosity modelling revealed the dominance of siltstones and sandstones as the main sedimentary facies throughout the sequence. Sandstones are extensive and prominent within the Cenozoic and Mastrichtian, while the unit dated to the Barremian is identified as having the best potential for CO_2 storage based on the overlaying capping unit. Quartz, Plagioclase feldspar (Albite), Biotite and Kaolinite are the major minerals identified in all four samples. Each of these minerals has an implication for which may influence the long term storage of CO_2 with the potential to form as they may form part of the inra-porous post-

depositional cementation and hence change the porosity and permeability properties. The presence of Albite as observed on the XRD may predict possible mineralisation of CO_2 to form Dawsonite when reservoir is injected with CO_2.

The Barremian sandstone which straddles the Aptian shale at the top and the Hauterivian Shale and Siltsone deposit at the bottom holds a good promise for a potential CO_2 storage.

An estimated volume of CO_2 that could be stored in the reservoir of the Barremian sandstone in zone 8 is limited to the lateral seal of shale above the reservoir in zone 7 of the Aptian age.

The method used to determine the potential storage capacity of CO_2 was performed by Alexandros Tasianas and Nikolaos Koukouzas (2016). The Equation used to determine CO_2 storage capacity is: $mCO_2 = RV * Ø * Sg * \delta(CO_2)$.

Table of Contents

LIST OF FIGURE

1 Chapter 1

1.1 Introduction

Carbon Dioxide (CO_2) is one of the main contributors to climate change and a by-product of many sources. Coal derived energy and the production of steel are just two of many processes that emit CO_2 into the atmosphere. The CO_2 emitted forms an invisible layer which in turn restricts heat from escaping the Earth's atmosphere. This process is called global warming. Consequently, there is a need to explore areas of scientific interventions that could be used to mitigate the effects of global climate change.

The offshore northern Orange Basin is the focus area of the study and specifically located on the west coast margin of South Africa which covers an area of 130,000 km^2. Previous studies dealt with the regional geology (Barton et al., 1993; Samakinde et al., 2016; Fadipe et al., 2011); which includes the depositional history, structural setting, petroleum systems, and thickness of reservoir layers, porosity and permeability suggests the feasibility for CO_2 storage in this part of the basin. A 3D Seismic block acquired in 2009, which has a well AF-1 within its survey area, is used in this study. The seismic block data set and the well logs of AF-1 are processed, interpreted and modelled on Petrel 2013®workstation to map potential reservoir rocks for Carbon Dioxide storage. The well data and geophysical logs are utilized to generate petrophysical properties and used to calibrate observations made from seismic interpretations. Although the basin is highly underexplored, consequently, investigating the rock units for possible CO_2 storage would increase the feasibility of supercritical carbon sequestration.

The abundance of CO_2 in the atmosphere is mainly caused by the demand for energy as industrialization and urbanization increases globally. The main contributor to energy used world-wide is Coal. Coal exposed to a high temperature generates energy which is used to operate large turbines to produce electricity. During this process, large amount of Carbon Dioxide is emitted into the Earth's atmosphere which increase anoxicity, and with consequences on the biological life. Capture and Storage/Sequestration (CCS) mechanism involves capturing CO_2 either before production or after production and stored indefinitely beneath the Earth's surface in geological formations. The identification of potential sites for carbon storage is the initial step in CCS, while potential sites have been identified in many countries for this purpose, less research has been done in South Africa to identify potential

storage sites for carbon storage, hence the justification for this study. The main outcome of this study will identify and delineate potential areas within the basin for possible carbon storage.

1.2 Aim and Objectives

The aim is to investigate the presence of key reservoir and caprock elements that are crucial for Carbon sequestration in the northern section of the Orange Basin. Potentially, a carbon capture and storage project could be a need in the near future as a geothermal energy source in this basin, and importantly, in an effort to reduce the amount of carbon in the atmosphere.

1.2.1 Objectives of Study

The objectives of this study are listed below;

- To provide a mapping of different Geological formations based on chronological timeline and estimation of thickness of each formation.
- Construction of a 3D Geological model for the study area to investigate the structural framework of this area.
- Modelling of reservoir properties like facies and porosity to investigate the suitability of the study area for CCS.
- To indicate chemical reactions by injecting CO_2 into rock samples.
- To utilise petrographic studies (Thin section and XRD) of rock samples for the identification of rock forming minerals and diagenetic minerals to predict reactions of these minerals with CO_2 after storage.

Seismic and well logs data purchased from the Petroleum Agency SA will be processed and interpreted on the Petrel 2014 workstation and a 3D Tectono-sedimentary framework will be constructed to understand the tectonic and sedimentary framework variation across the study area.

1.3 Study Area

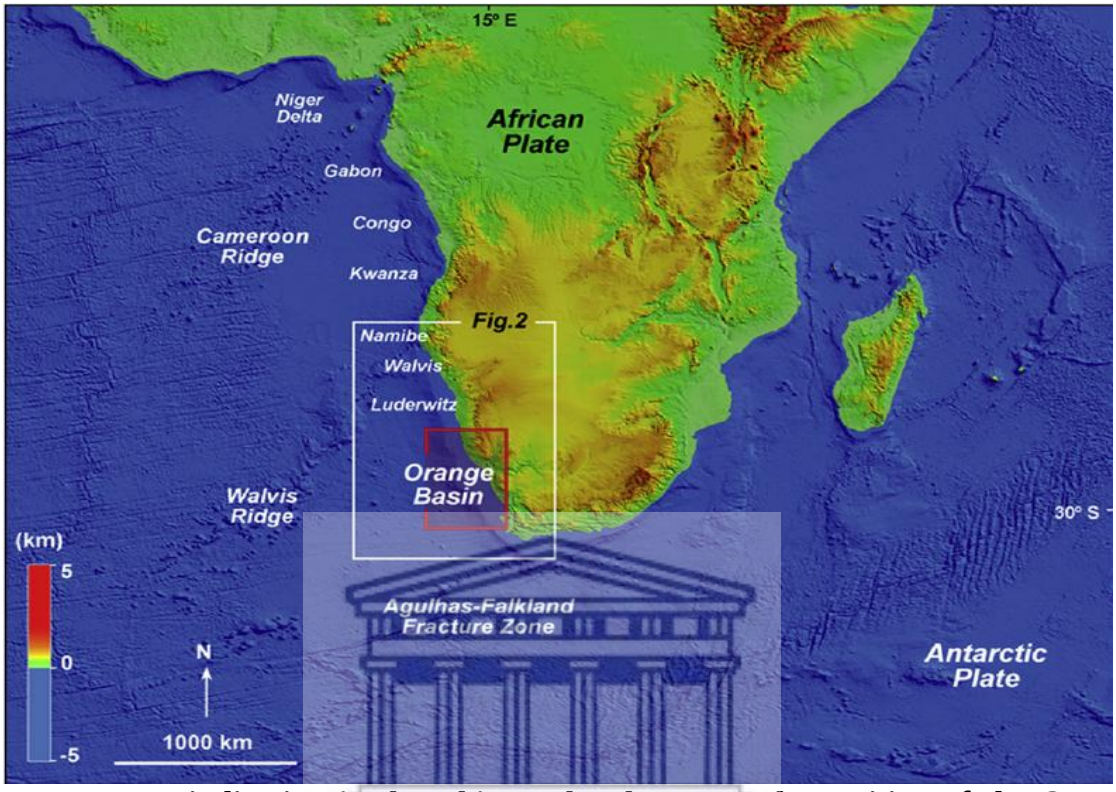

Figure 1-1: Map indicating in the white and red squares the position of the Orange Basin in relation to other West Africa sedimentary basins (De Vera, 2010).

The study area focuses on offshore, West coast, Orange Basin within well AF-1 just west of the Ibhubesi Gas field, located in the northern region of the Orange Basin (Figure 1-1). The Luderiwitz, Walvis and Namibe Basins bound the Orange Basin in the north and the Agulhas-Falkland Fracture Zone in the south (De Vera, 2010). The Orange Basin consists of upper-Jurassic synrift sequences overlain by Lower Cretaceous to present postrift passive-margin deposits (Doug, Dave 2008). The Orange Basin is located on the passive margin of the South Atlantic off the west coast of South Africa and is the largest Basin (160000 km^2) in terms of volume and area size in South Africa (CO_2 tech report).This passive margin was formed due to the break-up of the Africa and South America continental plates. The Orange Basin has records imbedded in its geological sequence presenting the development of the Late Jurassic to today's volcanic-rifted passive margin of Namibia. (De Vera, 2010). These

Records show a very complex rifting history and have widespread indications of massive volcanic activity (Hirsch, 2010).

The seismic stratrigraphy of the Orange Basin is divided into two depositional megasequences, namely the syn-rift and post-rift megasequences. From the late Jurassic to Hauterivian (160-127 Ma) in the Syn-rift Megasequence and Late Hauterivian to present day forms the Post-rift Megasequence. (De Vera, 2010).Initial faulting and forming of grabens and half grabens, which are nearly parallel to the present coastline, occurred during the rifting process. The Syn-rift grabeninfills consist of fluvial clay, sandstone and volcaniclastic sediments. The presence of these sediments indicates a continental depositional environment. These grabeninfills are then overlain by the Hauterivian unconformity where the eldest three source rock intervals were deposited. In the Aptian, regional organic-rich source rocks where then deposited (Hirsch, 2010). These stratigraphic layers that were deposited between the rifting initiation of Gondwana (Mesozoic mid Jurassic 180 ma) to late cretaceous formed the Orange basins petroleum system.

1.4 The Earth's Carbon Dioxide Count

Carbon dioxide is one of the key greenhouse gases responsible for elevated global temperature in the atmosphere. Carbon dioxide is needed in the atmosphere because it is one of the greenhouse gases responsible for not allowing the earth to freeze over (Pearson, 2000). The Earth's Carbon count has drastically increased over the years, in concentrations well over the amount needed for the earth to retain enough heat. The high levels of carbon dioxide in the atmosphere is causing the earth to retain too much heat and consequently, increasing temperatures of the Earth. Carbon dioxide concentrations are irreversible for at least a century after carbon emissions have stopped. It is uncertain that the atmospheric temperature would exponentially decrease if carbon emissions were to completely cease (Solomon, 2009).

One of the methods established in for the Earth's CO_2 count is the use of the boron-isotope ratios of ancient planktonic foraminifer shells to estimate the pH of surface-layer seawater. The pH levels recorded are then used to reconstruct atmospheric CO_2 concentrations (Pearson and Palmer 2000).

In the late Palaeocene and earliest Eocene periods about 60 to 52 Ma the Earth's CO_2 concentrations were well over 2000 Parts Per Million (ppm) followed by a drastic decrease in

CO_2 concentrations in the early Eocene epoch 55 to 40 Ma. The decrease in CO_2 in the Earth's atmosphere in the Eocene Epoch is still highly speculated due to the fact that there is not yet actual proof as to why the CO_2 levels erratically decreased. One speculation suggested the CO_2 decrease due to outgassing from ocean ridges, volcanoes and metamorphic belts and increased carbon burial (Le Quéré, 2007). From the Miocene Epoch about 24 Ma ,the CO_2 concentrations relatively stabilised at 500 ppm and were much more stable than before, although in the Neogene period there where evidence of rapid cooling about 15 to 3 Ma(Pearson,2000).Currently the CO_2 count has increased since the Neogene period and is continuing to increase.

1.5 Characteristics and the effects of Carbon Dioxide in the atmosphere

CO_2 is an inorganic compound consisting of two Oxygen atoms and one Carbon atom. These atoms share electrons equally and are bonded with a covalent bond. Carbon dioxide is produced into the atmosphere either by natural organisms or by human activity. The highest amounts of CO_2 released into the atmosphere are a by-product of fossil fuel consumption and manufacturing plants (Boden, 2009).

High levels of CO_2 in the atmosphere play a big role in the alterations of the Earth's biogeochemical cycle. Carbon a non-metallic element forms the basis of most living organisms on earth and Carbon dioxide found in the Earth's atmosphere acts as the primary resource for photosynthesis. Human activity increases the atmosphere's CO_2 levels by mining and by the use of fossil fuels as an energy source. Mining and fossil fuel combustion along with converting grasslands and forests to agricultural ecosystems represent the main contributors to the change that human alterations have on the Earth's system (Vitousek, 1997).

2 Chapter Two: Literature Review

2.1 What is Carbon Capturing and Storage?

Carbon dioxide capture and storage is a process that deals with separating CO_2 from industrial sources and sources from where energy is produced. The captured CO_2 is then transported to a different location and buried deep within the geology of the earth (Metz, 2005). The Carbon capture and storage technology uses fossil fuels to produce energy, but captures the by-product produced called CO_2. Normally fossil fuel combustion plants release the by-products into the atmosphere but over the year's evidence as shown that this normal process actually negatively affects the Earth. After the CO_2 has been captured the next step would be to store the CO_2 indefinitely within the deep seated geology of the Earth.

Figure 2-1 below indicates the processes responsible for the most CO_2 emissions starting from fossil fuel manipulation being the process emitting the most CO_2 emissions to other sources as well as oil and gas processing as the lowest CO_2 emitter.

This figure also indicates the process or industrial activity of worldwide large stationary CO_2 sources with emissions of more than 0.1 million tonnes of CO_2 ($MtCO_2$) per year.

Process	Number of sources	Emissions ($MtCO_2$ yr^{-1})
Fossil fuels		
Power	4,942	10,539
Cement production	1,175	932
Refineries	638	798
Iron and steel industry	269	646
Petrochemical industry	470	379
Oil and gas processing	Not available	50
Other sources	90	33
Biomass		
Bioethanol and bioenergy	303	91
Total	**7,887**	**13,466**

Figure 2-1: Indication of fossil fuel processes and the Emissions there of (Celia, 2009).

Atmospheric concentrations of CO_2 have drastically increased over the past 200 years. Concentration levels have increased from about 280 parts per million (ppm) to alarming values of about 380 ppm and continues to increase (Celia, 2009). The main contributors to

this pollution of CO_2 in the atmosphere are fossil fuel combustion and Biomass. Fossil fuel combustion is undoubtedly the main cause of the atmospheres CO_2 conditions.

Other options to reduce CO_2 emissions besides CO_2 storage include using less carbon-rich fuels and switching from coal as an energy supply to a more renewable source of energy. Carbon capturing and storage still has the most effective potential to reduce atmospheric CO_2 and for the world to apply this process the application would require their capability to apply the technology, the costs to successfully operate the process and all environmental and geological issues need to be researched and determined if CO_2 storage is possible (Metz,2005).

Industrial activities are dependent on fossil fuel combustion. More than 85% of the energy used to operate industries derives from fossil fuel combustion. Coal is the main contributor to energy and is on path to supply 28% of the world's energy by 2030 (Haszeldine, 2009). By the year 2050 carbon capture and storage technologies have a main goal to fit all coal and gas power plants with CO_2 capture capabilities and if this objective is achieved emissions from energy would reduce by 20% (Haszeldine, 2009).

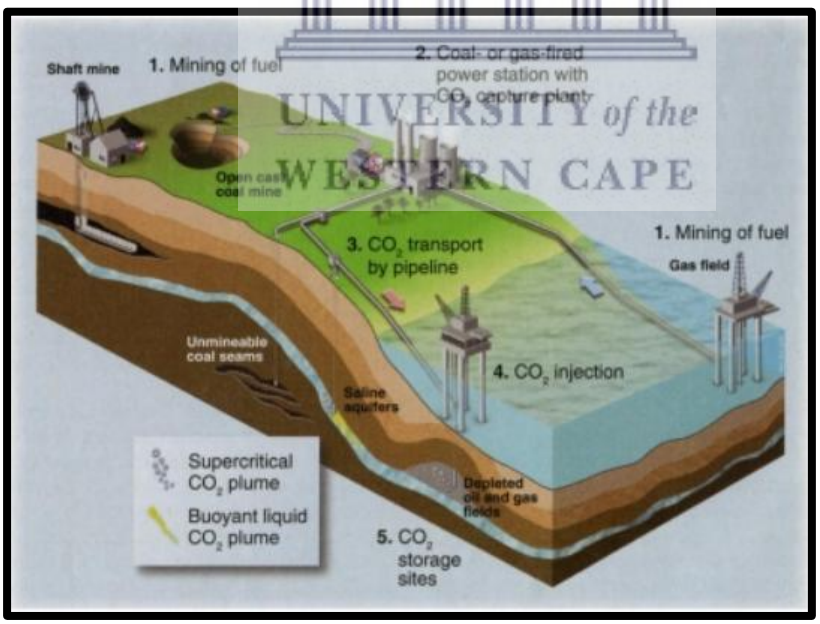

Figure 2-2: Representation of the life-cycle of fossil fuels with the use of a CO_2 storage plant.

There are three investigated methods of CO_2 capture and storage (see figure 2-3), the first method being Post-combustion capture. This method uses chemical solvents to capture and separate the CO_2. A secondary and final stage is added to the combustion process to remove almost all of the CO_2 from the combustion products before vented into the atmosphere. A process called Wet scrubbing uses an aqueous amine solution to capture the CO_2 and separate it from the waste gas previously captured in the combustion process (Gibbins, 2008). The solvent created after the wet scrubbing process is then re-heated to about 120 degrees Celsius then again cooled and then recycled continuously. The CO_2 is then extracted from the regenerated process and dried and compressed then transported for deep geological burial (Gibbins, 2008).

The second method used for CO_2 capture is Pre-combustion capture. This method partially combusts the fossil fuel by using calculated quantities of oxygen and some steam at a higher pressure to generate a mixture of CO and H_2(Gibbins, 2008).

This mixture is then passed through catalyst beds and with adding steam and reducing the temperature this last process converts CO to CO_2.This process is however much less efficient than Post-combustion. The turbines needed for fossil fuel combustion use CO_2 to generate power and with the CO_2 already captured before combustion the turbines operate on CO and generate much less power (Gibbins, 2008).

The last method used for CO_2 capture is oxyfuel combustion. This method burns the fossil fuel in denitrified air to produce only CO_2 and water (Haszeldine, 2009). The oxyfuel option gives a flue gas mixture consisting of mainly CO_2 and water vapour. The CO_2 is then very easily extracted by an added compression process. The Oxyfuel process shows good results for capturing CO_2 with little to no change in the power generated and the costs are also relatively low and can compete with the Post-combustion capture process (Gibbins, 2008).

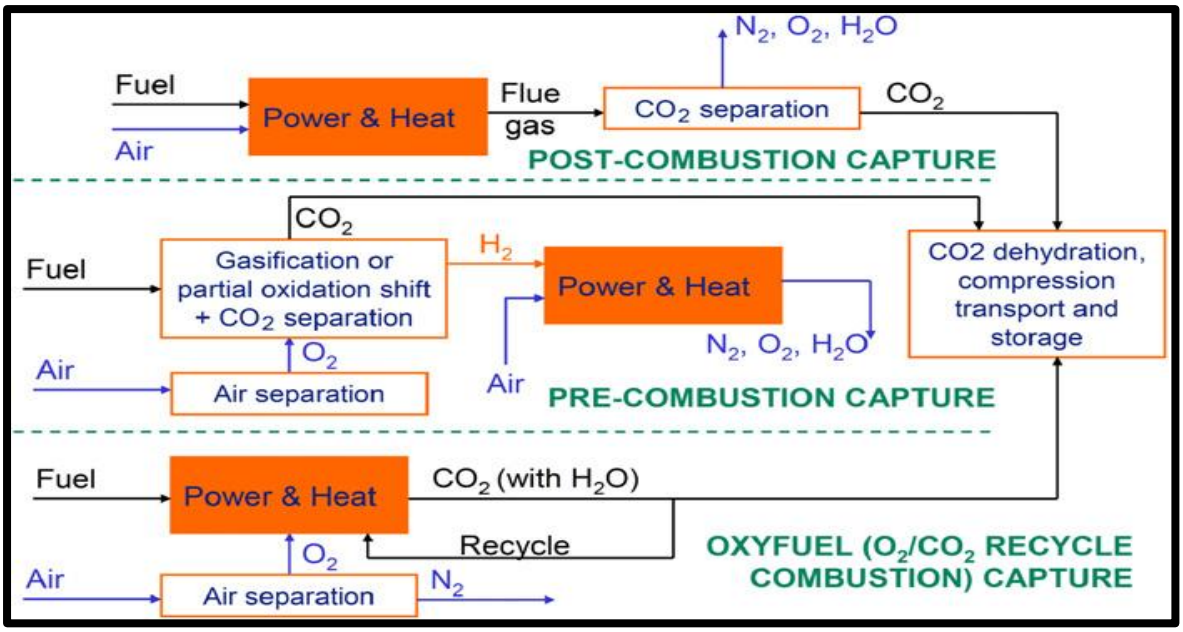

Figure 2-3: Principles of three main CO_2 capture options (Jordal et al, 2004).

2.2 Geological features for CO_2 storage

Deep geological formation storage is the most effective option for CO_2 storage. These types of formations can include oil and gas reservoirs, deep saline aquifers and coal seams as indicated in figure 2-4. The most effective storage option would be in deep saline aquifer sowing to the saline aquifers and have a large potential storage capacity (Celia, 2009).

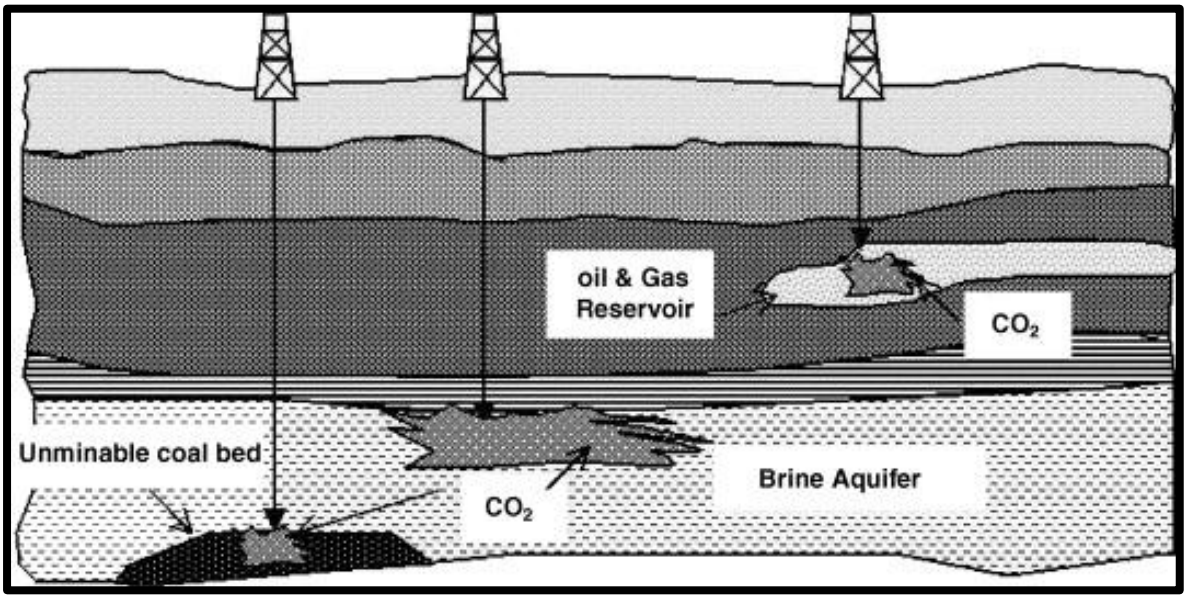

Figure 2-4: Carbon Dioxide sequestration possibilities(X, Xu 2006)

2.3 Storage of CO_2 in reservoirs

A subsurface sandstone reservoir can be a highly porous storage space, and if capped by a shale deposit, it can serve as a potential reservoir which makes it an ideal storage place to store CO_2. Efficient reservoirs for storing CO_2 should have high porosity and minimal amounts of faulting. Faulting could cause the CO_2 to migrate out of the reservoir if the faults are non-sealing and cut through the seal above the reservoir rock.

CO_2 storage in the subsurface is undoubtedly the best option for safely discarding unwanted CO_2. Storing CO_2 in active oil and gas reservoirs could help the recovery rate of oil or gas by adding pressure to the system and forcing the hydrocarbons to the surface (Koide, 1992). Injecting CO_2 into a gas reservoir could help in the recovery of the gas present. The process called Carbon Sequestration with Enhanced Gas Recovery (CSEGR) was simulated on the Rio Vista Gas Field in California (Oldenburg, 2001). The Rio Vista Gas Field is a methane (CH4) gas field that could potentially use the CSEGR process to successfully retrieve most of the small amounts left of the methane within the reservoir and at the same time store CO_2 (Oldenburg, 2001). The reservoir simulator which models the gas reservoir simulates CO_2 injection to find out if the CSEGR process could work. As it simulates CO_2 injection, relevant parameters needed for indefinite CO_2 storage are also calculated and tested. The caprock sealing capacity (breakthrough pressure), reservoir porosity, degree of faults and fractures and interaction of CO_2 with other gases and solutions already present in the reservoir are tested to see if the reservoir in question can hold the injected CO_2 (Oldenburg, 2001). The only disadvantage of this process is that the recovered methane would be diluted and would not have the same concentration as when methane is extracted normally from the reservoir (Oldenburg, 2001).

However, because these oil and gas reservoirs are distributed across a large area into small reservoir units, it leaves this method to be very limited as their volumes are small (Koide, 1992). When referring to storage in saline aquifers, these aquifer units are far larger and could contain much more volumes of CO_2. Storage in either active or depleted oil or gas reservoirs have an advantage over saline Aquifer storage because these reservoirs already have exploration and production wells giving the geological data needed and can be used to

reach these deep underground reservoirs to place the CO_2 (Koide, 1992). The Pipelines and well equipment are already in place and would help cut down a CO_2 projects cost and time.

Depleted hydrocarbon fields have successfully sealed the hydrocarbons that were once there meaning that the reservoir had a good sealing capacity. The seal capacity however will become less due to the CO_2 replacing the Hydrocarbons (Zhaowen, 2005). The surface tension of the CO_2/water system within the reservoir would be much lower than the hydrocarbon/water system that was once there. In replacing the hydrocarbons with CO_2 this process lowers the capillary sealing pressure of the caprock. Therefore, seal capacity tests are calculated before injection of CO_2 to determine the reservoir pressure so that migration to other formations above the caprock is avoided (Zhaowen, 2005).

2.4 Storage of CO_2 in deep saline aquifers

Deep saline aquifer storage is definitely a possibility and should not be overlooked. Saline aquifers are porous and fractured space deep beneath the Earth's crust filled with brine connate water. These connate waters are hazardous for human consumption and are useless in any regard. This is one of the reasons why saline aquifers are an ideal storage space for CO_2 sequestration (Bachu, 2000).

There are a few reasons why saline aquifer storage qualifies as a second option after hydrocarbon reservoir storage. This is because firstly, deep saline aquifers are situated deep within the geology of the earth and would require time for research and money to reach the target. Secondly, the saline aquifer is an unexplored area and would need exploration work before any drilling to store for CO_2 storage can take place. After the aquifer and its surrounding geology have been examined, then the drilling to store process could commence. These drilling steps along with the exploration of the target area are very expensive processes and because of the high costs involved, CO_2 storage projects have more interests in shallower and already explored depleted hydrocarbon reservoirs.

Deep saline aquifers however do have the largest volumes to store CO_2. An estimated range for the capacity to store CO_2 is from 100 to 10,000 $GtCO_2$ (Bruant, 2002).CO_2 injected into the saline aquifer for sequestration could be in one of the three phases; gases phase, liquid phase or as a supercritical phase. Supercritical CO_2 has a lower density and viscosity compared to the host fluid of the saline aquifer (Nordbotten, 2005). When a supercritical CO_2 fluid is injected into the brine aquifer, multi-fluid flow occurs within the aquifer, this could lead to multi-fluid flow problems. One of the flow problems are difference in viscosity and density of the two or more fluids present in the formation. CO_2 has much less density and viscosity than the residual fluids in the formation, causing the CO_2 to migrate upward which could lead to leakage from the injection formation (Nordbotten, 2005).

As supercritical CO_2 is injected into the aquifer the CO_2 will dissolve in the residual fluid of the aquifer (approximately up to 29 %) and the rest of it forms a plume structure with an upwards direction due to hydrodynamic flow and its buoyancy in water (Bachu, 2000). Another problem that could arise from aquifer injection is the leakage of CO_2 through other pre drilled wells within the area on injection. A CO_2 plume could grow greater than 5km in radius size and could leak out in neighbouring wells (see figure 2-5) (Nordbotten, 2005). These large volumes of CO_2 injection could also affect shallow groundwater. CO_2 plumes over years of burial grow in diameter and have a tendency to travel upward. These plumes are restricted by the low-permeable cap but could potentially affect groundwater by infiltrating fresh water aquifers due to pressure variations and saline water displacement (Birkholzer, 2009). Injecting CO_2 into saline aquifers also changes the hydraulic connectivity that fresh water aquifers have with the lower seated saline aquifers. The change in hydraulic connectivity between the two (brine and fresh water) solutions could alter the water table and the zones of discharge and recharge. If the water table should rise, then changes such as water quality will occur due to the upward force of the lower seated brine water. CO_2 mixes and becomes in equilibrium and makes one solution instead of different solutions in one aquifer. This process happens over years of burial (Birkholzer, 2009).

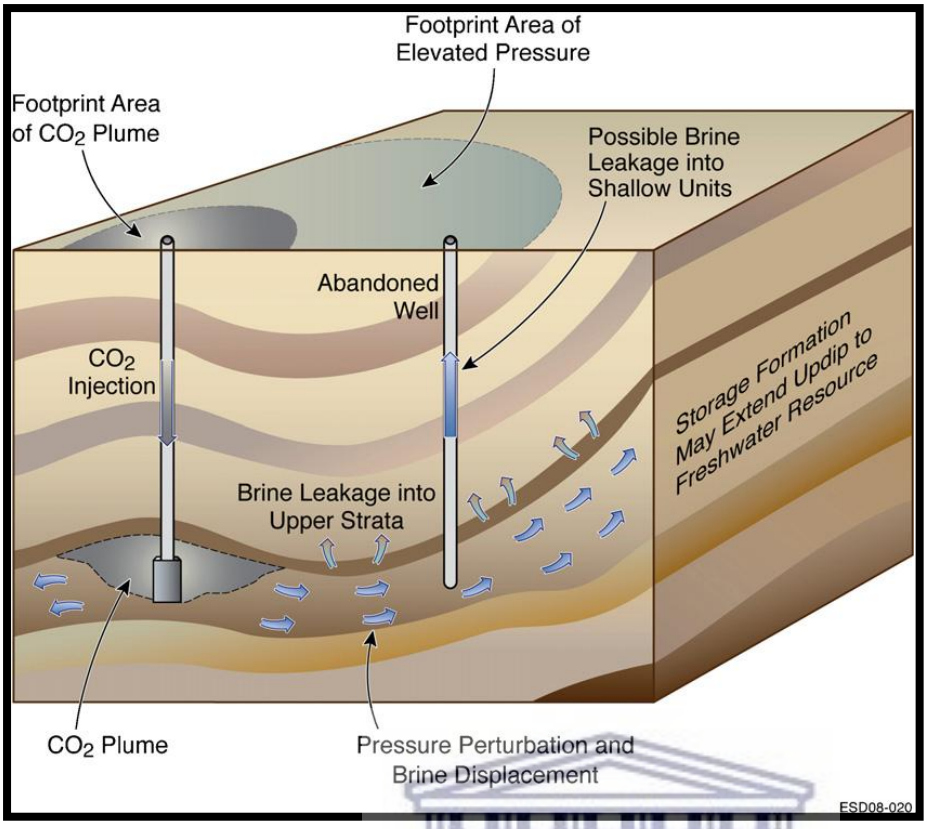

Figure 2-5: Schematic of CO_2 injection and migration of CO_2 post injection (Birkholzer, J 2009)

2.5 CO_2 sequestration in coal seams

Injection of CO_2 into coal seams is one of the three options for CO_2 sequestration due to the ability of coal having a high storage capacity for gas (Karacan, 2003). Un-mineable Coal seams are estimated by the IPCC report (IPCC, 2005) to store from 3 to 200 $GtCO_2$ and these figures indicate that Coal seam storage is a definite possibility for CO_2 sequestration. Coal seam CO_2 storage targets are in areas where coal mining is impossible (refer to figure 2-4) due to the depth of the coal which makes it difficult to near impossible to reach (X, Xu 2006). Coal seam targets for CO_2 sequestration could also be used if the coal seams are too thin or too high in sulphur or too low in BTU (heating value of coal) for the coal extraction process to be viable or if the locations of the coal seams are too dangerous to mine (White, 2005). These conditions determine if the coal seams are CO_2 sequestration targets. Coal seams are perfect for CO_2 sequestration because the technique for gas production from coal seams are well understood and the experience of this process can contribute to relevant information needed with regards to CO_2 storage in coal seams (Karacan, 2003). Storing CO_2 in coal

seams is also beneficial in terms of enhanced methane gas recovery. Coal has a strong tendency to attract gas particles, especially CO_2 gas. During the sequestration process, the CO_2 gas adsorbs into the coal mass thus desorbing the methane gas from coal (Perera, 2011). Coal is a highly porous sedimentary rock with great surface area that not only favours CO_2 over Ch4 but also can store considerable amounts of it (Perera, 2011).

CO_2 sequestration in coal seams depend on three factors: Firstly, the type of coal within the coal seam, secondly the degree of the coal seams permeability and thirdly the ability of the injected CO_2 to attach to the coal (Perera, 2011). A successful coal seam CO_2 sequestration project depends on the sorption capacity of the coal in question. The rank of coal, swelling, coal under stress and permeability are the main factors that need to be understood before any production of CO_2 storage can commence (Garnier, 2011).

There are many different techniques to determine gas sorption on coal and these techniques show the coals ability to adsorb CO_2 for sequestration. A coal sample called Filtrasorb 400 (F400) was used in the study of (Gensterblum, 2009) to imitate natural coal seam conditions. This coal sample has a similar pore structure and chemical composition of undisturbed deep seated natural coal seams. Before the sorption process the sample is placed in a heating sleeve to extract the moisture within the coal to mimic natural conditions. The sorption process techniques used typical coal seams conditions suitable for CO_2 sequestration, ranging from temperatures of 300 to 330 Kelvin (K) and Pressures from 6 to 15 Megapascal (mpa)(Gensterblum, 2009) .There are three techniques which are used more often to determine the gas sorption isotherms on coal and they are the Manometric, volumetric and gravimetric methods. The Manometric method injects gas from a calibrated reference cell into a measuring cell that contains the coal sample. The gravimetric method uses a high-pressured compartment controlled by a magnetic suspension balance. The coal sample is placed in the high-pressured compartment and CO_2 is injected into the compartment giving results of CO_2adsorption at different pressures. When referring to the volumetric method to determine the adsorption properties of a specific coal seam the coal sample is crushed and placed into automated high-pressure volumetric equipment (Levy, 1997). Amongst these three methods of obtaining coals adsorption properties the manometric and gravimetric methods give the most accurate results (Gensterblum, 2009).

2.6 Geological criteria needed for CO_2 sequestration

CO_2 sequestration requires sedimentary basins for indefinite storage. Sedimentary basins consist of permeable and porous rock types needed for CO_2 sequestration. Active Mountain belts and craton continental crust are areas not suitable for long term storage of CO_2 (Bachu, 2000). The conditions found in active mountain belts are not suitable for CO_2 sequestration due to the fact that these mountain formations are dominated by fractures and faulting with no continuous seal present. Craton crust is also not suitable for CO_2 sequestration mainly because these areas consist of crystalline structures and metamorphosed rock types (Bachu, 2000). Craton continental crusts are also subjected to rifting aided by mantle plumes and mafic dyke swarms which indicates no continuous seal properties which means this area is not suitable for CO_2 sequestration (Bleeker, 2004). Geological areas dominated by volcanism and earthquakes, for example convergent basins such as basins found in Japan or New Zealand are also not suitable for geological sequestration. Natural disasters such as volcanism and earthquakes could lead to large scale fracturing and faulting which intern could lead to a break in the seal of a sequestration storage site. Geological CO_2 storage is favoured in divergent basins mainly due to the basins tectonic stability and its low probability to any Earth changing events (Bachu, 2000).

2.7 Properties

Petrophysical properties are required to model a functional reservoir model. Interpreting physical rock core samples, thin section analysis and wire line logs are a few ways to determine a rocks porosity and permeability.

2.7.1 Porosity

Porosity values in a rock unit indicate the amount of pore space between grains. It can be divided into primary (Original) and secondary porosity. The primary porosity of a rock is determined when the rock was initially deposited and secondary porosity values are recorded after diagenetic changes have been made to the rock and could either increase or decrease porosity (Fraser, 1935). Pore spaces can be altered as a rock is subjected to various diagenetic processes such as cementation and compaction. Dissolution of a rock as well as fracturing and faulting are considered secondary porosity and ultimately increases the porosity values.

To determine sandstone or shale sediment properties there are five sedimentary structures that can be measured. The five are (1) Sorting of grain, (2) shape of grains, (3) size of grains, (4) degree of angularity and (5) displacement of grains (packing) all of which could be measured to calculate porosity and permeability. Grain size and sorting of sedimentary structures are the most important quantities used to determine porosity, whereas the shape and roundness of the grains are not as important but would assist in identifying porosity values (Beard, 1973). Just as important it is to have an adequate reservoir, source rock and trap formation for hydrocarbon accumulation the same applies when wanting to store carbon dioxide. Thus, having even one of these elements missing would not allow for proper hydrocarbon accumulation or CO_2 sequestration (Bloch, 2002).

The amount of pore space allowing fluid flow within a rock is termed as the effective porosity; on the other hand total porosity refers to porosity in pore spaces that are in constraint. Effective porosity could be estimated using the phenomenon discovered by Darcy (see figure 2-6), this equation can determine the flow through porous media where q is the flux of the fluid, U is the viscosity of the fluid, p is the fluid pressure and K being the permeability coefficient (Koponen, 1997).

$$\mathbf{q} = -\frac{k}{\mu}\nabla p,$$

Figure 2-6: Darcy's law of Fluid flow through a wide variety of natural porous media. (Koponen, 1997).

The wire line data previously obtained during the drilling process of well AF-1 was used in this study. To display the wire line data petrel 2014 software was utilised, the computed data displays a porosity log throughout the well indicating the change in porosity values. A porosity map can be generated by using an upscale value of the porosity. This can display a three dimensional model which indicates the porosity values of the entire 3D seismic.

2.7.2 Permeability

Fluid mechanics forms part of understanding of permeability when dealing with rocks and their petrophysical properties. The degree to which a rock unit allows fluid or gas to pass through it without chemically or physically changing the substance is termed permeability. Henry Darcy defined the term by modifying the heat transfer equation he initially developed to describe fluid flow; hence permeability measurements are in Darcies or millidarcies.
Permeability defined by Darcy is:

$$K = Q \mu / A (\Delta P/L),$$

K = Permeability (Darcy), Q = Flow /time (cm/s), μ=Viscosity of medium in motion (cp),
A = Cross section of rock (cm2), L = Length of rock (cm), ΔP = Change in pressure (psi)
Permeable and impermeable rocks are the two divisions when referring to the permeability of a rock. A permeable rock contains large interconnected pores to allow substances to flow through easily and is commonly known as sandstone rocks. Impermeable rocks commonly called shale or siltstone are rocks that are finer in grain size with less interconnected pore spaces which restricts substance flow through the rock.

Determining the permeability of a specific rock can be done in many ways. The first being wire line log analysis where by the data obtained from a well is loaded into either petrel or interactive petrophysics (IP) and a well log is generated indicating permeability changes with depth. Secondly by interpretation of core samples or by microscope thin section analysis to identify the interconnected pore spaces. Also by well testing and laboratory analysis permeability values can be determined.
Over the years geologists tried to establish the relationship between the random arrangements of pore spaces and the material properties of a rock. Permeability, expressed by Katz, A. J., and Thompson, A. H. (1986)" as the unit of length squared as a function of hydraulic radius" which is the pore volume divided by the pore surface area.
Permeability of a rock could either be absolute or effective. Absolute permeability deals with the measurements of rocks permeability when only one phase is present within the rock and effective permeability is when other immiscible fluids are present in the rock but flow of another fluid is possible. Effective permeability is affected by the saturation of the immiscible fluids and the mineralogy of the reservoir. Shlumberger Oilfield Glossary Quotes "Relative

permeability is the ratio of effective permeability of a particular fluid at a particular saturation to absolute permeability of that fluid at total saturation."

2.8 Status of the Carbon Capture and Storage process

A special report on CO_2 capture and storage by the IPCC (2005) verified the CO_2 capture and storage process and found that there was relevant information not yet understood when referring to storage in deep aquifers. 10 plus aquifer injection operations were put in place to give answer for the knowledge gaps of the process, these exploration injections needed to explain the unknown before commercial implementation of CCS can begin(Michael, 2010). These 10 wells have been monitored for about ten years and have answered some of the questions asked about the CCS process. However, besides the unanswered questions there are also other factors contributing to the setbacks in the progress of CO_2 storage and these factors include the cost and availability of anthropogenic CO_2, injection wells are of poor quality, cost of monitoring and private property cite access (Michael, 2010).

The CO_2 injection process started its first injection as early as the 1990's when Canada disposed of acid-gas (H_2S and CO_2) in saline aquifers. Canada implemented this process of acid-gas injection due to their gas wells having a high concentration of H_2S (Michael, 2010). In the Sleipner gas field in the Norwegian North Sea the first official CO_2 injection started in October of 1996. This CO_2 injection project was the first commercial scale sized project implemented for the purpose of minimising CO_2 emissions from a natural gas project. 1000m below the sea floorCO_2 was injected in the sand layer containing salt water, this layer is called the Utsira formation. This formation up until today stores over 5 million tonnes of CO_2 and has no recorded issues of leakage from the capture plant or the injection well (Torp and Gale, 2004). To ensure that all operations of the Sleipner CO_2 storage project are well a separate project called The Saline Aquifer CO_2 Storage project (SACS) was implemented in 1998. The SACS project monitored the CO_2 injection project using 3D seismic surveys, these 3D seismic surveys allowed monitoring of the movement of the injected CO_2 within the reservoir. The SACS and Sleipner CO_2 Storage project is a successful learning curve project and could assist new projects by answering many unanswered question when starting a new CO_2 storage project (Torp and Gale 2004).

Another CO_2 gas project active since 2004 is the In Salah Gas Joint Venture CO_2 storage project. This project is based in Algeria and is the largest operating onshore CO_2 project in

the world (Iding, 2009). The In Salah storage project is based on the Krechba field in Algeria and the storage saline aquifer is situated at a depth of 1880m with a pressure of 175 bars. The storage unit is of carboniferous age and consists of a heterogeneous geology. The krechba field has medium to low permeable sandstone and small amounts of fractures and faults, these fractures and faults are found in both the reservoir sandstone and slit and mudstone cap rock (Iding, 2009). The Faults and fractures identified in the Krechba field are important factors to take into account when storing CO_2 underground, they could cause either migration or trapping of CO_2. Fractures and faults are regarded as pathways and can have a negative effect on CO_2 storage. Studies of this deep saline aquifer gives incite to the reliability of long-term underground storage. Successful CO_2 Storage in such aquifers depends on parameters such as trapping mechanisms, seal efficiency and well status.

In the Barents Sea north of Finland and Sweden, lies the Snohvit Gas Unit (see figure 2-9). This gas unit consists for three oil and gas bearing formations called Askeladd, Albatross and Snohvit (Maldal, T &Tappel, 2004). The Snohvit unit is a subsea gas-producing project with a connected stream pipeline to Melkoya a small island north of northern Norway. The Melkoya Island is host to the liquefied natural gas (LNG) storage plant, which is located 160km away from the production site. Studies on the production of the Snohvitunit indicated eight gas producers and one CO_2 injector more specifically in the Snohvitfield (Maldal, T &Tappel, 2004). From the Snohvit gas unit CO_2 amounts are about 5 to 8 mol%, so the gas pumped from this unit needs to dispose of the concentrations of CO_2 in order for the liquefaction process to commence. Underground storage was chosen as the concept for the disposal of the captured CO_2 upon that decision several formations in the Snohvit field where evaluated for potential CO_2storage (Maldal&Tappel, 2004). The Snohvit Tubaen Formation was chosen for injection and storage of the unwanted CO_2. The Tubaen Formation has an expected storage capacity of 23 million tons and could store the Snohvit LNG projects CO_2 for approximately 30 years (Maldal, T &Tappel, I. M 2004). Extensive research has been done on the Tubaen Formation and results show that this formation is ideal for storage. The highly porous (Porosity ranging from 10 to 16 % and permeability from 130 to 880 mD) Tubaen sandstone formation is a perfect storage reservoir not only because of the amounts of CO_2 it can hold but because of the 25-30 m thick shale which lies above the Tubaen formation (Maldal, T &Tappel, 2004). The massive shale cap rock gives indication that the Tubaen Formation is perfect for sealing CO_2.

The Gorgon Project is located offshore in the Northwest coast of Australia and is also along with the Snohvit project a LNG production plant. This major LNG development is a joint

venture consisting of three well-established oil companies. Chevron who is the operator and owns 50% of the project, ExxonMobil (25%) and Royal Dutch Shell (25%) (Flett, M, 2009). The Grogon Field reservoir contains not only large amount of gas but also CO_2. The LNG process needs to extract large amounts of CO_2 from the reservoir fluid before the liquefaction process commences. The Greater Gorgon field contains high volumes of CO_2 (approximately 14%) within the reservoir fluid and disposing of this CO_2 is important for preserving our environment (Flett, 2009). The Dupuy Formation located a few kilometres below the Barrow Island (Nature Reserve with a quarantine management regime in place) was the selected reservoir for CO_2 storage. The Dupuy formation dates back to the Late-Jurassic with deposits of sandstone and siltstone and consists of four rock units (see figure 2-7) namely; Basal Dupuy, Lower Dupuy, Upper Massive Sand and Upper Dupuy (Flett, 2009). As the figure shows, the Upper Dupuy and Basal Barrow Shale both contribute as a seal for the Dupuy Formation. The Basal Barrow Group Shale extends throughout Barrow Island and is considered as a continuous barrier above the DupuyFormation (Flett, 2009). The Upper Dupuy unit also serves as a barrier due it consisting of mostly siltstone with small sandstone lenses (Flett, 2009). The Upper Massive Sand and Lower Dupuy are medium to fine grained highly porous sandstone rock units which will be the storage unit for the CO_2 (Flett, M, 2009). To date the Gorgon Project is the most lucrative LNG project and the most successful CO_2 storage project disposing of about 40% of the Gorgan LNG projects CO_2. The In Salah Algeria project, Norwegian Sleipner project, Grogon Australia project and Snohvit unit project all give relevant information regarding CO_2 Storage and could help future CO_2 projects. Most of the CO_2 projects active today used the Sleipner project as a reference in the initial stages of the Carbon storage projects.

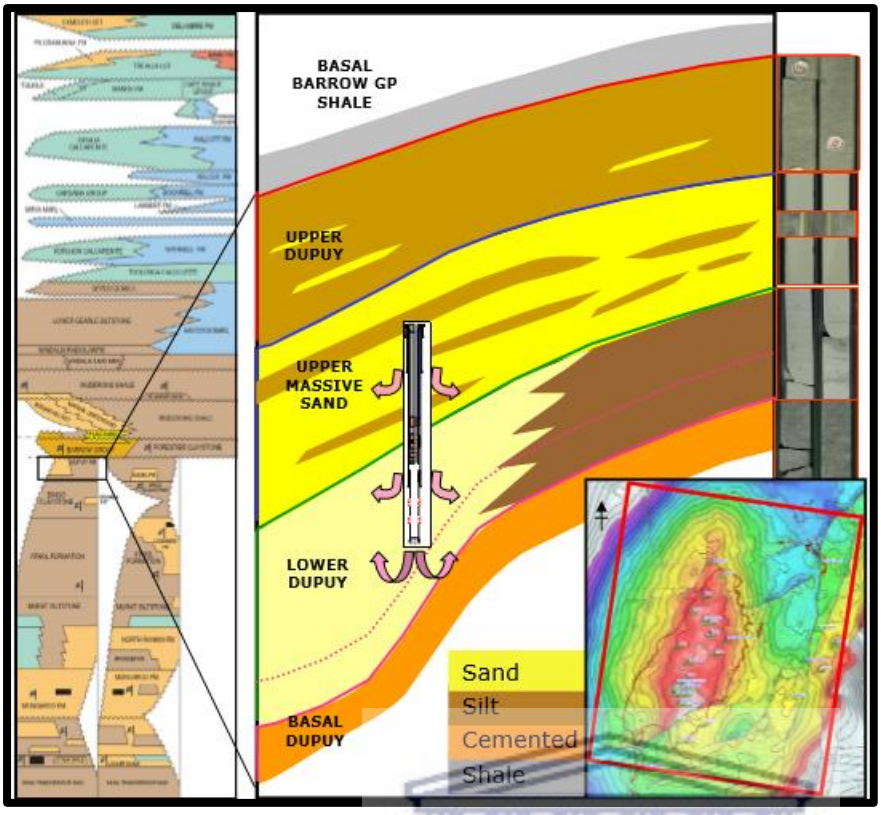

Figure 2-7:Depositional history of the Dupuy Formation (Flett, M, 2009)

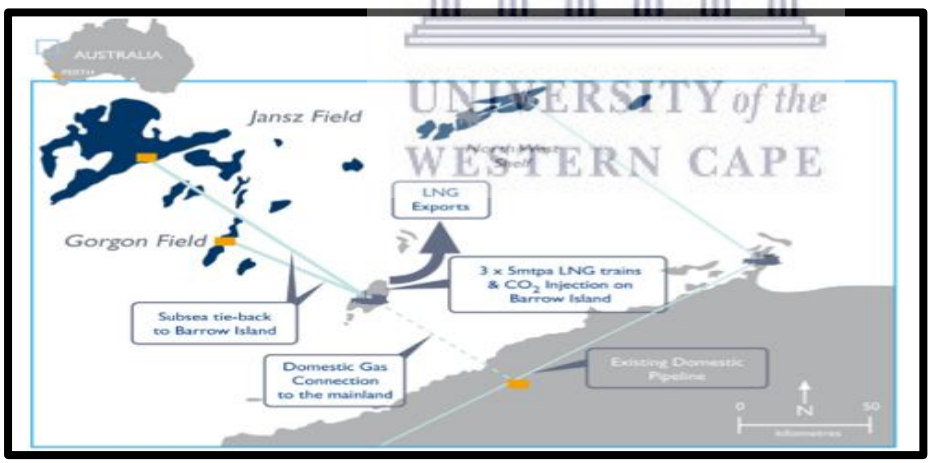

Figure 2-8: Location of the Gorgon Gas Field and Barrow Island (Flett, M, 2009).

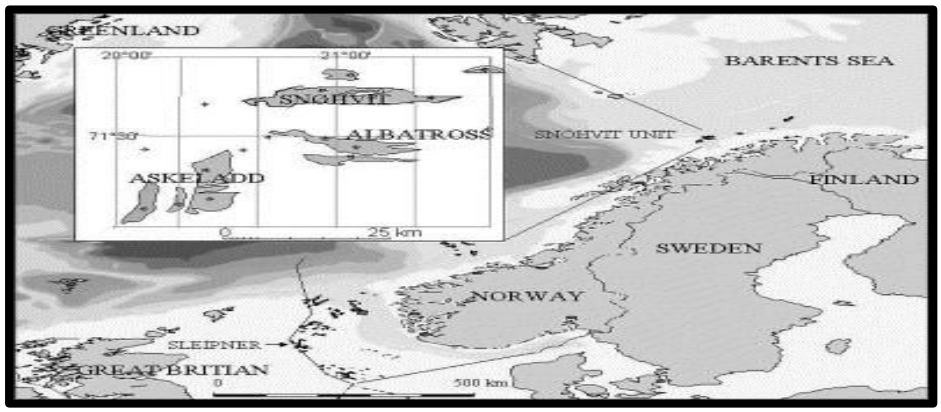

Figure 2-9: The Snohvit Unit Coordinates. Maldal, T., &Tappel, I. M. (2004)

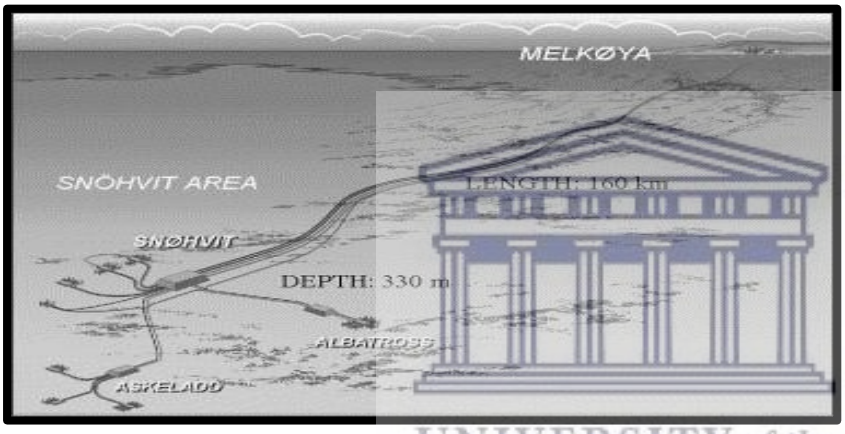

Figure 2-10: LNG Stream Pipe from the Snohvit unit to the Melkoya Storage plant (Maldal, T&Tappel, I. M 2004).

3 Chapter 3: Geology of the Orange basin

The geology of the Orange Basin is sectioned into two parts, Regional and local geology. Regional geology would give information about the depositional history and other geological disciplines to understand the geological history on a large scale. Local geology also describes the depositional history and geological disciplines but on a smaller scale, in close proximity to the area of interest.

3.1 Regional geology

The Orange basin lies offshore and bounded by Namibia at Alexander Bay in the North and Cape Town South Africa in the South. The Orange basin is a post rift basin formed over multiple rift basins with the depositional history dating back from as early as the Early Cretaceous age (Muntingh, 1993). These rift basins that form the Orange basin lies beneath the Atlantic Ocean and consist of fifteen seismic reflections from Upper-Jurassic to the upper Cretaceous age. These layers of deposits throughout the depositional history (see figure 3-2) occurred during the Transition and Drift tectonic stage after the breakup of Gondwanaland (Paton, 2007). The rifting process of Africa and South America continental plates generated grabens and half-grabens. These graben structures were formed subparallel to the present southwest African margin (Muntingh, 1993). These rifted basins consist mostly of lower Cretaceous siliciclastic shoreline rocks and volcanic type rocks (Muntingh, 1993). Kuhlman in 2010 recorded the Orange basin as one of the biggest sedimentary basins on the West coast within the South Atlantic Ocean. This basin formed on a passive continental margin and has a total basin area of 160,000 km^2 (Kuhlman, 2010).

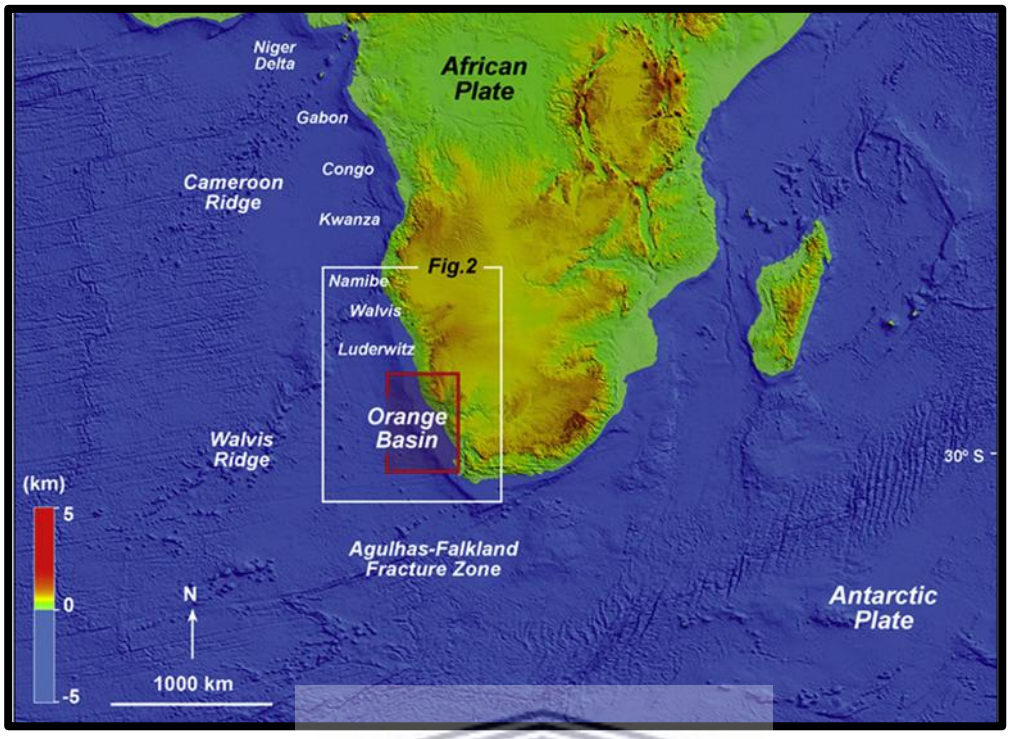

Figure 3-1: Location Map of the Orange Basinafter De Vera, J. (2010).

3.2 Tectonic history and Stratigraphy

This basin history indicates three tectonic phases; pre, post and syn-tectonic phases. The pre-tectonic rift phase, which dates up until the Triassic is dominated by a destructive boundary that formed a stable unyielding block of the Earth's crust which is known as Gondwanaland. During the late Jurassic about 130ma the rifting of this basin formed northwest trending half grabens. This rifting sequence lies beneath the Barremian- Aptian aged rifted transitioned to drifted sequence (Hartwig, 2012). Above this sequence lies the mid-Albian to Cenomanian sequence. This sequence accumulated fluvial marine and deltaic deposits with a thickness of 3500m and this sequence was then overlain by organic shale deposited during the cenomanian and Turonian age. Above the Cenomanian and Turonian aged deposition lies ocean current deposits deposited in the Coniacian to late Santonian/early Campanian age. During the late Cretaceous tilting, uplift and erosion of the inner shelf resulted in the Campanian-Maastrichtian seaward build-up sequence (Hartwig, 2012). Akinlua, (2010) identified a rock type called postglacial black shale deposited in the late Permian age that aremarine environment deposits. This rock type forms a regional seal for the Orange basin. In the late-Permian age, about 260Ma, sandstone volcaniclastic deposits dominated, these

deposits are not of good reservoir quality but in the Triassic period, more suitable reservoir quality sandstones were deposited (Akinlua, 2010).

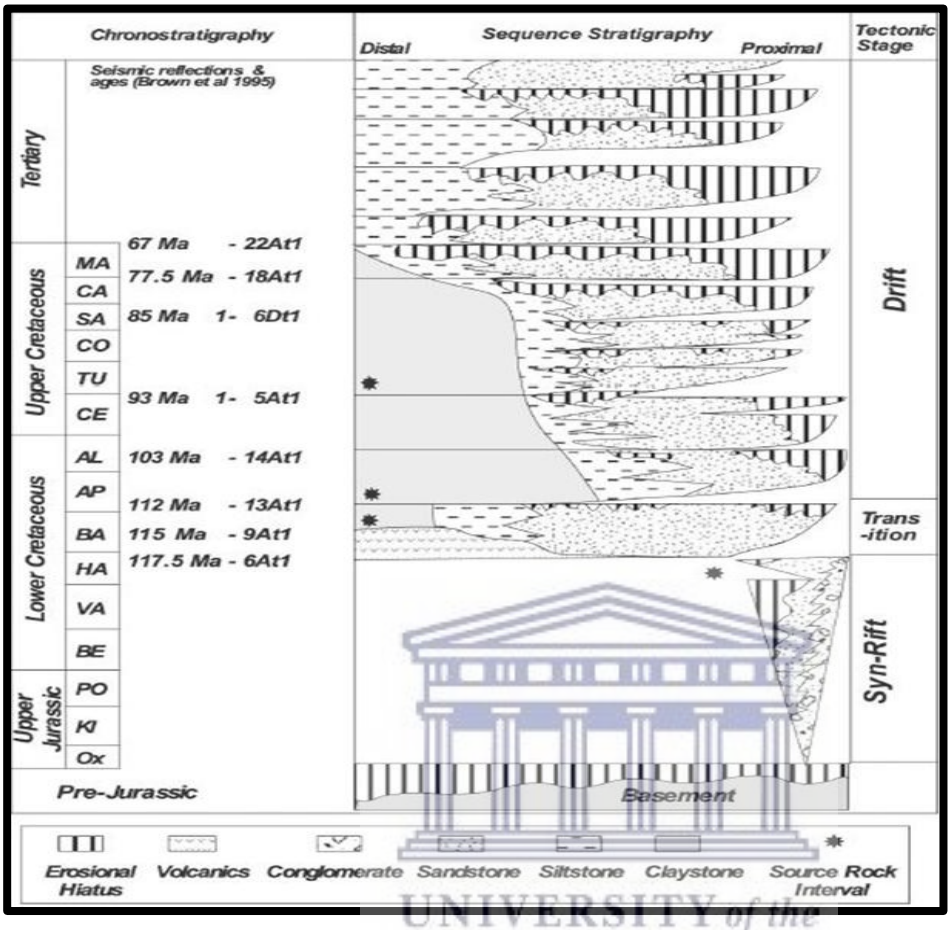

Figure 3-2: Sequence stratigraphy and chronostratigraphy of the Orange Basin (Paton, D. A., Di Primio, R., Kuhlmann, G., Van Der Spuy, D., &Horsfield, B. 2007)

3.3 Introduction to petroleum systems

In order to determine the viability for storage opportunities within geological oil and gas reservoirs, the parameters that construct a petroleum system need to be in place. A petroleum system needs a viable regional seal or caprock, low permeability and high porosity sandstone or carbonate reservoir unit and understanding of the mineralogy and stratigraphy that would determine the rate and direction of migration of the injected CO_2.

3.3.1 Petroleum Systems

A petroleum system is classified as a natural system containing an active source rock, reservoir rock, seal or trap and overburden rock (Magoon, 1994). The formation of a viable petroleum system depends on the depositional history of the basin under review. The deposition of organic material (Kerogen type) along with temperature pressure and time would determine the type of hydrocarbon (oil or gas prone) that will be produced (Tissot, 1987). A sedimentary basin consists of a basement rock on which the first layer of deposition is deposited. The layers of deposition occurred throughout geological time until the present day sedimentary layer, all of which is collectively termed a sediment stratigraphy. The deposition of each layer occurred at different times in different conditions, for example marine deposits or volcaniclastic deposits. During the deposition time, the layers could encounter erosion or tilting and uplift and can alter the geology. The depositional history of the basin is a starting point that needs clarification to determine basins petroleum system abilities(Barker,1988). A petroleum system consists of three categories: The first category being the source rock which is limited to a single source rock (Charged formation), secondly the Migration stage leading to the reservoir rock and thirdly the trapping style which entraps the hydrocarbons or in the case of this thesis the entrapment of CO_2 (Demaison, 1991). Forming a petroleum system requires physical and chemical alterations. These alterations are diagenesis, compaction and deformation due to geological tectonics. All of which can affect the sediments which form the basin and ultimately affect the concentration and dispersion of hydrocarbons (Perrodon, 1984).

3.3.2 Reservoir rocks

Understanding the rock properties of a specific reservoir rock and the relationship the rock has with oil, gas, hydrocarbons and liquid is referred to as petrophysical rock studies. A reservoir with an ability to store gas or liquids would need layered deposits of geological sediments that are highly porous with three-dimensional connectivity. The interconnected pores between sediments would allow for storage of CO_2 or hydrocarbons as well as to allow the fluids or gas present to migrate throughout the reservoir rock (Tiab, 2015). To determine a reservoirs ability to store hydrocarbons or in the case of this thesis to store CO_2 one needs to understand the reservoirs characterization. Petrophysical parameters dealing with the reservoir rocks porosity, permeability and saturation can give the information needed to

determine the viability of a specific petroleum system in question (Lucia, 1995). Rock properties are determined by the composition, structure of sediments and texture with the latter being the most important property that helps understand the amount of gas or fluid a rock can hold and transport (Tiab, 2015). These three properties are mutually dependant on each other. The composition of a rock would be determined by the mineralogy that in turn determines the texture of the rock and the structure of the sediments depends on textural and compositional components. When referring to texture one looks at the shape, orientation, packing, sorting and grain size. The shape of a grain is important because it determines the flow of substance within the rock. The grain shape is calculated by the degree to a spherical shape and the shape of the grain is a function of its size. The sorting of grains within a reservoir rock section evaluates the sizes of grains about the median grain size and the packing of grains determines the size of the pores between grains. The sorting along with the packing of grains both exerts an elemental control on the rocks permeability (Berg, 1970).

To determine the reservoir rocks characteristics, the geological facies of the reservoir formation need to be assessed. The facies assessment provides information about the rocks texture, the diagenetic processes and rock-fluid interaction. To determine the texture, the parameters namely; permeability, porosity and pore space size would need to be examined. The diagenetic processes would give information about the minerals present within the reservoir section, which would suggest the reservoir formations depositional history. A carbonate reservoir unit is more likely to undergo diagenesis than what a sandstone reservoir would. Understanding the diagenetic processes provides information about the reservoirs degree of cementation. Cementation within a rock unit occurs during burial. The cementation process could alter a reservoir by transforming the lithofacies (grain type, sedimentary structure and sedimentary texture) type from a highly porous reservoir rock to a low to no reservoir quality rock (Gomes, 2008). It is recommended to conclude the degree of diagenesis within a potential CO_2 storage unit to identify the reservoir unit's mineral composition to determine whether the diagenesis process degrades the reservoirs ability to store sequestrated CO_2.

Further investigation to evaluate reservoir rocks storage capabilities would aim at identifying the reservoirs longevity for storage. Understanding the long term affects the CO_2 would have on the reservoir rock would determine the ability to indefinitely store CO_2. Bickle, 2007 used modelling accumulation results to determine the alterations the captured and stored CO_2 would have on the reservoir and the layers of sediment deposited above it. Migration paths

determined by the reservoirs grain structure, physical structures (faulting, fracturing, strata displacement) and mineralogy are important to understand to predict pathways and CO_2 plumes that form after years of burial.

3.3.3 Traps and seals

A geological trap is defined as a disposition of rock that enables oil or gas to accumulate within the subsurface. Geological traps effectiveness depends on the reservoir rock and seal ability which all together form a petroleum system. A seal or multiple seals (refer to Figure 3-3 A) are an important element for storage capabilities, and without a successful seal Carbon Dioxide will escape the reservoir rock (Biddle, 1994).

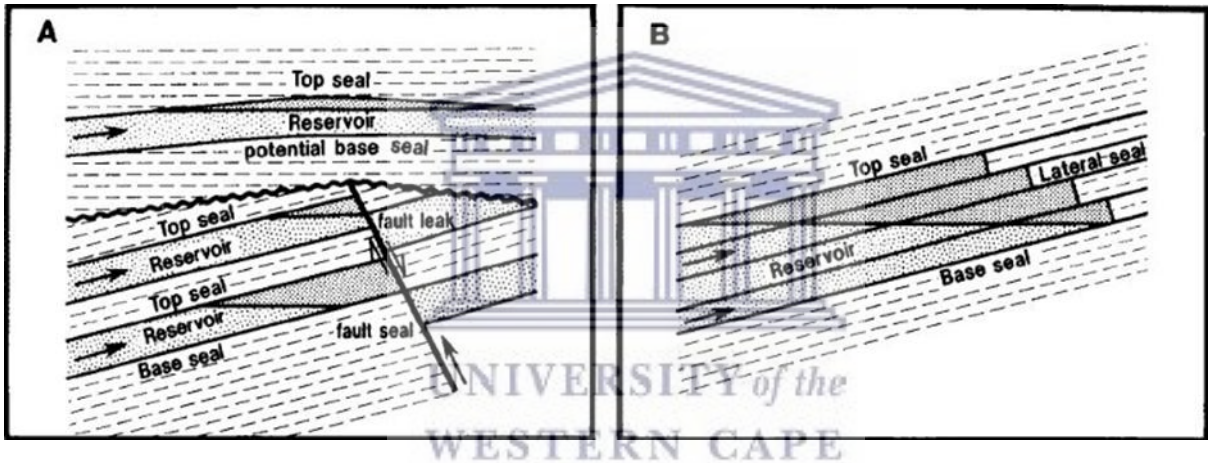

Figure 3-3: (A) Structural traps and seals (B) Stratigraphic Traps and seals (Biddle, 1994).

The presence of a seal or multiple seals within a petroleum system is a very important component. Without a seal hydrocarbons or any form of gas or oil stored within the reservoir rock will migrate out of the storage space. Ductile rocks are usually what a seal consists of, but alternatively seals are composed primarily of volcanic rock material and fault zone material. The seal barriers are mostly thick and continuous throughout the reservoir section with a high surface threshold. For an effective trapping mechanism there would need to be a laterally continuous top seal and base seal as indicated by figure 3-3 (A) and (B).
Reservoir traps subdivide into stratigraphic traps and structural traps.

Structural traps are formed by deformation of deposited strata. A structural trap example is folds within strata due to deformation of already deposited sediments. Folding of geological surfaces usually occur due to plate tectonic movement but can also be formed by slumping of sediment due to gravity forces and overlaying sediment compaction. Folds are subdivided into fault folds and fault-free folds (refer to figure 3-5). The most common fault-related folds are fault bend folds (Figure 3-5A) and fault propagation folds (Figure 3-5B). These fault-related folds occur from shortening of strata and extension.

Fault-free folds on the other hand occur in deposited sequences dominated by shales and evaporites. Upon movement of strata, these shales and evaporites tend to buckle, lift off and kink (refer to figure 3-5) with no faulting due to the ductile nature and composition of the sediments. Most fault free folds are formed by twisting and bending above material that has horizontal or vertical movement with little to no shortening or extension of strata near the reservoir level. Figure 3-5 indicates fault- related and fault free structural fold traps. It is also important to note that a fault free fold can transform into a fault related fold over time. A good example would be a formed fault free fold changing into a propagation fold over time as strata encounters additional tectonic movement. It is very important to identify the type of folds present using seismic data to predict migration pathways and plume generation structures in order to determine if CO_2 storage is viable in the reservoir under review.

Another structural trap is referred to as a fault. A fault usually occurs when the folding strata exceeds its threshold due to tectonic plate movement. Fault dominated traps can either act as a seal or can be a pathway for migration of the intended trapped substance. Fault traps are divided into three categories, these categories are determined if the slip of the fault is known. These faults are normal faults, strike slip faults and reverse faults.

A normal fault is the most common fault trap and can either be a basement attached normal fault or a curved (listric) normal fault. The basement attached normal faults are formed during crust extension and listric faults form during ground sinking or deposition of sediments. A reverse fault trap is the opposite of a normal fault. The hanging wall rises relative to the footwall. These reverse fault trap are usually accompanied by folding and could exhaust the traps efficiency. A strike-slip fault is defined by the strata displacing horizontally in parallel to the strike of the fault. Strike-slip faults do not usually act as good trapping mechanisms although basement connected strike-slip faults could produce anticlinal structures in overlaying sediments and alternatively form a new trap.

Stratigraphic traps are divided into primary stratigraphic traps, unconformity stratigraphic traps and secondary stratigraphic traps.

Primary stratigraphic traps otherwise known as depositional stratigraphic traps are formed from depositional changes which occurred during the same period of time. Facies changes and depositional pinchouts are the general subdivisions of primary stratigraphic traps.

Facies changes refer to changes in grade of rock size and composition as sediments are deposited over time. Highly porous sandstone will be composed of larger grain sizes with larger pore spaces between each grain. Shale and siltstone deposits otherwise will be composed of finer grains with minute pore space between each grain. Shale or siltstones are impermeable with very low porosity which is ideal for a seal or trapping mechanism. A porous sandstone accompanied by an overlaying shale or siltstone are perfect areas for accumulation of hydrocarbons or Carbon dioxide. Examining seismic reflections of a specific reservoir and seal gives an indication of facies changes and how these stratigraphic traps work.

A depositional pinchout occurs when the reservoir rock transitions either rapidly or gradually (depending on the areas depositional history) into the seal rock. These pinchouts form stratigraphic traps in the subsurface and could be one of the potential areas to store Carbon Dioxide.

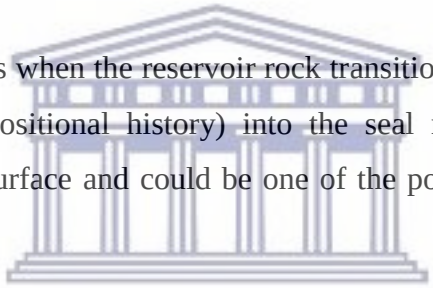

Another type of stratigraphic trap for potential CO_2 storage is traps associated with unconformities. This type of trapping style could either form above the unconformity or beneath. Trapping mechanisms associated with unconformities are subdivided into three types; shortening of tilted strata, shortening of strata associated with valleys or canyons and buried erosional relief. Shortening of tilted strata is the most common type of trapping style associated with unconformities. This type of trapping style forms beneath the unconformity and has impermeable rock material directly above the unconformity acting as a top seal. The overlaying rock acting as the top seal needs to be impermeable for this trapping mechanism to be a viable trap. Another unconformity trapping style uses shortening of reservoir strata where filled valleys and canyons form the trapping styles lateral seal. Filled valleys and canyons can also form a trapping mechanism above the unconformity and this type of trapping mechanism is a very common type found in petroleum systems. Erosional relief is another form of stratigraphic trap style associated with unconformities. This type of trapping style is controlled by the shape and relative arrangement of the surface of bedding undergoing erosion and the underlying layers of strata. This type of unconformity related trap could also

form above an unconformity. Halos form bordering buried eroded strata above the unconformity ultimately trapping oil and gas. A secondary stratigraphic trap is also a type of stratigraphic trapping style that forms within layers of previously deposited strata. The composition of the strata is subjected to alterations due to various reasons. Strata could form from a non-reservoir quality rock to a reservoir rock or from a reservoir rock, which was highly porous and permeable to a more impermeable seal type rock. These alterations could occur to any type of rock due to cementation (refer to figure 3-4) or diagenetic processes depending on the rocks environment and conditions the rock layer is subdued to.

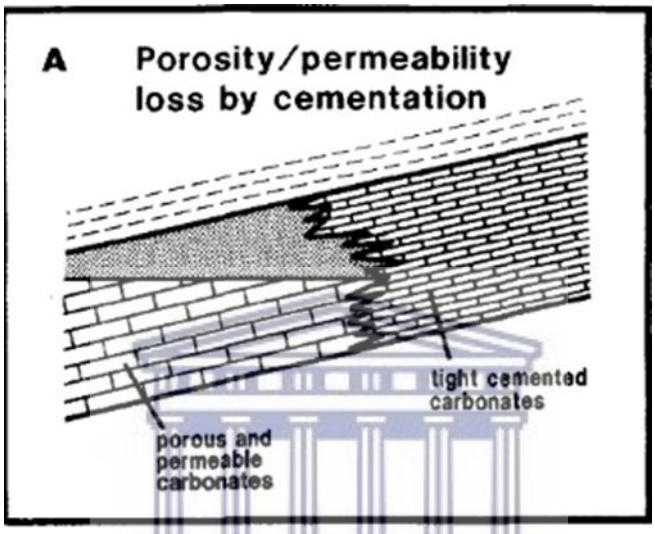

Figure 3-4: Secondary stratigraphic trap by porosity and permeability alterations due to cementation of rock strata (Biddle, 1994).

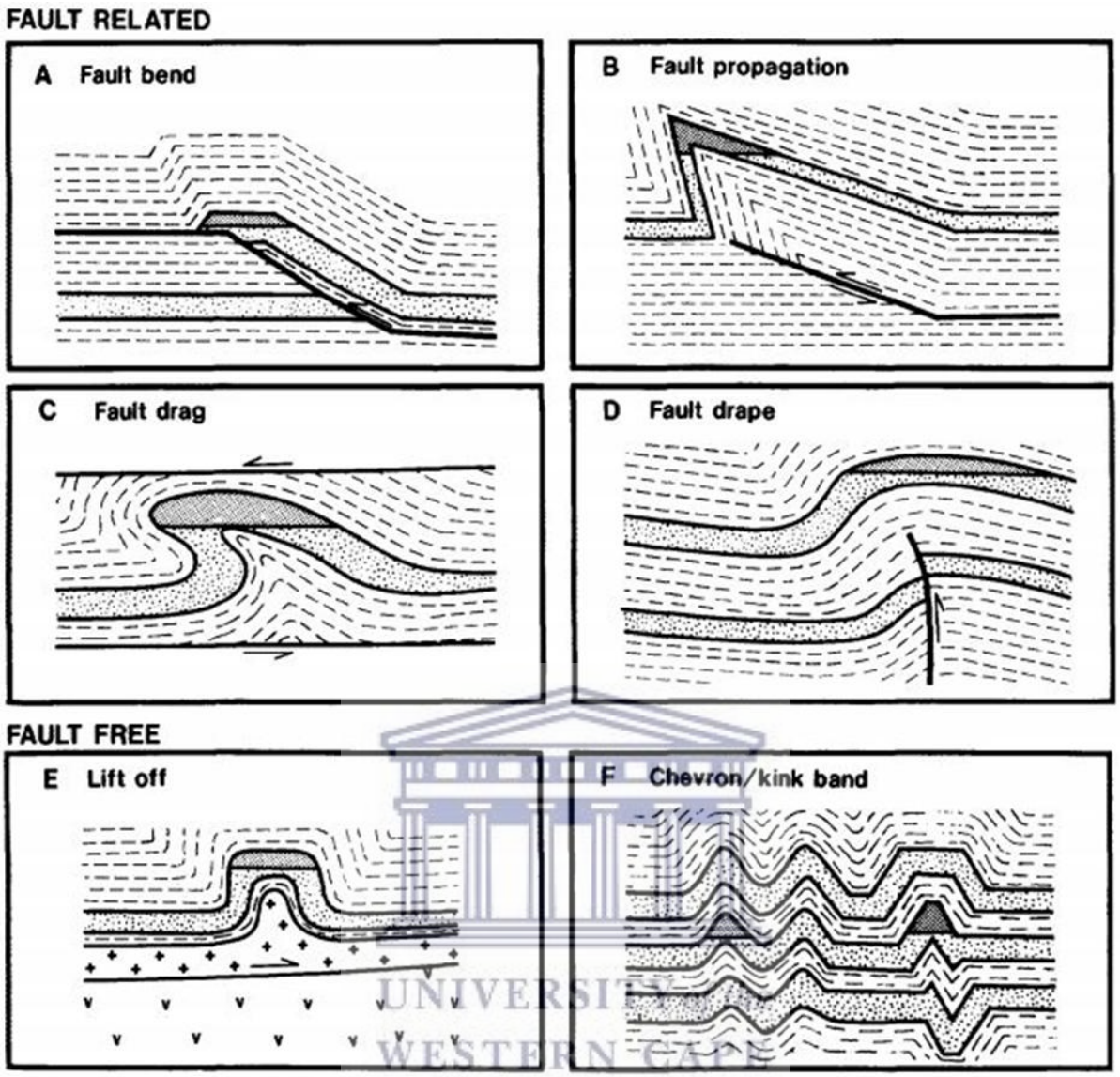

Figure 3-5: Structural traps dominated by folding. (A) Fault bend, (B) Fault propagation, (C) Fault drag, (D) Fault drape, (E) lift off, (F) chevron/kink band Biddle, K. T (1994).

4 Chapter 4: Methodology

4.1 Materials

This chapter discusses the materials used to determine the viability for storage opportunities within the Orange basin, specifically focusing on well AF-1. Different analyses and there results would give insight and answer the main research questions of this thesis. There are various methods that can be used to estimate CO_2 storage capacities, either by using seismic data or through the development of geological models. A three-dimensional seismic volume set which covers 130 000 km^2 contains one well called AF-1. Rock samples were also acquired from well AF-1 along with geophysical wireline logs of gamma-ray, Density, neutron and sonic logs. In addition the well report completion and formation tops were also obtained. The seismic data will be used to map major unconformities which are the major horizons. The faults will be mapped on the seismic volume by looking at the plain of discontinuities of the seismic section.

The outline as follows:

1. 3D seismic bock data set for Seismic Interpretation and depth conversion
2. 4 rock samples from well bore AF-1
3. Facies definition from wireline logs
4. Petrophysical modelling: porosity, saturation
5. Structural modelling
6. Facies modelling
7. Injection of CO_2

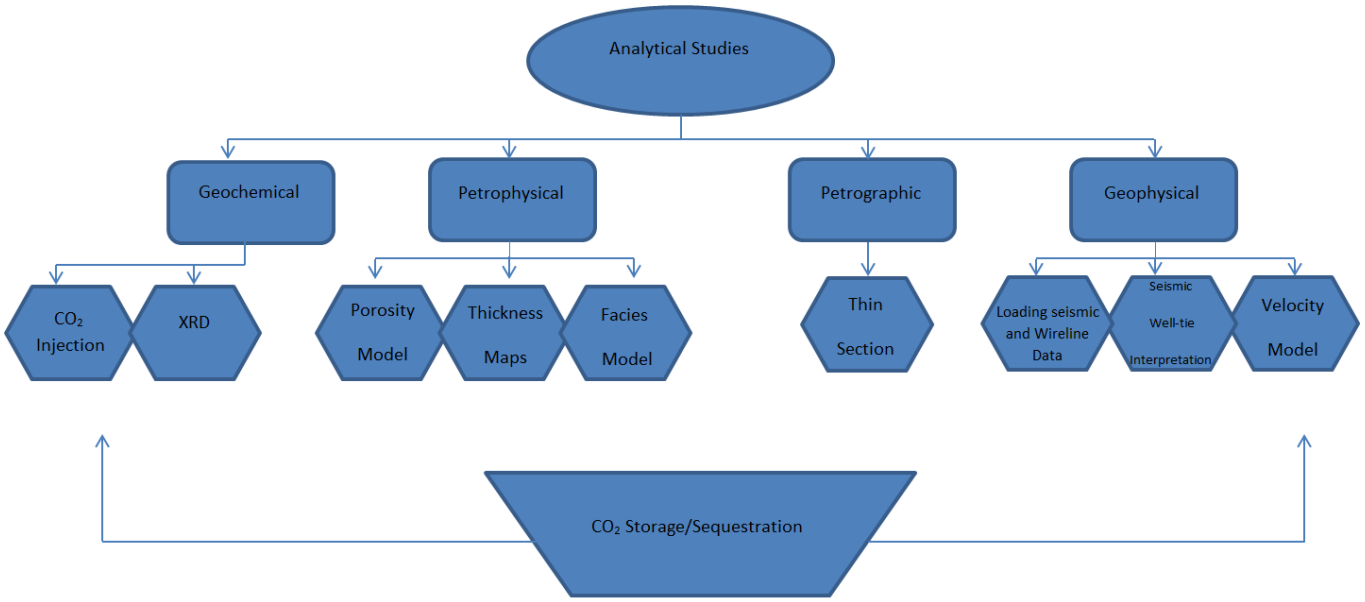

Figure 4-1: Methodology flow chart

4.2 Methods

4.2.1 Introduction to methods

The methods and techniques used to determine the Orange basins storage abilities are also discussed in this chapter. Extensive research has been done to understand the geology of the Orange basin. A regional study of the area has been done to understand the tectonic movements as well as the order and positioning of the deposited strata that form the basin in question. The Petroleum system of the Orange basin is also an important factor under review in this thesis, which highlighted the Orange basins reservoir and seal abilities for Carbon Sequestration.

The software used in this study is Petrel 2014. Followed by the loading of the data set was the identification and mapping of all major faults within the data set. After the faults were mapped then the horizons of each deposited layer were picked. The next step was to create surfaces of each deposited layer using the horizons that were previously picked. With the surfaces created, various models were built. The models built include; Velocity model, Facies model and Porosity model, these models all assist in identifying the different rock layers and their abilities to store or trap injected CO_2.

Rock samples from well AF-1 were taken at different depths. These rock sample depths were used according to the data given by the wireline Gamma ray log. The Gamma ray log

indicated the specific depth samples as potential seals and reservoir intervals, which gives an understanding of the quality of these intervals. These rock samples were used for the geochemical, petrophysical and petrographic studies. Thin section slides made from the four rock samples identify the mineralogical and textural characteristics such as types of minerals present, grain (size and shape) and degree of cementation and diagenesis to determine porosity and permeability values of these rock intervals.

To assist in identifying the minerals present within these rock intervals the rock samples were milled and given to ithemba labs where X-ray diffraction analyses were performed.

The milled rock samples were also used in another geochemical method, where all four samples were placed one at a time in the Carbon injection machine. The carbon injection machine injected CO_2 into each rock sample at temperatures of 200 degrees Celsius at four hour intervals. This method indicates the affect each rock unit has when CO_2 is exposed to it, giving a simulated result as to the effects of the reservoir and seal rock layers when CO_2 is injected into the reservoir for storage.

4.2.2 Seismic data loading:

The seismic data acquired was loaded into Petrel 2014 workstation. Seismic data is normally saved in SEG-Y format, SEG-Y format means the Society for Exploration Geophysicist code.

4.2.3 Seismic-Well tie

Seismic-well tie starts with sonic log and check shot calibration. Sonic calibration is performed to generate a sonic log to calibrate the well AF-1 with the seismic. The sonic logs are used to determine the travel time of sound waves. After sonic calibration, by using the sonic log a synthetic seismogram is generated within the well. The synthetic seismogram along with the seismic cube will indicate the seismic amplitude peaks and troughs within the well and on the seismic volume. Matching the peaks and troughs are then performed, which is called integrated seismic-well tie. This process will enable you to position the well within the seismic cube forming a time-depth relationship between the seismic and well AF-1. As indicated on figure 4-2, by looking at the highlighted yellow circles, its shows that the blue and red amplitudes on the well match with the blue and red amplitudes on the seismic section. This is an indication of a good seismic-well tie.

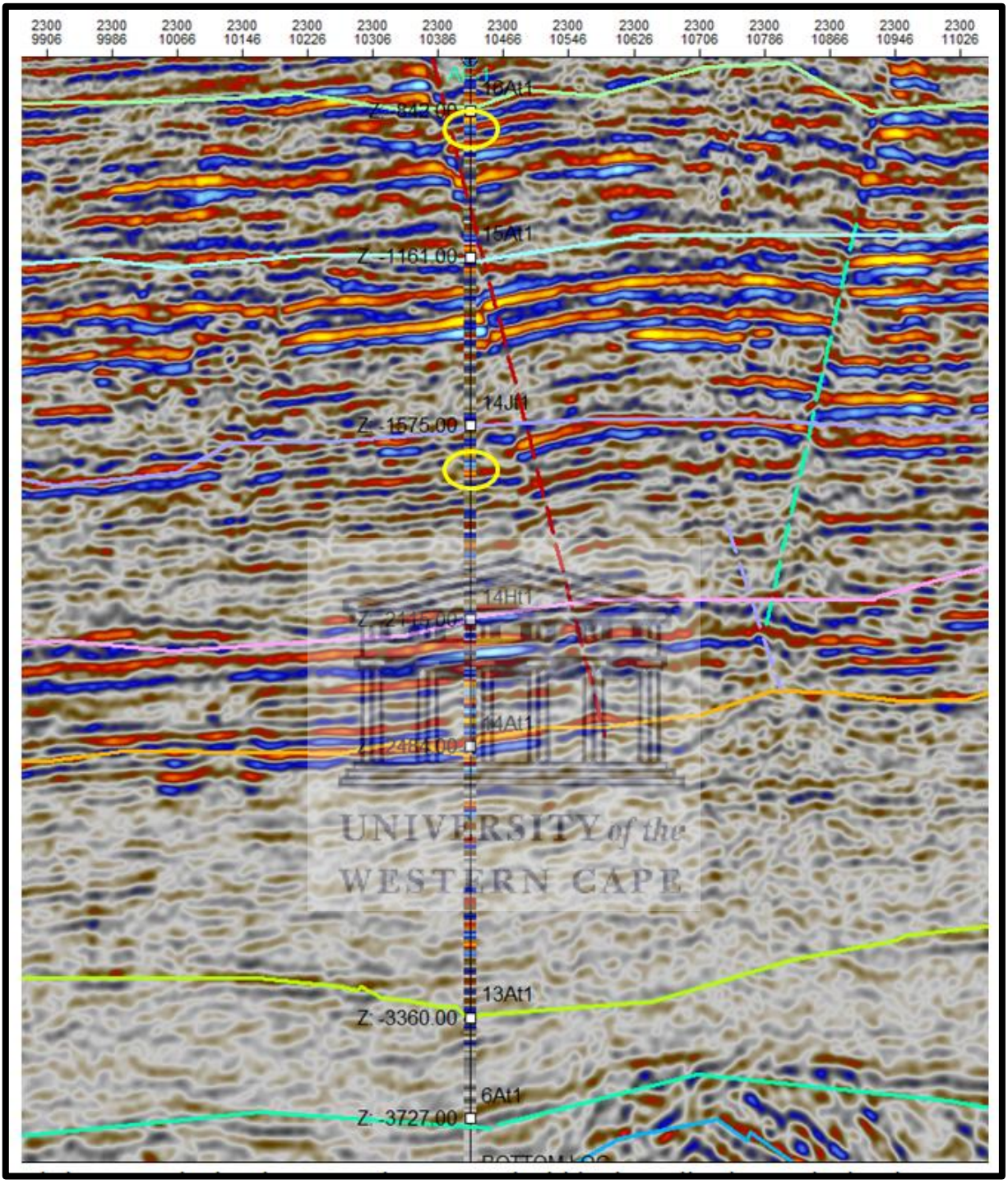

Figure 4-2: indicating a good Seismic-well tie.

The horizons picked were then converted into surfaces for each formation. After mapping the seismic horizons and creating surfaces for each formation, thickness (isopach) maps were created. The process uses one horizons distance between the next directly beneath it, which gives an indication of that specific formations thickness.

4.2.4 Seismic data interpretation

The first step in seismic interpretation was fault mapping as shown in Figure 4-3. The seismic section was displayed in an interpretation window on petrel 2014. The faults were picked on the in-line which indicates some faults that run throughout the full volume of the seismic section (extensive faults) and some are minor faults which do not carry throughout the seismic volume.

Mapping of seismic horizons require a thorough sonic log and check shot calibration process called seismic-well tie to identify the positions of the horizons in the well and on the seismic section. Once this first step is complete, then each horizon will be displayed within the well and can give an indication as to the starting point of each formation that needs to be picked on the seismic volume. Refer to Figure 4-2 for an example.

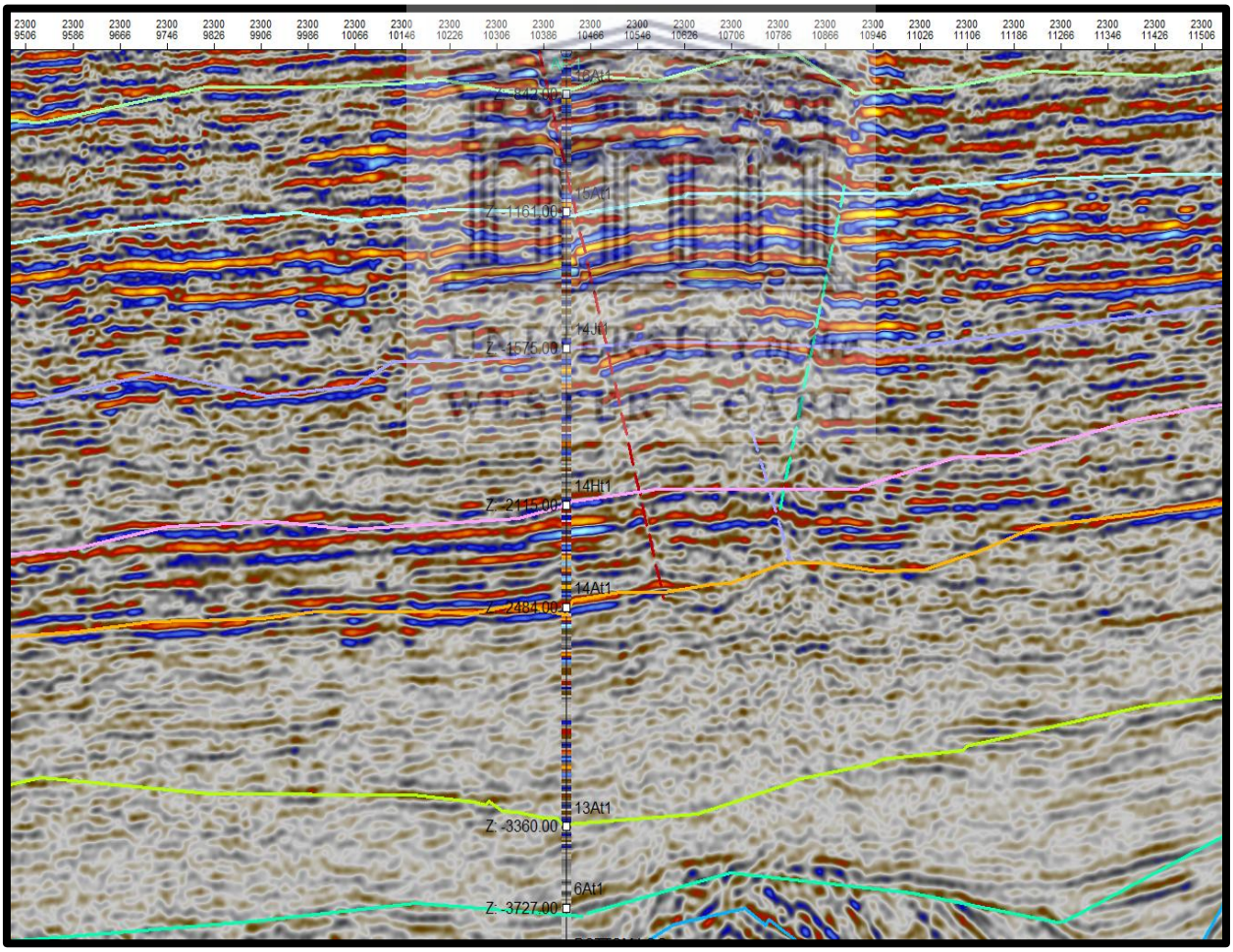

Figure 4-3: Indicating a seismic interpretation with the major faults picked and horizons mapped.

4.2.5 Velocity modelling

Velocity modelling was performed to convert my surfaces which were in time to depth. The velocity models output sheet can be viewed by figure 4-4. The essence of performing velocity modelling is to determine a good level of certainty for the depth of prospect for the driller's target. Therefore it is important to map depth and thicknessmaps of subsurface formations in order to identify sweet spots (hydrocarbon rich sandstone reservoir and source rock) and subtle stratigraphic features that can be potential charged sandstones and continuous seals for effective Carbon storage.

Velocity model							
user							
JADE PROJECT.pet							
Monday, December 05 2016 15:35:23							
TWT [ms]							
Z [m]							
[m]							
Well	**X-value**	**Y-value**	**Z-value**	**Horizon after**	**Diff after**	**Corrected?**	**Information**
Well	**X-value**	**Y-value**	**Z-value**	**Horizon after**	**Diff after**	**Corrected?**	**Information**
AE-1	624909.9	6692823.8	-1425.00	Outside		No	
AO-1	613595.5	6797161.1	-375.00	Outside		No	
AF-1	616587.9	6766560.8	-475.00	-457.24	-17.76	No	
Well	**X-value**	**Y-value**	**Z-value**	**Horizon after**	**Diff after**	**Corrected?**	**Information**
AE-1	624909.9	6692823.8	-1282.00	Outside		No	
AF-1	616587.9	6766560.8	-842.00	-828.48	-13.52	No	
Well	**X-value**	**Y-value**	**Z-value**	**Horizon after**	**Diff after**	**Corrected?**	**Information**
AE-1	624909.9	6692823.8	-1518.00	Outside		No	
AO-1	613595.5	6797161.1	-1135.00	Outside		No	
AF-1	616587.9	6766560.8	-1161.00	-1136.74	-24.26	No	
Well	**X-value**	**Y-value**	**Z-value**	**Horizon after**	**Diff after**	**Corrected?**	**Information**
AE-1	624909.9	6692823.8	-1986.00	Outside		No	
AO-1	613595.5	6797161.1	-1473.00	Outside		No	
AF-1	616587.9	6766560.8	-1575.00	-1591.45	16.45	No	
Well	**X-value**	**Y-value**	**Z-value**	**Horizon after**	**Diff after**	**Corrected?**	**Information**
AE-1	624909.9	6692823.8	-2139.00	Outside		No	
AO-1	613595.5	6797161.1	-1805.00	Outside		No	
AF-1	616587.9	6766560.8	-2115.00	-2084.98	-30.02	No	
Well	**X-value**	**Y-value**	**Z-value**	**Horizon after**	**Diff after**	**Corrected?**	**Information**
AE-1	624909.9	6692823.8	-3195.00	Outside		No	
AF-1	616587.9	6766560.8	-2484.00	-2452.37	-31.63	No	
Well	**X-value**	**Y-value**	**Z-value**	**Horizon after**	**Diff after**	**Corrected?**	**Information**
AE-1	624909.9	6692823.8	-4389.00	Outside		No	
AF-1	616587.9	6766560.8	-3360.00	-3311.50	-48.50	No	
Well	**X-value**	**Y-value**	**Z-value**	**Horizon after**	**Diff after**	**Corrected?**	**Information**
AO-1	613595.5	6797161.1	-3502.00	Outside		No	
AF-1	616587.9	6766560.8	-3727.00	-3680.36	-46.64	No	
Well	**X-value**	**Y-value**	**Z-value**	**Horizon after**	**Diff after**	**Corrected?**	**Information**
AO-1	613595.5	6797161.1	-4545.00	Outside		No	
AF-1	616587.9	6766560.8	-3974.40	-3942.64	-31.76	No	

Figure 4-2: Velocity model output sheet.

The last step was to form a structural framework; this process uses the faults and surfaces previously created within petrel to give an overview of the tectonic and stratigraphic interactions within the study area. The first step when forming a structural framework is to create cells within the framework, which is termed gridding. Gridding would allow you to

populate the petrophysical properties within the structural framework in order to display facies and porosity distribution throughout the study area. The facies model identifies the distribution of sandstone and shale within each formation, which would assist in exploration for potential reservoir targets and trapping mechanisms. Along with the facies model a porosity model was also created. The porosity and facies logs were both upscaled and inserted into the gridded cells of the structural framework in order to display the property modelling values across the study area. Both the facies and porosity models help to identify potential areas for highly porous sandstones for carbon storage as well as to identify shale formations which act as potential seals to assist in trapping the stored Carbon dioxide.

4.2.6 Wireline logs:

Wireline geophysical logging is a measuring tool that logs electrical properties to determine the composition and physical properties of rock layers within a borehole. Wireline logs are used extensively by geoscientists to map subsurface properties to discover oil and gas reservoirs. This method of measuring in situ rock formations was performed with the tool called a sonde, this tool was invented by Conrad and Marcel Schlumberger in 1927. The wireline tool is connected to a cable and guided down a man-made borehole. Geologists also suspend more than one sonde tool attached to one steel cable in order to receive multiple measurements at once. This measurement tool records the formations from the top of the bore well to the end of the bore well and displays the results in a well log. There are two types of ways logs can be recorded. Openhole logging logs well data after the well has been drilled and the other type of logging is called logging while drilling (LWD). The later type of logging method has logging tools connected to the drilling tools so that the logging of results can commence at the same time as the drilling of the well.

4.2.7 Loading of wireline logs

Four wireline logs are used in this thesis to distinguish the differences between the rock layers and to emphasise the petrophysical properties of each deposited rock unit. A brief description of each log and their results are discussed below.

Well AF-1 was loaded into petrel workstation using the longitude and latitude of the well. The different logs used for this study were loaded in the global wells log folder and subsequently despiking and splicing (editing of log data) was performed in order to join

different log runs to make a complete run for well AF-1. The data sets acquired from PASA contained Log ASCII Standard (Las) files. These Las files were imported into petrel 2013 and each wireline log mentioned above was generated. These wireline logs along with seismic maps, XRD analysis and Carbon injection test will give a good representation of the area to finally determine the Carbon sequestration abilities.

4.2.8 Gamma-Ray log:

Geologists determine the type of deposited rock using a gamma-Ray log. The gamma-ray log calculates the amount of gamma radiation each formation emits and returns the information to the sonde tool. The formations radiation mostly derives from Potassium, Uranium and Thorium elements, which is dominant in shale and clay deposits. The main reason why gamma ray logs are used is to distinguish between lithology's to determine which intervals of deposited strata are reservoirs or seals. The gamma ray log will measure in API (American Petroleum Institute) ranging from 0 to 45 API being clean sand or in other words reservoir sand and from 45 to 75 and is referred to as shaly sand and higher values close to 100 API and above being shale. Refer to figure 4-5 to see the gamma ray log output responding to different lithologies. This figure shows a generated gamma ray log from well AF-1 data. As you can see the curve shifting far right means shale present at a specific depth and when the curve shifts to the left, we have reservoir sandstone sediments.

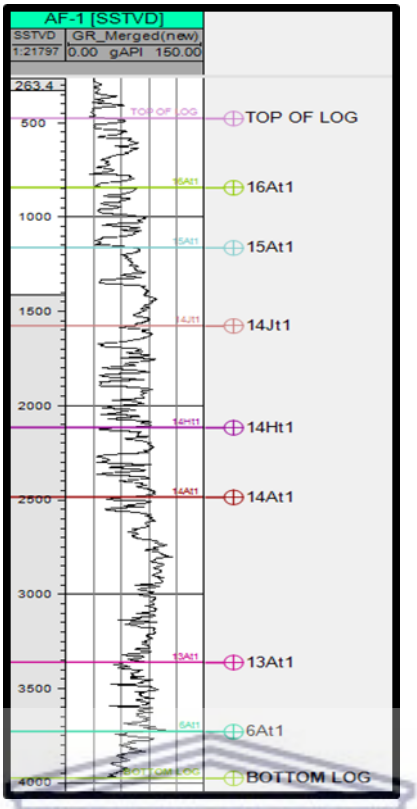

Figure 4-3: Representation of a gamma-ray log from well AF-1

4.2.9 Density log

The density log is used to measure the Compton scattering of the gamma rays. This measurement results derive from the amount of scattered gamma rays to identify the level of density within the borehole. Specifically the density tool shoots gamma rays derived from a chemical apparatus located at the bottom end of the tool. The gamma rays penetrate the borehole strata and absorb some of the gamma rays. The number of gamma rays that were not absorbed reach another detector called a scintillation Counter, this value gives the electron density of the surrounding rock and this value of electron density is proportional to the actual density of the rock unit. Density logs are used for lithology analysis using recorded photoelectric capture and can too display porosity in the rock. Refer to figure 4-6 to see an example of the density tool and detectors. Indicated below is the density log for well AF-1.

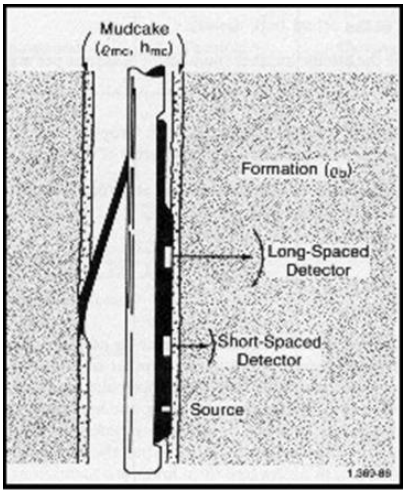

Figure 4-4: Density log tool with detectors. After Crain, E. R., &Eng, P. (2006)

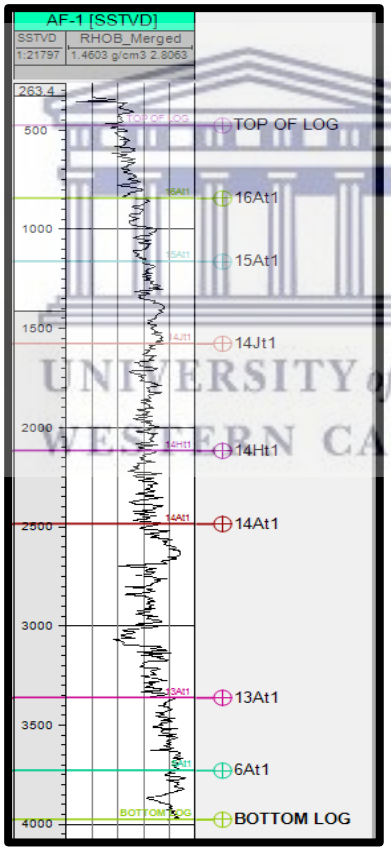

Figure 4-5: Example of a density log output on a well section window indicating density for well AF-1.

4.2.10 Porosity logs

Porosity of a specific rock unit is the measure of the void spaces between each grain of the material, for example void spaces within a sandstone or shale deposit. The degree of compaction and characteristics of the materials (grain size, grain shape, grain orientation) would determine the porosity value of that specific rock unit under review. Porosity values for rocks range from 1% (mostly shales with little to no pore spaces due to the close proximity of the grain matrix) to about 40% (mostly sandstones with large pore spaces) and can be calculated using this equation;

$$Pt = \frac{Vp}{Vt}$$

Figure 4-6: Porosity equation where (Pt) is porosity, (Vp) being Volume of pore space and (Vt) being volume of total rock

Porosity values were derived from well AF-1 data and from the previously generated density log. The porosity log generated was upscaled to form porosity map models for each surface within the 3D seismic. The porosity log along with the gamma ray log and density log give a direct identification of potential sandstone layers that can be used as a storage unit for CO_2. Figure 4-9 shows well AF-1 porosity values throughout the log section from the top of log to the bottom of log.

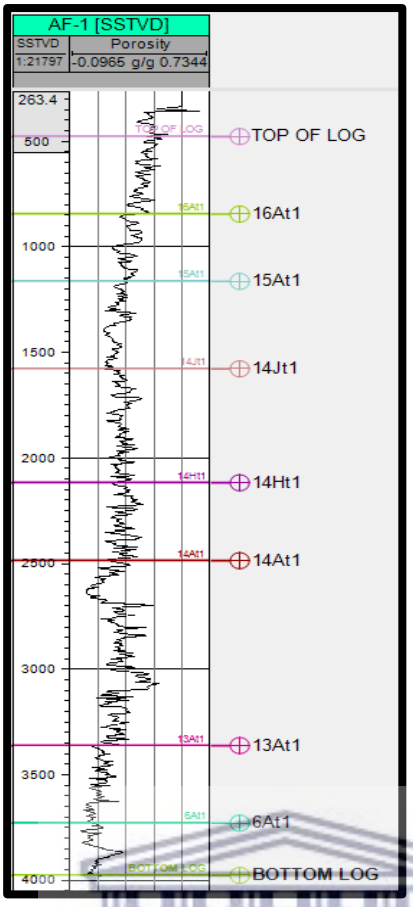

Figure 4-7: Typical representation of a porosity wireline log from well AF-1.

4.2.11 Acoustic Impedance log

The Acoustic Impedance, a basic physical property of a rock is determined using the values of seismic velocity and density and are displayed in a log window. This log presents important facts dealing with the rocks lithology and nature, highlighting the necessary information which helps to understand reservoir and seal rock properties. Figure 4-10indicates the acoustic impedance values for well AF-1.With the Acoustic impedance values a Reflection Coefficient can be generated. The reflection values indicate changes in lithology, if diagenesis occurred in a rock layer or simply indication of a new deposited layer, to changes in porosity and saturation, which is critical for understanding the physics of a particular rock unit.

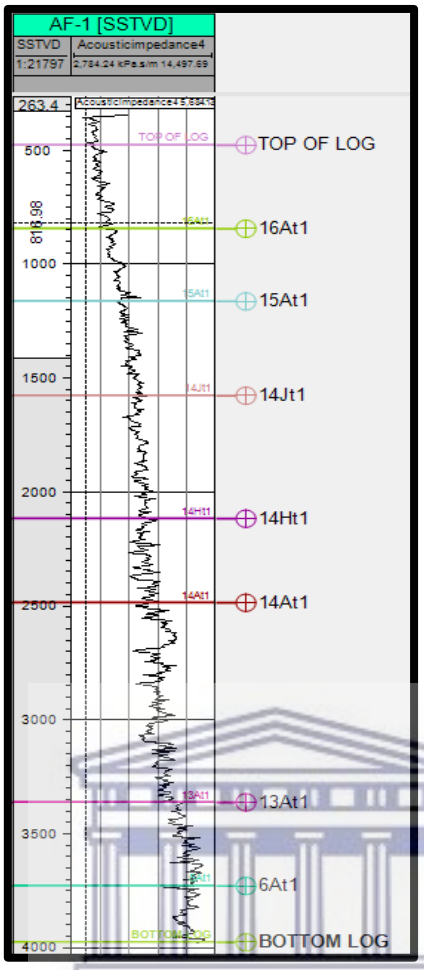

Figure 4-8: typical results of Acoustic Impedance displayed in a log window for well AF-1.

4.2.12 X-Ray Diffraction (XRD) analysis

The X-ray diffraction analysis is a method whereby a rock sample is placed into the XRD machine to identify the crystallinity and chemical composition of that specific rock. The XRD method also identifies grain size, crystal texture and structure which ultimately indicate the minerals present that form the rock sample. The process bombards a monochromatic X-ray beam into the sample at an angle of incidence. The X-ray beam would then be absorbed by the material and a portion of the x-ray will be deflected. The intensity and angle of the deflected beam is then measured and compared with pre-recorded diffraction patterns from a database of measurements for all compounds.Peak shapes and intensity values collected during the analysis reveals the percentage of a specific mineral and its crystalline size. Four samples from depths1178m, 2322m, 2542m and 3190m in well bore AF-1 were given to ITHEMBA labs were the Bruker D8 advance diffractometer was used to perform the XRD

analysis. An example of one of the results obtained from the XRD diffractometer can be seen from figure 4-11.

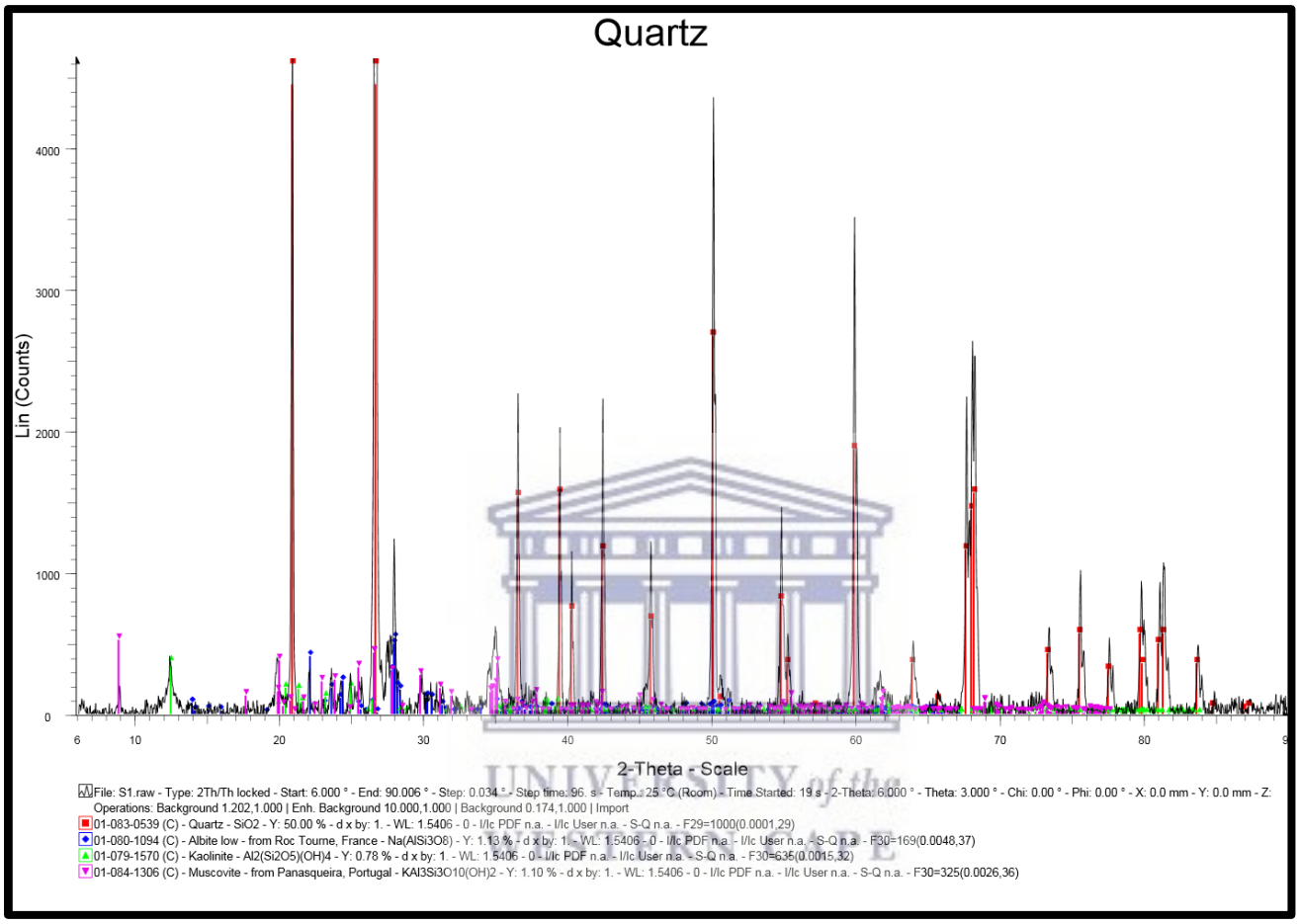

Figure 4-9: XRD analysis result for sample 1 at the depth of 1178m in well AF-1.

4.2.13 Thin Section analysis

Thin section analysis is a crucial step to understanding the mineralogy and chemical structure of the specific sandstone and shale deposits which act as the Orange basins reservoirs and seals respectively. The petrographic descriptions of each rock sample helps to identify minerals and their abundance, the sorting of these minerals, grain size and an estimated porosity value. The initial step to creating a thin section starts with preparation of the rock sample. The rock sample is impregnated with epoxy to allow cutting of the rock sample. This

epoxy helps the loss of material when the rock is subdued to cutting and grinding. The rock sample is then cut to about 5mm in thickness and thinned to 30 microns after. After the cutting process the sample is then mounted and polished to two plates. The results of the thin sections are complimented by the XRD results to determine the authenticity of the observations made by the petrographic descriptions. Below is an example of sample 2 from the depth of 2322m in well AF-1.

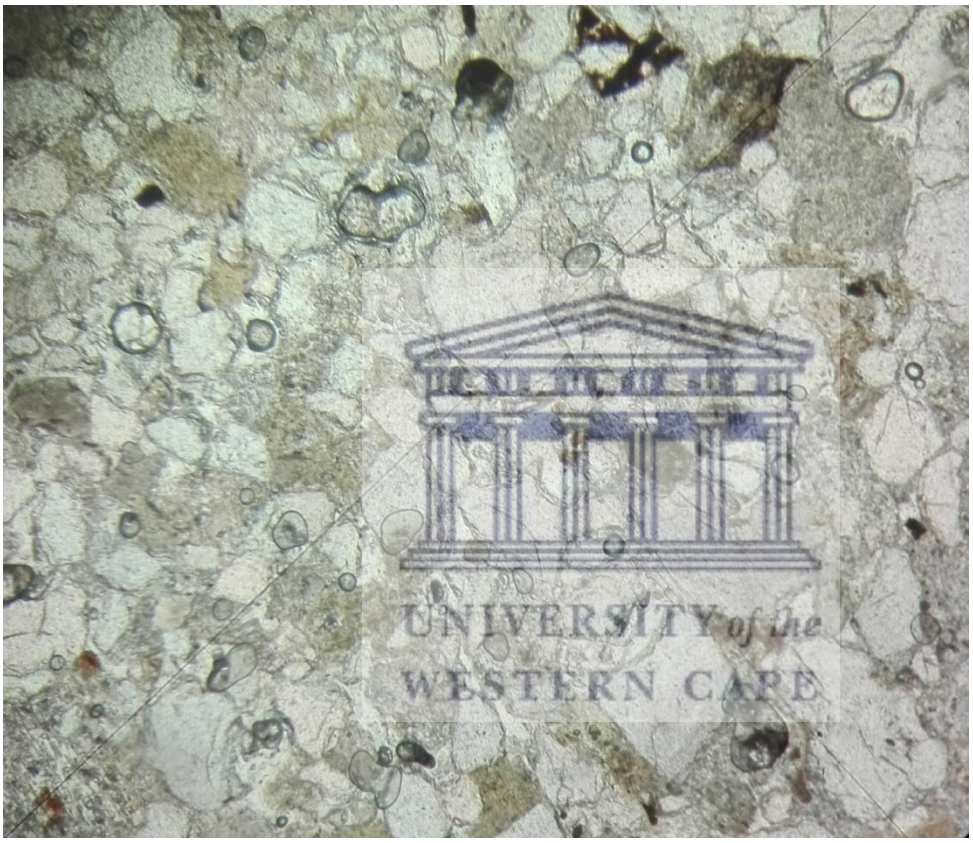

Figure 4-10: (sample 2 depth 2322m) microscopic thin section (Plane Polarised light) obtained from well AF-1, Orange Basin, South Africa.

4.2.14 Carbon Injection analysis

This analysis was performed in the laboratory. A rock sample is placed in the PerkinElmer Simultaneous Thermal Analyzer machine and injected with a controlled amount of CO_2 at a controlled temperature and pressure for a certain amount of time. This process simulates what would happen to a rock unit if subdued to CO_2 during the process of CO_2 sequestration.

The initial stage of this process removes the water vapour and all gasses found within the pore spaces of the rock sample. The injection machine applies immense pressure, temperature and nitrogen to the sample forcing out all substances within the pore spaces of the sample. After this step is complete, the pore spaces will only have nitrogen present. The next step injects CO_2 into the sample replacing the nitrogen in the pore spaces. The last step once again forces nitrogen back into the sample giving a CO_2 desorption percentage. This final stage results show the samples ability to adsorb $CO_2$and also shows the porosity value for that specific rock unit.

5 Chapter 5: Results Interpretations and Discussions

5.1 Petrography interpretations

Four rock samples from well AF-1 at depths of 1178m, 2322m, 2542m and 3190m were obtained from core samples given by the Petroleum Agency of South Africa. These four rock units were subjected to petrographic analyses (Thin section and XRD) to identify the rock forming minerals and diagenetic minerals which may impact on carbon storage within the formations. The first sample under review was taken from well AF-1 at the depth of 1178m which is referred to in this study as sample 1. The second sample was taken from the depth of 2232m and is referred to in this study as sample 2. Sample 3 and sample 4 were taken from depths of 2542m and 3190m respectively and are named in this study as sample 3 and sample 4. The core samples at these depths were taken within well AF-1 based on the lithology at these depths, which is either sandstone or shale. While sandstone formation is adequate for storage, shale is a potential seal unit. These depths were matched with the actual depths seen on the gamma ray log to calibrate the lithology identified on the core samples with the lithology inferred from the gamma ray signatures.

5.1.1 Sample 1 (1178m)

The description shows that this sample is predominantly sandstone. The general colour is dominantly washed out grey with minimal brownish and orange colour. There are also black carbonate speckles found throughout the sample as well as greenish minerals identified as Glauconite (Figure 5-1).

Petrographic description

- Angular to rounded grain shape
- Poorly sorted
- Quartz
- Glauconite- greenish colour
- Biotite- brownish colour
- Speckles of carbonate material
- Iron stain on quartz grains
- Well consolidated

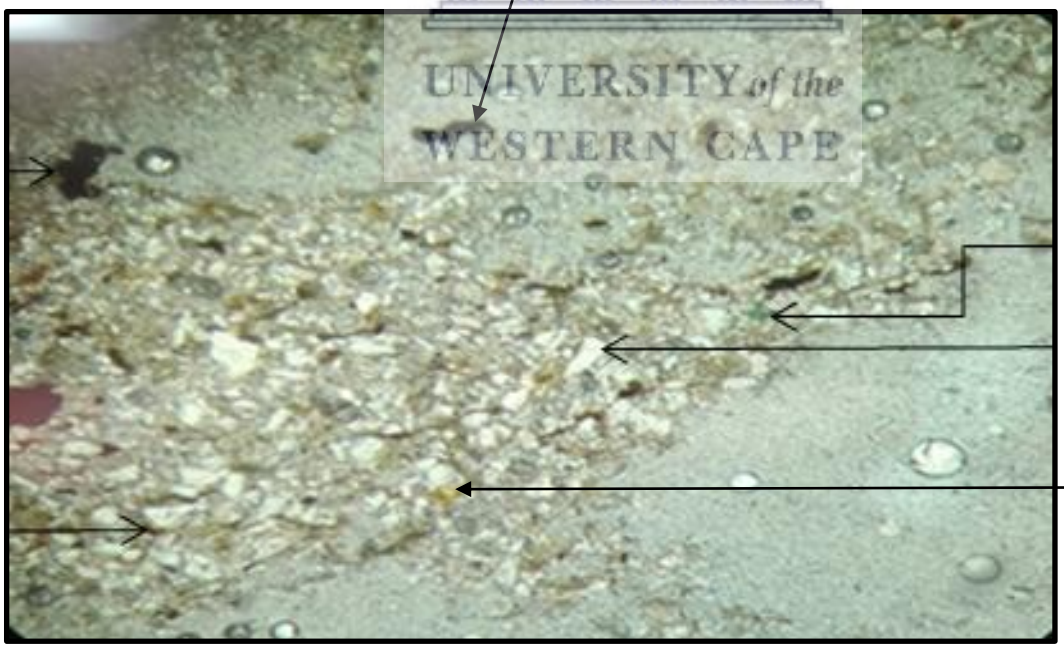

Figure 5-1: XRD result of sample 1 (1178m) indicates the dominance of Quartz, Albite, Kaolinite and Muscovite (Figure 5-2). Kaolinite and quartz do co-exist in marine environment while the presence of Albite as seen here, support similar observation

made on the thin section which suggest the presence of a brownish grain identified as Plagioclase.

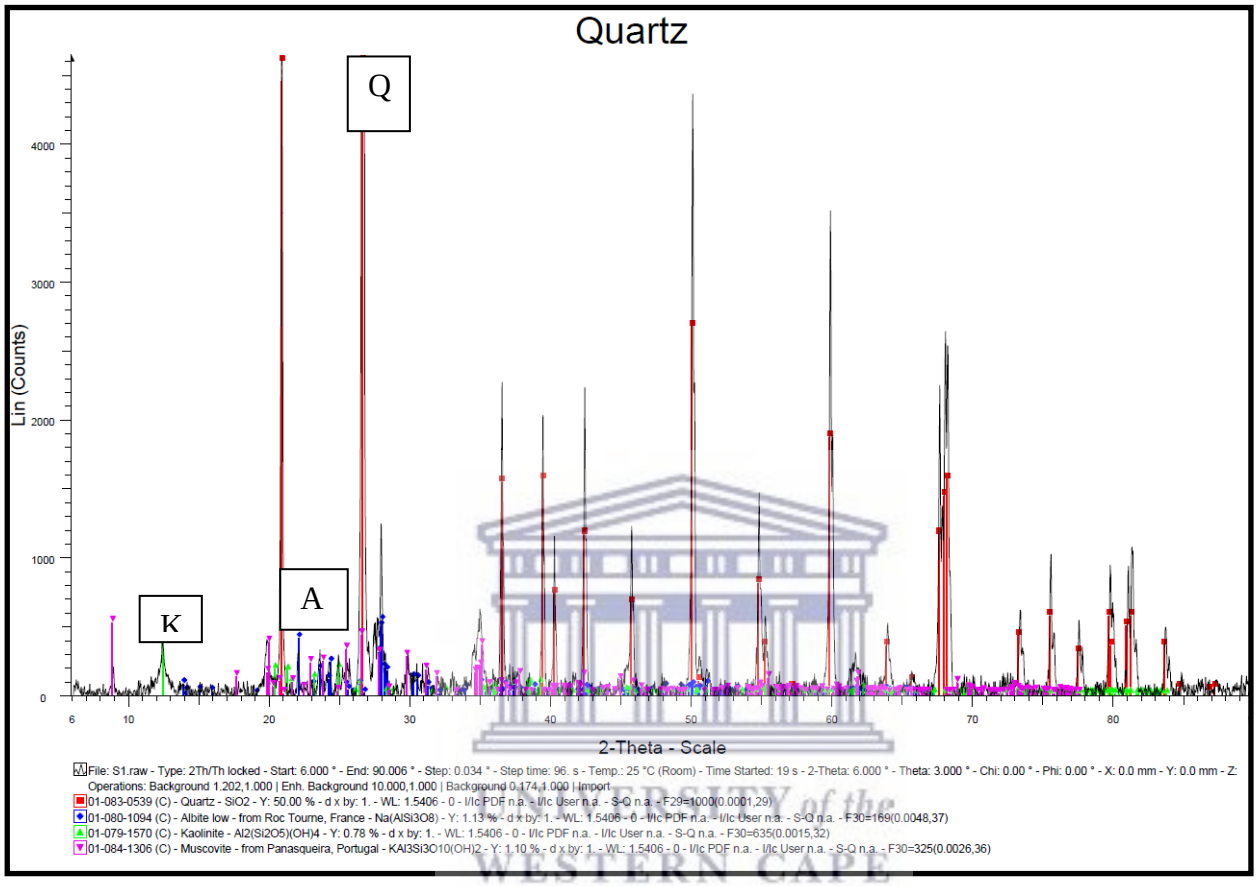

Figure 5-2:K-Kaolinite, Q-Quartz, and A-Albite

Rock sample 1 (Depth: 1178m) shows poorly sorted sandstones with minerals and rock fragments dominantly angular in shape (Figure 5-1).XRD result shows the presence of Kaolinite, Quartz and Albite as the dominant minerals (5-2).

5.1.2 Sample 2 (2322m)

Sample 2 derived from well AF-1 at the depth of 2322m indicate the lithology to be dominantly sandstones. The rock is dominantly light grey with minor brown contents and darker grey, slightly rounded grains. There are also small amounts of carbonate speckles found within the sample. The sample is rich in quartz. The Quartz minerals are the large angular grains found throughout the sample (Figure 5-3). Plagioclase feldspar is also present within the sample as indicated by a darker grey slightly rounded mineral compared to the dominant quartz minerals.

Petrographic description

- Angular to sub-rounded grain shape
- Moderate to poorly sorted grains
- Large Quartz minerals
- Biotite- brownish spots
- Black angular grains
- Poorly consolidated
- Plagioclase feldspar
- Calcite cement forming a rim around a quartz grain,

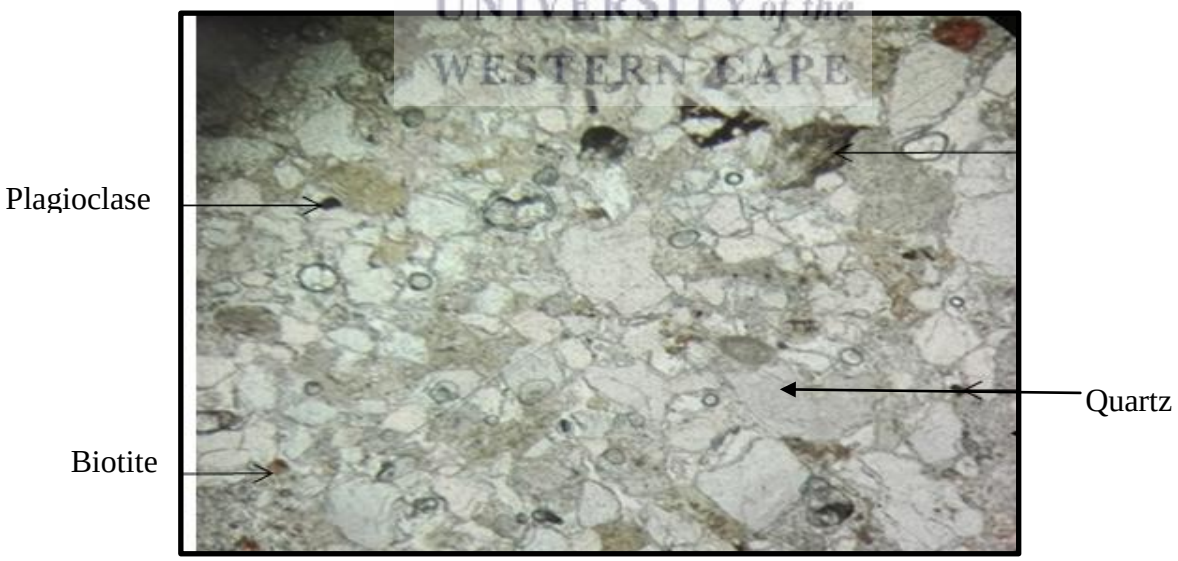

Figure 5-3 Rock sample 2 from depth 2322m (Sandstone formation rock). Rock minerals and grains are closely packed but poorly sorted.

XRD result (Figure 5-4) indicates the presence of Quartz, Muscovite, Kaolinite and Albite. This complements the observation made from the thin section where Muscovite and Biotite were observed (Figure 5-3). This suggests that the rock unit might have been sourced of from mica-rich older rock units. In addition, the presence of Albite suggest that it could have been formed from the Plagioclase feldspar as observed on figure 5-3

Mu-Muscovite, K-Kaolinite, Al-Albite, Q-Quartz

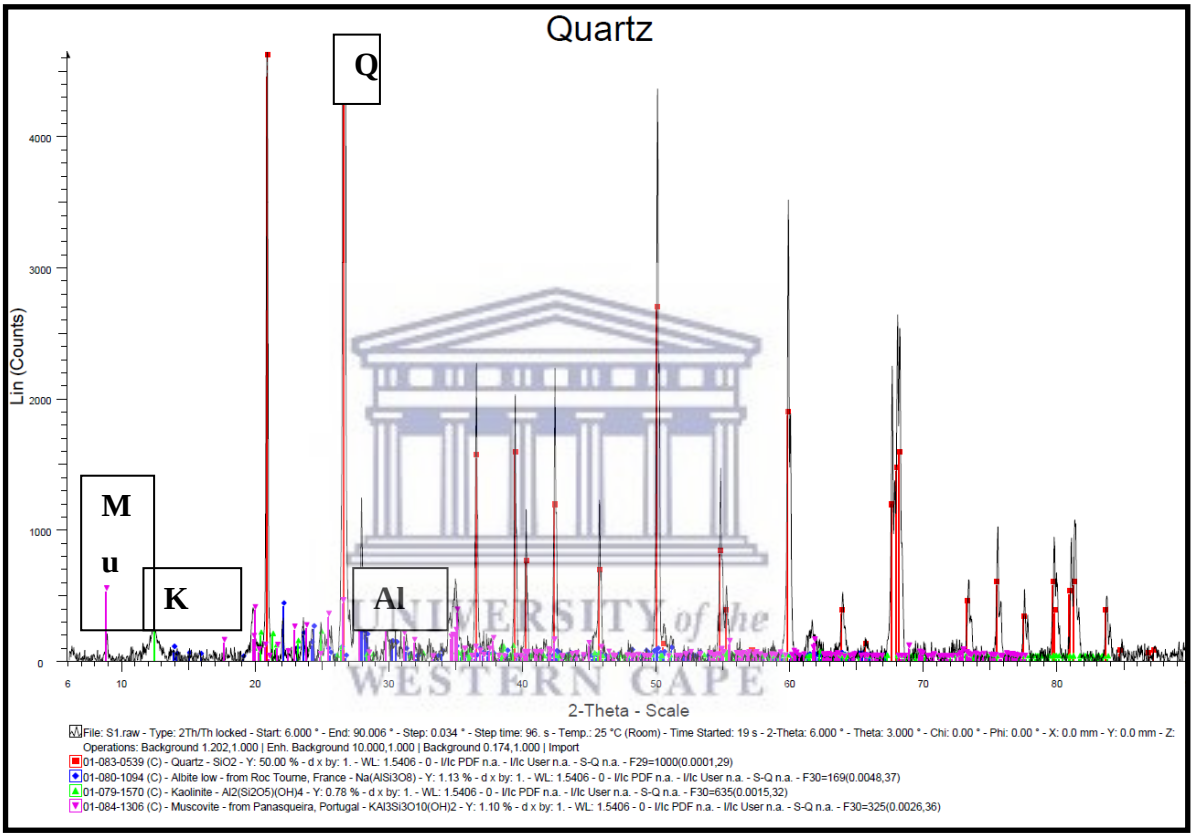

Figure 5-4: XRD result indicates the dominance of Quartz and Kaolinite

5.1.3 Sample 3 (2542m)

Sample 3 was taken from well AF-1 at the depth of 2542m. The sample is dominantly reddish/brown in colour with quartz grains supported by shaly content (Figure 5-5). This sample contains a lot of organic carbonaceous material judging by the presence of dark stained minerals and fragments throughout the sample.

- Mineralogy mostly contains quartz and shaly material.
- Dominantly brownish to red in colour with small white rounded minerals.
- Small black spots which could be carbonate minerals.
- The sample at this depth seems to be well consolidated with closely packed minerals.
- Brownish matrix throughout the sample indicates shaly carboniferous material which acts as the cement supporting the grains within the sample.
- Quartz is cemented by calcite.
- Muscovite- shiny white minerals found throughout the sample.

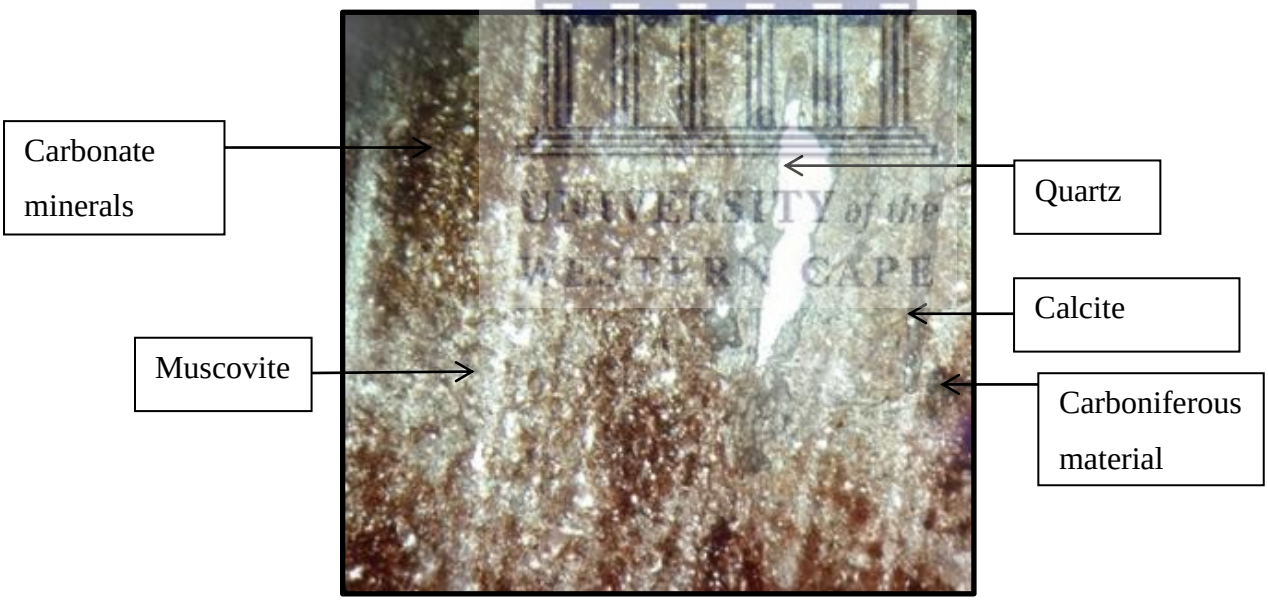

Figure 5-5: Rock sample 3 from depth 2542m (shale formation rock).Thin section shows the dark coloured sample suggestive of high organic content.

The XRD result shows the presence of Muscovite, Quartz, Albite and Haematite. Considering the lithology of the sample to be predominantly marine shale, which is often formed in deeper waters, this explains the presence of Haematite as seen on the XRD. Haematite is renowned

not to form in shallow waters but often formed within the continental shelf to the Abyssal plain and could form under both reducing and oxidizing conditions depending if it exist as an oxide, silicate, carbonate or sulphide facies. Because of the presence of carbonaceous materials (organic materials) as seen from the thin section coupled with the haematite on the XRD (Figure 5-5), it could be inferred that the rock sample was deposited under reducing conditions.

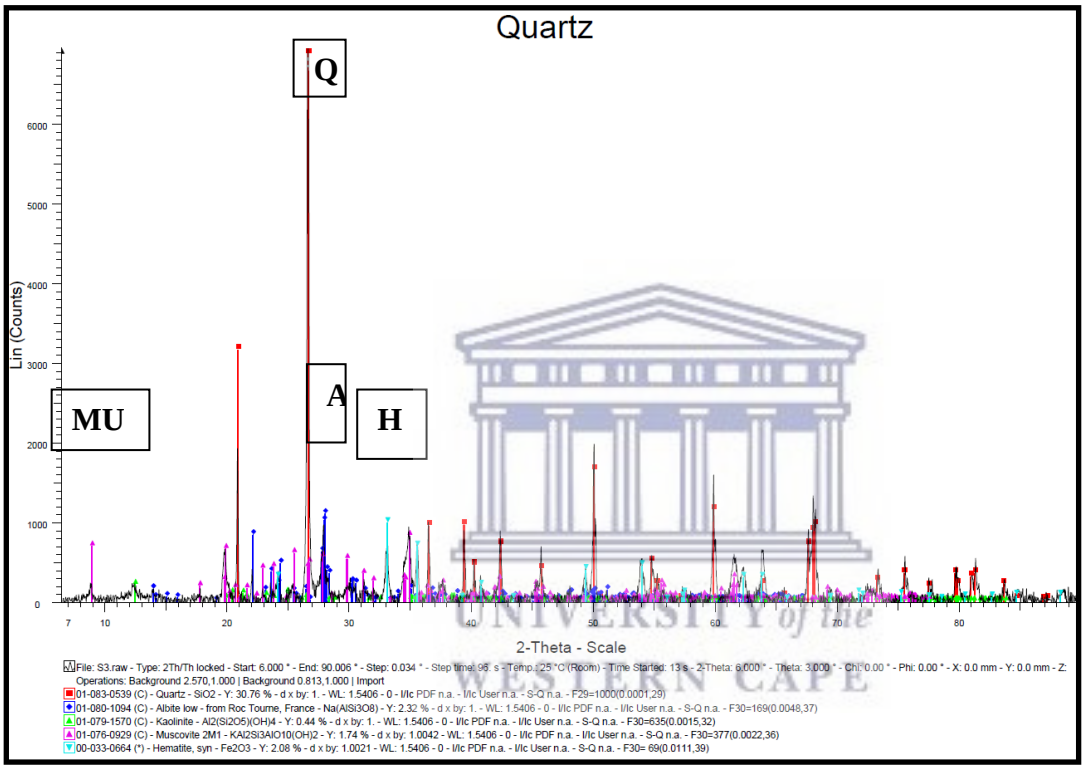

Figure 5-6: Muscovite-MU, Albite-A, Haematite-H, Quartz-Q

XRD shows the presence of dominant rock forming minerals and haematite which suggest the sample was deposited in deeper waters.

5.1.4 Sample 4 (3190m)

Sample 4 is taken from well AF-1 at the depth of 3190m. This sample is very fine grained and shaly in nature. The general colour is dominantly brownish/black with light green/grey minerals which suggest micaceous minerals.

- Mostly angular grains
- Moderate to poorly sorted grain size
- Organic rich clay matrix- cementation in between very angular quartz of moderate grain size.
- Contains angular/sub- rounded shaped, grey minerals suggesting plagioclase feldspar.

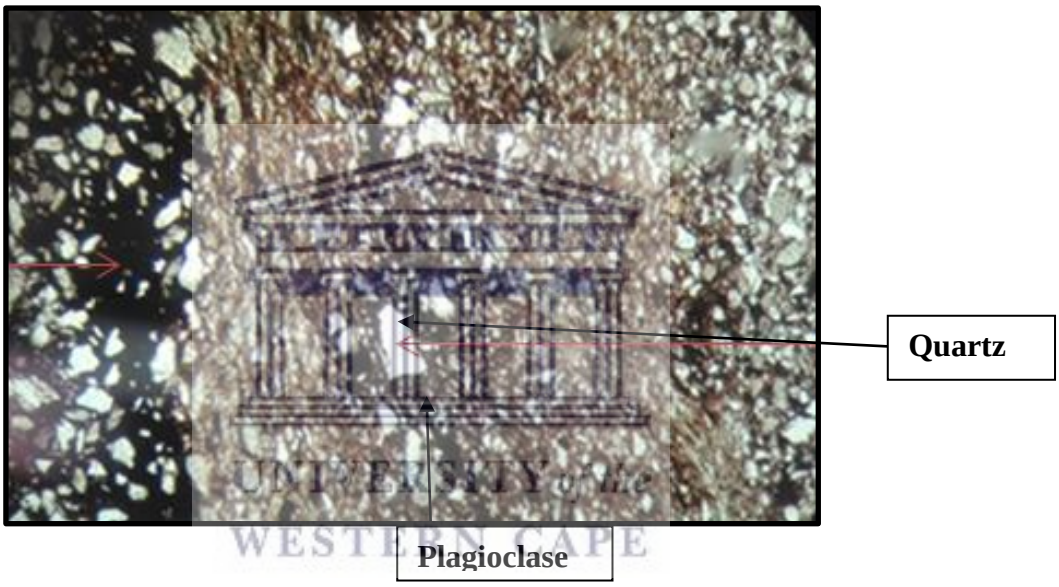

Figure 5-7: Rock sample 4 from depth 3190m .Thin section shows the dark coloured sample suggestive of high organic content.

XRD result indicates the presence of Quartz, Kaolinite, Muscovite, Haematite plus low Albite content. The presence of haematite in this shale sample is consistent with the observation made on the shale sample in figure 5-8. This implies that both samples may have been deposited under the same depositional environment conditions.

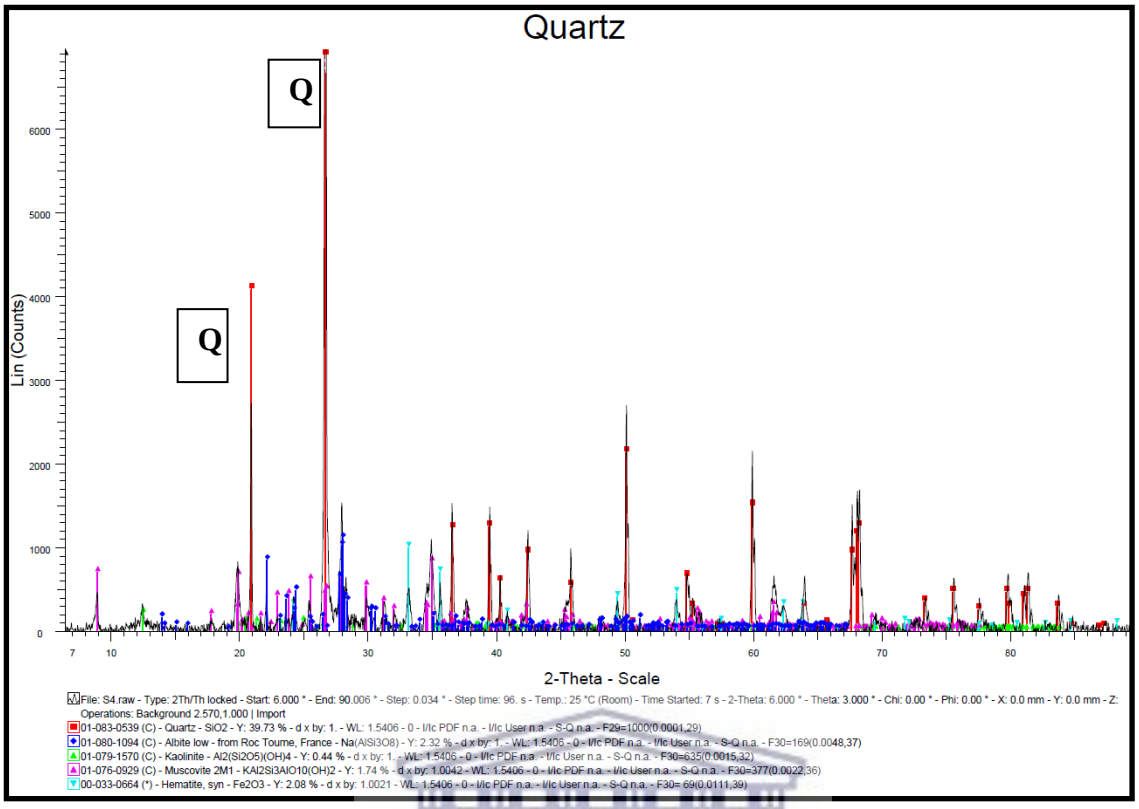

Figure 5-8: Muscovite-MU, Albite-A, Haematite-H, Quartz-QXRD shows the presence of dominant rock forming minerals of Quartz and Albite. The presence of Haematite suggests the sample was deposited in deeper waters.

5.1.5 CO_2 Mineralisation by Diagenetic Minerals.

Likely mineralisation of CO_2 is predicted based on the results obtained above from the XRD and thin section analyses. Muscovite, Kaolinite, Albite and Quartz are minerals identified (Figures 5-3 and 5-4). Study byHangx and Spier 2009, suggested that that sedimentary formation rich in Plagioclase feldspar (Albite) could precipitate Quartz and Dawsonite when reacted with supercritical CO_2. Dawsonite is an alumina-carbonate mineral which commonly serves as a raw material for the ceramics industry. Thedissolution of an aluminosilicate mineral like Kaolinite is expected when CO_2 is injected in to the reservoirs and could trigger an adsorbent systemin which the Kaolinite captures the CO_2 to its surfaces and interlayers; a mechanism of CO_2 storage in clay minerals rich reservoirs. In figures 5-6 and 5-8, Haematite (Fe_2O_3) was identified in the samples, mineralisation of carbon is expected with the presence of Haematite as there is a likely reaction between Haematite and CO_2 which could precipitate Ankerite and Siderite.

5.1.6 Summary of Petrography Interpretations.

Quartz, Plagioclase feldspar (Albite), Biotite and Kaolinite are major minerals identified in all four samples. Each of this mineral has an implication for long term storage of CO_2 with the potential to form secondary cements which could enable trapping of CO_2 to its layers and surfaces.

5.2 Geological modelling (Geostatistical Porosity and Facies Modelling)

To model the porosity and facies, the porosity log and facies log of well AF-1 were upscaled and populated unto the 3D grid using the Sequential Indicator Simulator. This allowed the average weighted scale of each property to be populated on each grid cell.Below are the results of the porosity and facies modelling. Each map represents each zone in a chronological order; from the youngest age to the oldest. In other words, from the Cenozoic- to the Hauterivian age.

5.2.1 Porosity and Facies Model of Zone 1(Cenozoic).

As indicated by figure 5-9 below, the porosity is higher in the north-eastern section of the Cenozoic unit and parts of the south-eastern region. The porosity is relatively lower in the north-western region compared to the Northeast and Southeast region with an approximate average of $0.33m^{3/}\ m^3$. The quantitative porosity estimate in the Northeast is an average of $0.55m^3/m^3$.The facies distribution map indicates sandstones deposit (bright yellow on the map) to be dominant in the south-eastern and north-eastern section (Figure 5-10) while siltstone (light brown on the map) is predominant in the southwestern section of the zone.
The observations above implies that subject to the presence of an effective caprock and good thickness of the sandstones reservoir, the sandstone deposit in the north-eastern section of the Cenozoic zone will be an ideal target for carbon storage.

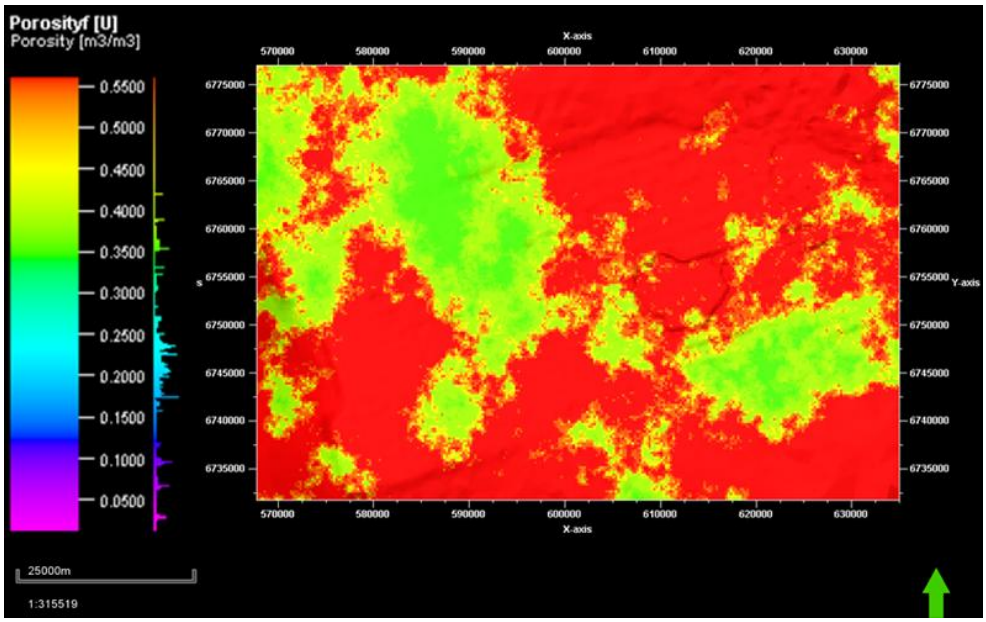

Figure 5-9: The Porosity Map of the Cenozoic Unit, northern Orange Basin. Porosity is higher in the north-eastern section.

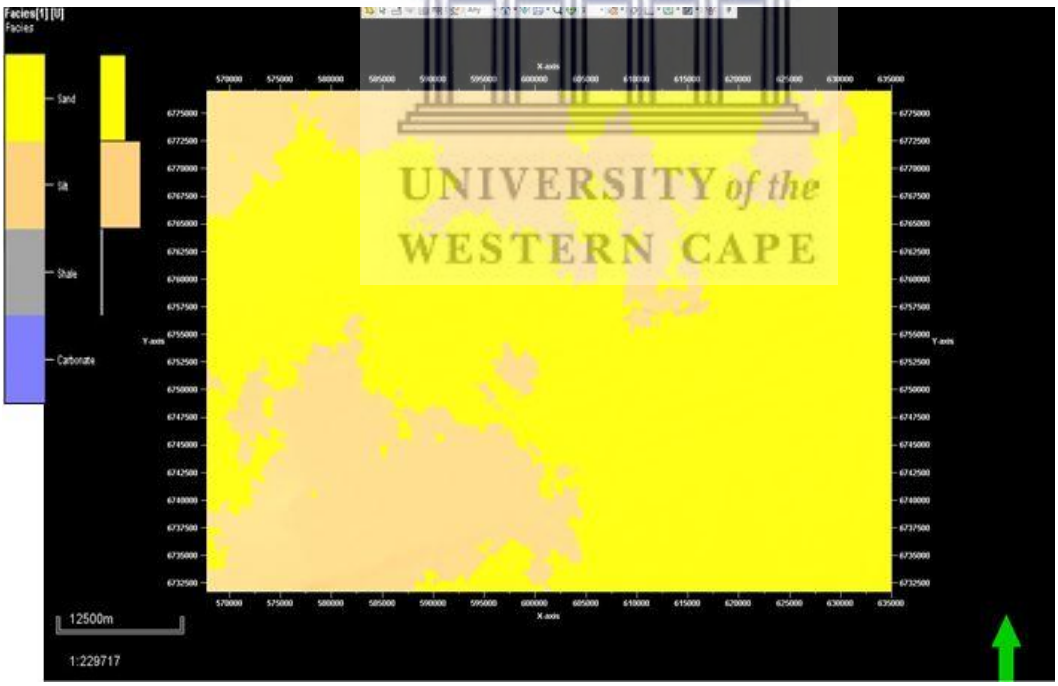

Figure 5-10:The Facies distribution Map for the Cenozoic Unit, northern Orange Basin. Two major lithofacies(Sandstones and Siltstone) are dominant within the Cenozoic unit. Sandstone deposits dominate the Southwestern section of the Cenozoic.(Dark grey-Shale, Yellow-Sandstones, Biege-Siltstone).

5.2.2 Porosity and Facies Model of Zone 2(Maastrichtian).

Figure 5-11 shows the porosity distribution throughout zone 2. The north-eastern, north-western and south-eastern region of this zone indicates porosity values ranging from $0.4m^3/m^3$ to $0.45m^3/m^3$. The central part show porosity values range of 0.3- $0.35m^3/m^3$ .In comparison to other zones, the central and southern section of the map havelower porosity with values range from $0.2m^3/m^3$ to about $0.29m^3/m^3$ and is indicated by the light blue colour. The Facies model distribution map of this zone indicates sandstone to be the main sedimentary deposit in the eastern and western portion of the zone. In the central and Northwest of zone 2, siltstone deposits are dominant.

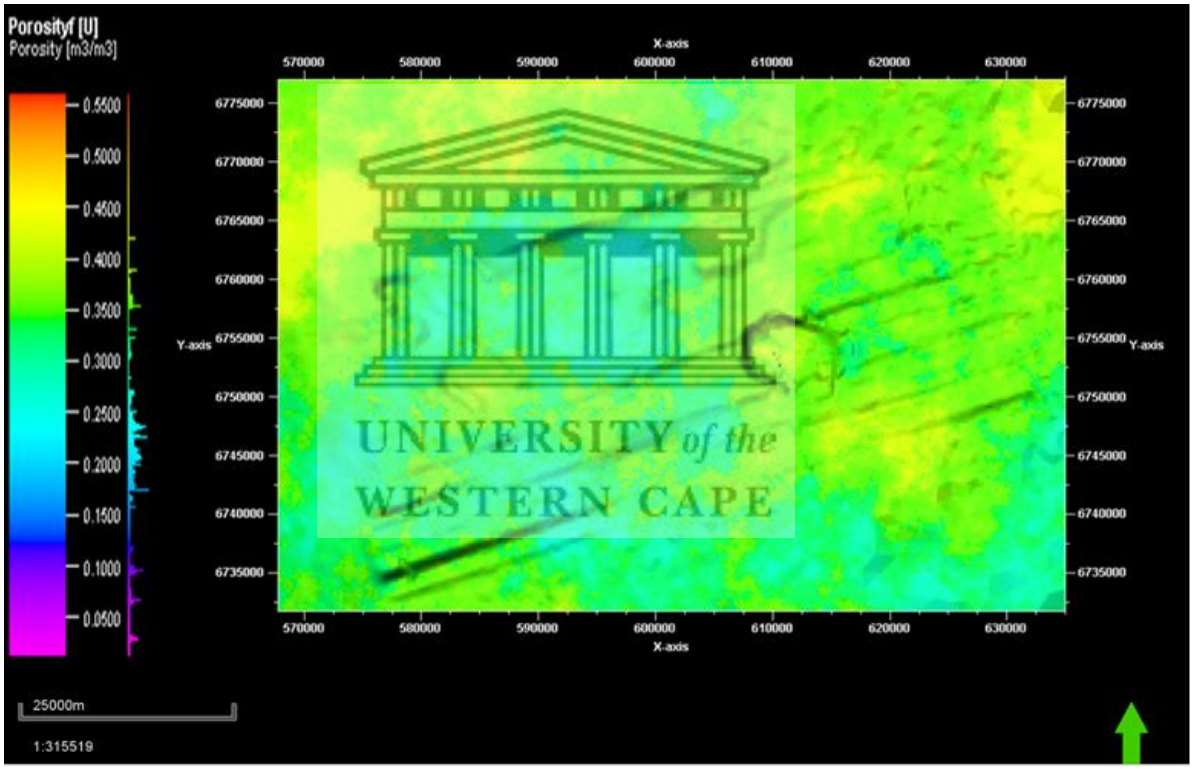

Figure 5-11: Porosity map for the Maastrichtian age sedimentary Deposits.Porosity is slightly higher in the North-eastern and North-western section of the Maastrichtian unit.

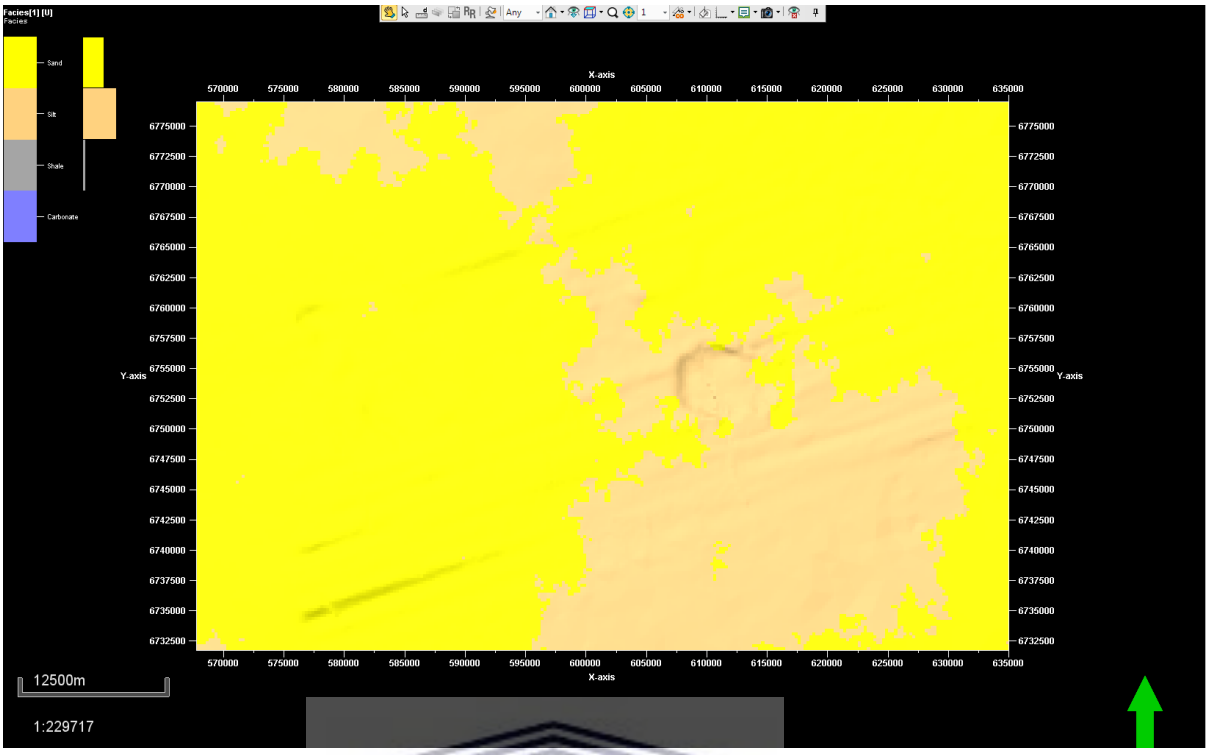

Figure 5-12: Facies distribution map for the Maastrichtian age sedimentary deposits. Sandstone deposit dominates the North-eastern section. Siltstone is dominant in the south-eastern section of the Maastrichtian unit. (Dark grey-Shale, Yellow-Sandstones, Biege-Siltstone).

5.2.3 Porosity and Facies Model of Zone 3(Turonian age)

The dominantporosity values for this age range between 0.18m^3/m^3 to 0.28m^3/m^3 except for the North eastern position where a slight increase in porosity ranging from 0.31m^3/m^3 to 0.35m^3/m^3 was observed (Figure 5-13). There is a slight decrease in porosity in the western section and far South-west indicated in a slightly darker blue colour showing a porosity value of 0.12m^3/m^3. This depositional history displayed by the facies model indicates more siltstone deposits than sandstone (Figure 5-14). The northern area of the zone as well as the southern area consists mostly of siltstone deposits indicated by the beige colour. More centralised following from west to east and the north-eastern sectionlies deposits of sandstones.

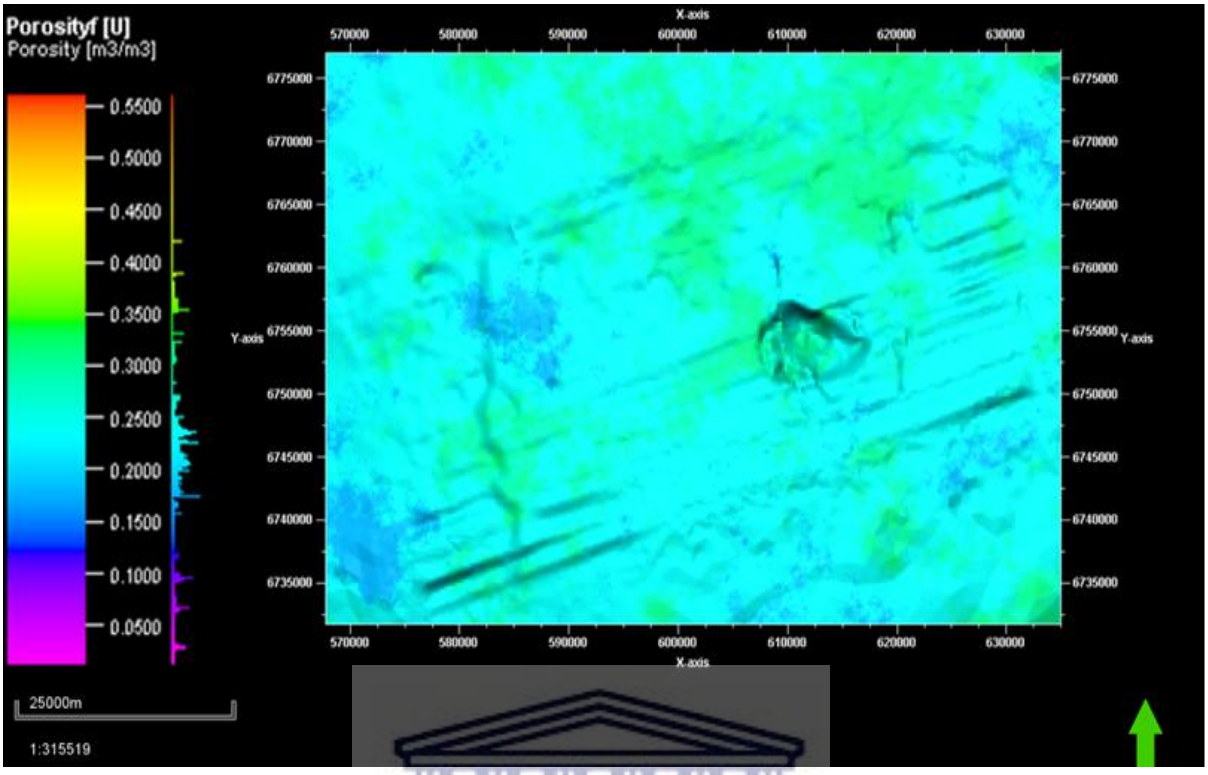

Figure 5-13: Porosity map for the Turonian age sedimentary Deposits. Porosity is within a uniform range but slightly higher in the Northcentral section of the Turonian unit.

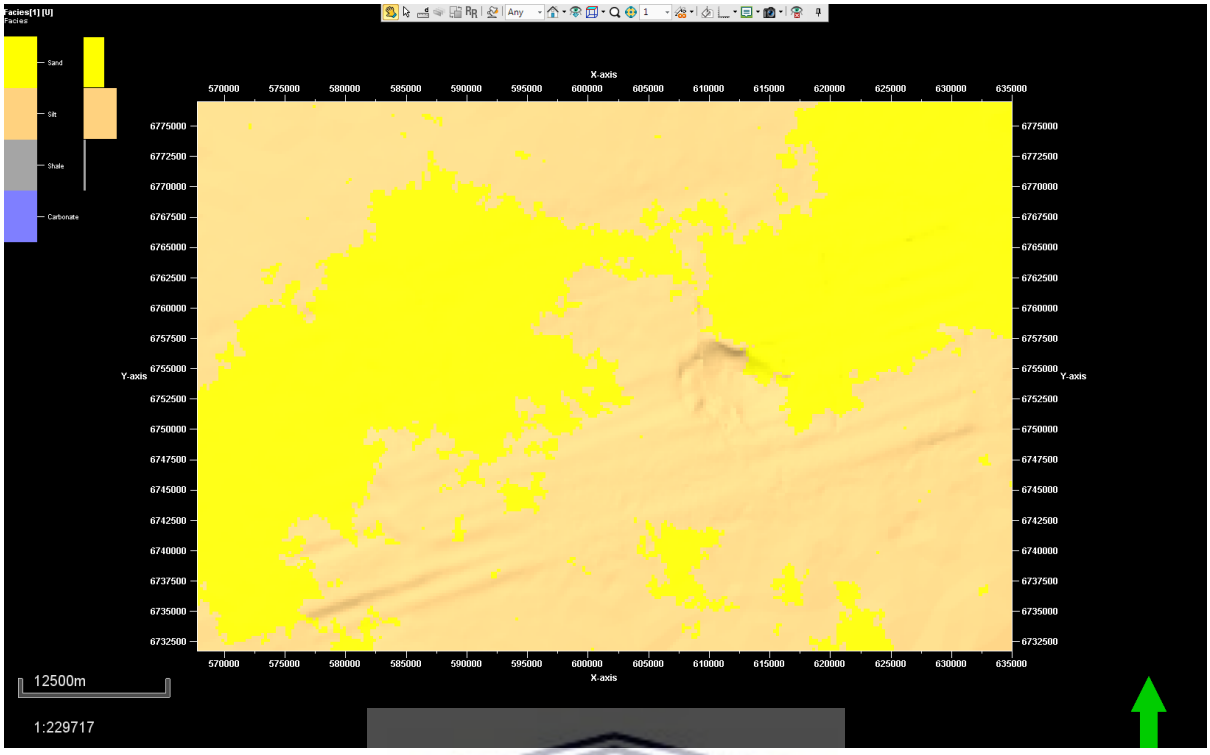

Figure 5-14: Facies distribution map for the Turonian age sedimentary deposits. Siltstone deposits dominate the Turonian unit. Sandstone is more localised to the Northeast and the Southwest. (Dark grey-Shale, Yellow-Sandstones, Biege-Siltstone).

5.2.4 Porosity and Facies Model of Zone 4(Cenomanian age)

This zone shows the western section and a small section in the eastern zone have porosity values range of $0.12m^3/m^3$ to $0.15m^3/m^3$(Figure 5-15). The North eastern and South eastern section show higher porosity values ranging from $0.18m^3/m^3$ to $0.26\ m^3/m^3$. The facies distribution in this zone is dominated siltstone deposits while the eastern and a part of the South East havedeposits of Sandstones(Figure 5-16).

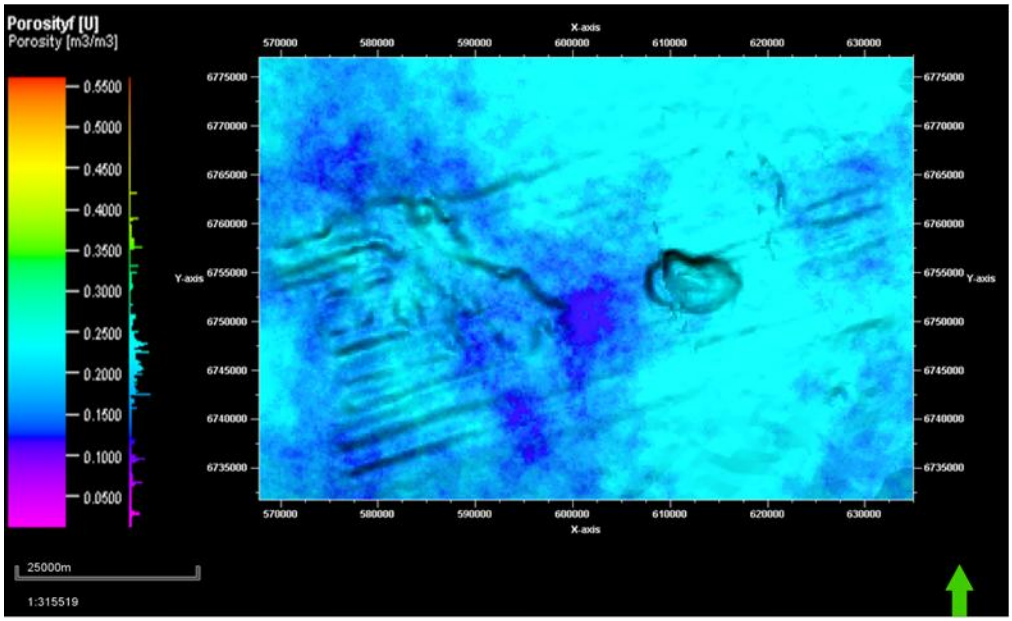

Figure 5-15: Porosity map for the Cenomanian age sedimentary Deposits. Porosity is within a uniform range but slightly higher in the North central section of the Cenomanian unit.

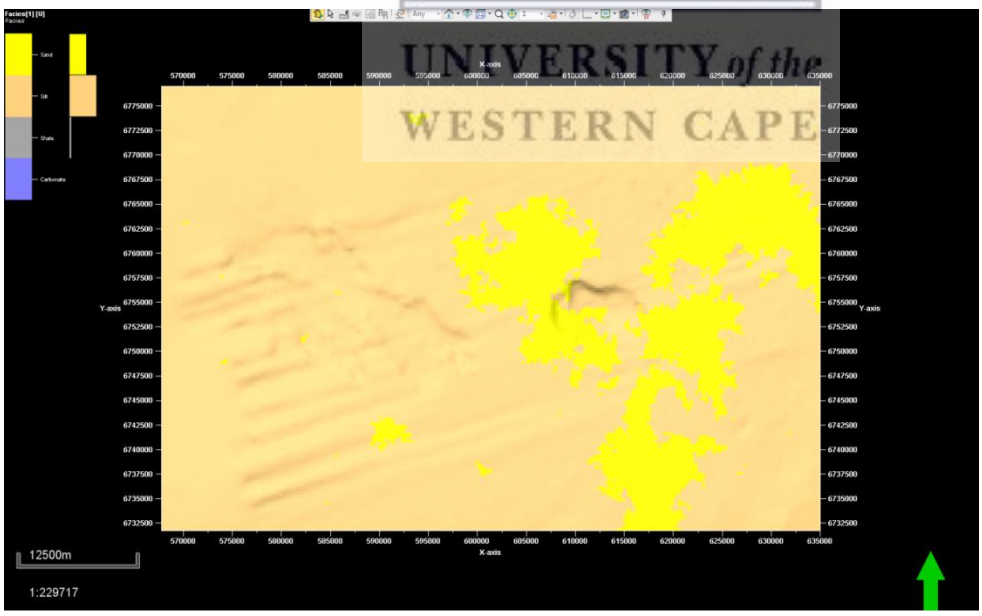

Figure 5-16: Facies distribution map for the Cenomanian age sedimentary deposits. Siltstone deposits dominate the entire unit but with localised sandstone deposit in the Northeast and the Southwest. (Dark grey-Shale, Yellow-Sandstones, Biege-Siltstone).

5.2.5 Porosity and Facies Model of Zone 5(Late Albian age).

Porosity distribution in this zone displays values within the range of 0.16 m^3/m^3 to 0.27m^3/m^3. A minor part of the Northeast, Northwest and Southeast of zone 5 does show a slight decrease in porosity, indicated by the darker blue colour with values range from 0.13 m^3/m^3 to 0.14 m^3/m^3 (Figure 5-17). The facies distribution model in this zone shows siltstone deposits to be dominant except in the North West and Southeast where some sandstone deposits are found (5-18).

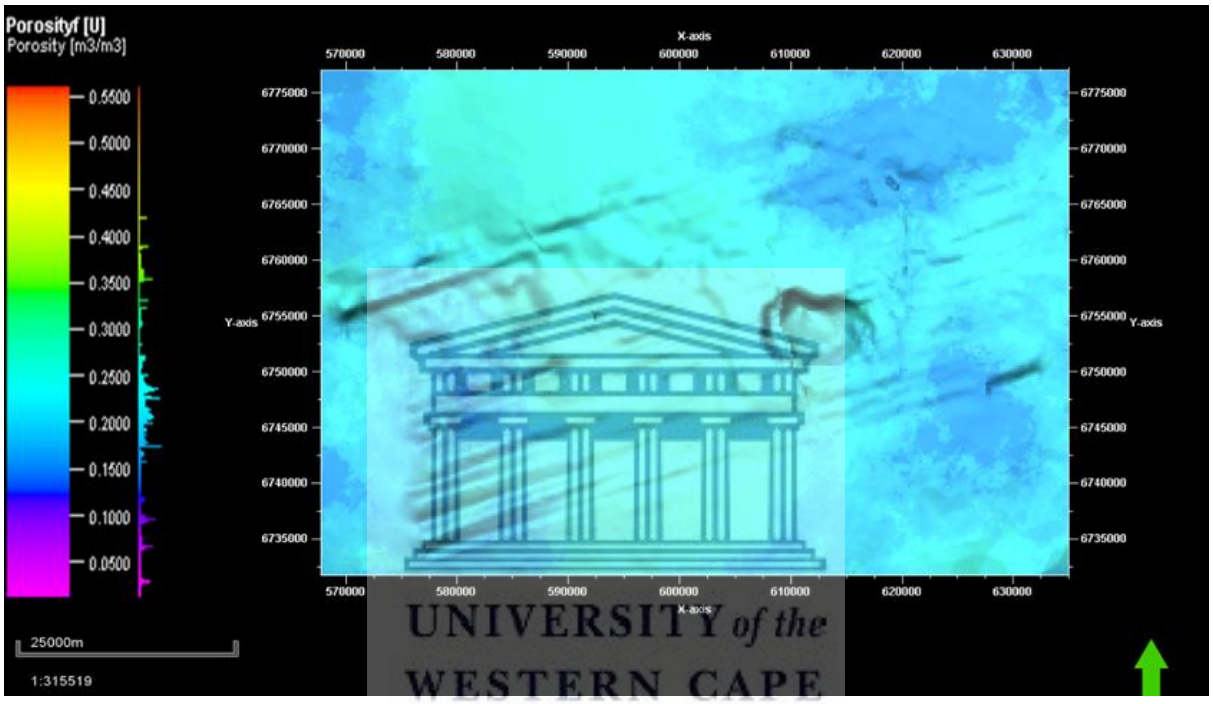

Figure 5-17: Porosity map for the Late Albian age sedimentary Deposits. Porosity is within a uniform range but slightly lower in the North-eastern section of the Late Albian unit.

Figure 5-18: Facies distribution map for the Late Albian age sedimentary deposits. Siltstone deposits dominate the entire unit except for the Southeast section dominated by Sandstones deposit. (Dark grey-Shale, Yellow-Sandstones, Biege-Siltstone).

5.2.6 Porosity and Facies Model of Zone 6(Albian age).

The porosity distribution in this zone ranges from 0.17 m^3/m^3 to 0.26 m^3/m^3 except for the North West and South East section which shows slightly lower porosity values (Figure 5-19). The lower values as indicated on the map ranges between 0.14 m^3/m^3 to 0.15 m3/m3.The facies distribution indicates dominance of siltstones within the unit. There are deposits of sandstone also within the zone, but localised tothe North West section (Figure 5-20).

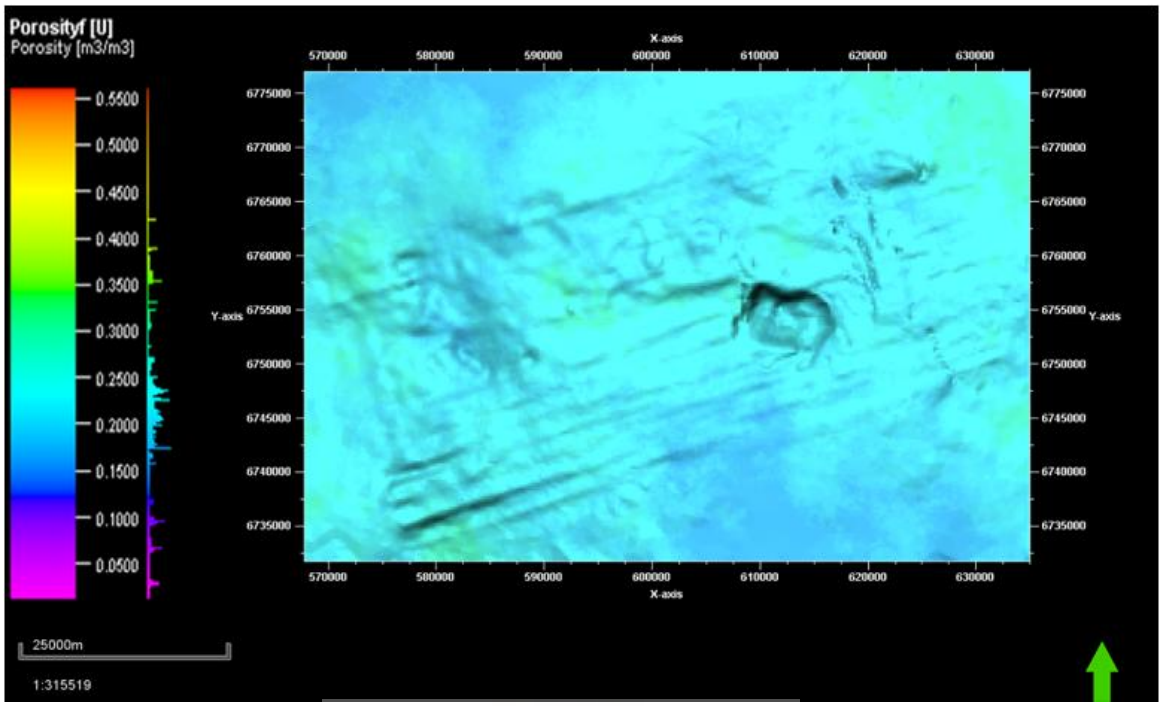

Figure 5-19: Porosity map for the Albian age sedimentary deposits. Porosity is within a uniform range but slightly lower in the North-eastern section of the Albian unit.

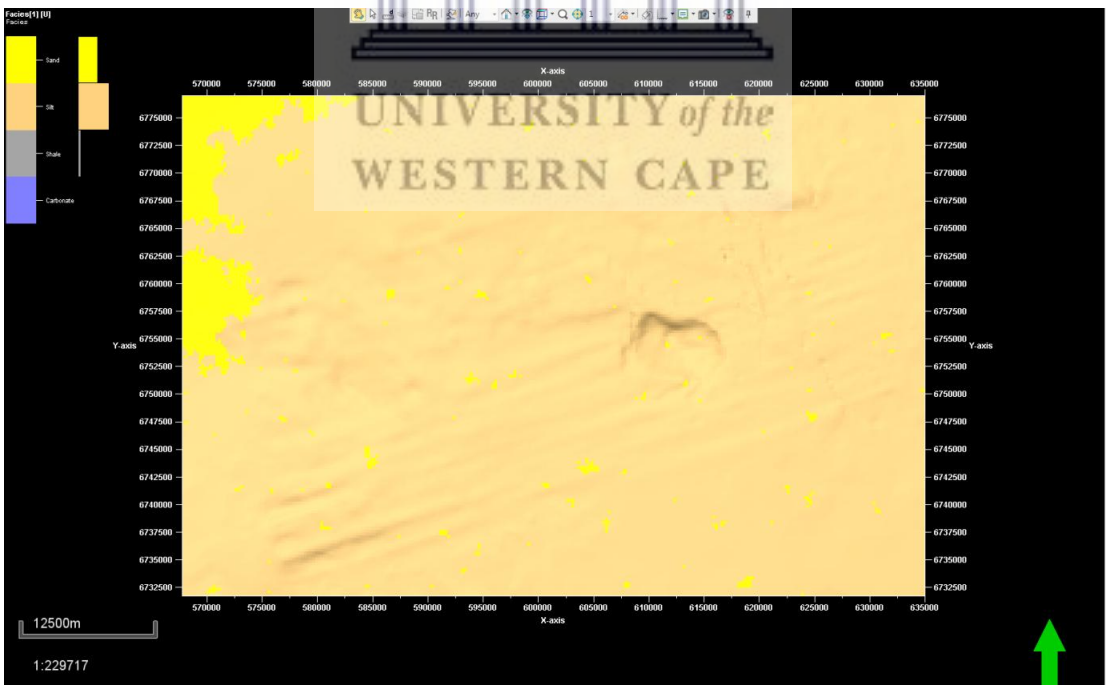

Figure 5-20: Facies distribution map for the Albian- age sedimentary deposits. Siltstone deposits dominate the entire unit except for the Northwest section with localised Sandstones deposit. (Dark grey-Shale, Yellow-Sandstones, Biege-Siltstone).

5.2.7 Porosity and Facies Model of Zone 7(Aptian age).

Zone 7, compared to other zones shows a significant decrease in porosity as shown on the map, specifically, in the southern section, west and north eastern section. The dominant porosity values range from $0.15m^3/m^3$ to about $0.2\ m^3/m^3$. However, there is random distribution of porosity values in the range of $0.05m^3$ to $0.1m^3$ around the South central section of the unit (Figure 5-21).Shale deposits are evident by the dark- grey sections found on the facies model map. Specifically, in the Northwest region as well as in the Southeast and Southwest section. In the western section, sandstone deposits are found in minimal amounts as seen in the North east and southern region of the facies map (Figure 5-22). The eastern region and a section of the south west region of the map are dominated by siltstone deposits. This zone could be a potential trapping mechanism for carbon sequestration due to the majority of the sediments being finer grained.

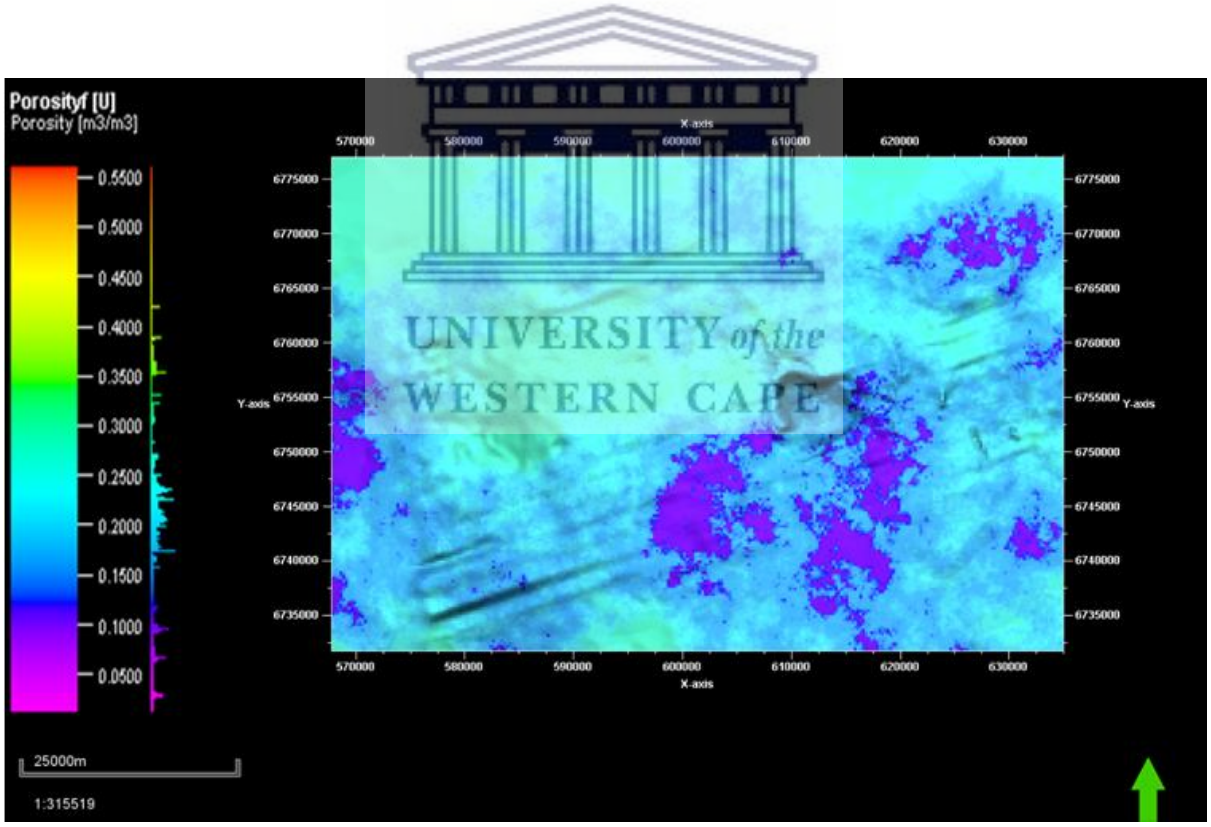

Figure 5-21: Porosity map for the Aptian- age sedimentary deposits. Porosity is within a uniform range but slightly lower in the Southeastern section of the Aptian unit.

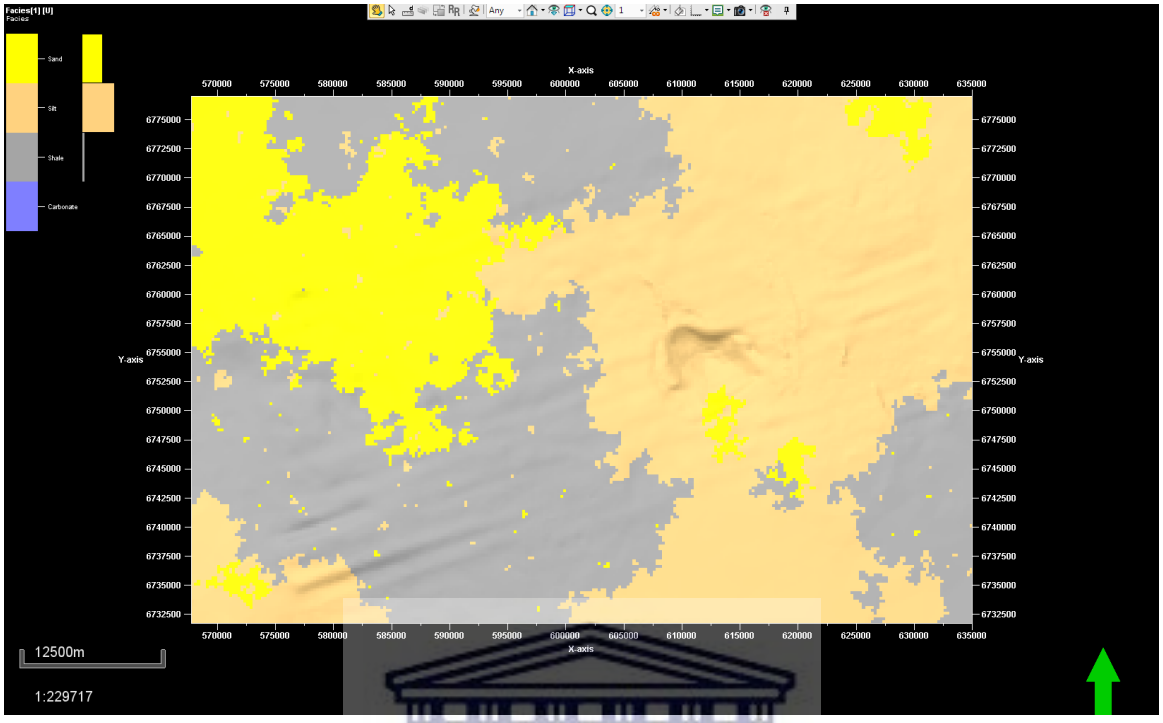

Figure 5-22: Facies distribution map for the Aptian- age sedimentary deposits. Siltstone deposits dominate the Northeastern section of the. Shale deposits dominate the Southwest and the northern section. (Dark grey-Shale, Yellow-Sandstones, Biege-Siltstone).

5.2.8 Porosity and Facies Model of Zone 8(Barremianage).

The map displays low porosity values across the entire zone. These values range from 0.08 m^3/m^3 to 0.10 m^3/m^3 as shown on the map. In the North central section, the porosity values slightly increase to a range between 0.13m^3/m^3 to0.15 m^3/m^3(Figure 5-23). The facies distribution map indicates siltstone is dominant within theunit except for the South eastern and South central section, where sandstones deposit is prominent (Figure 5-24).

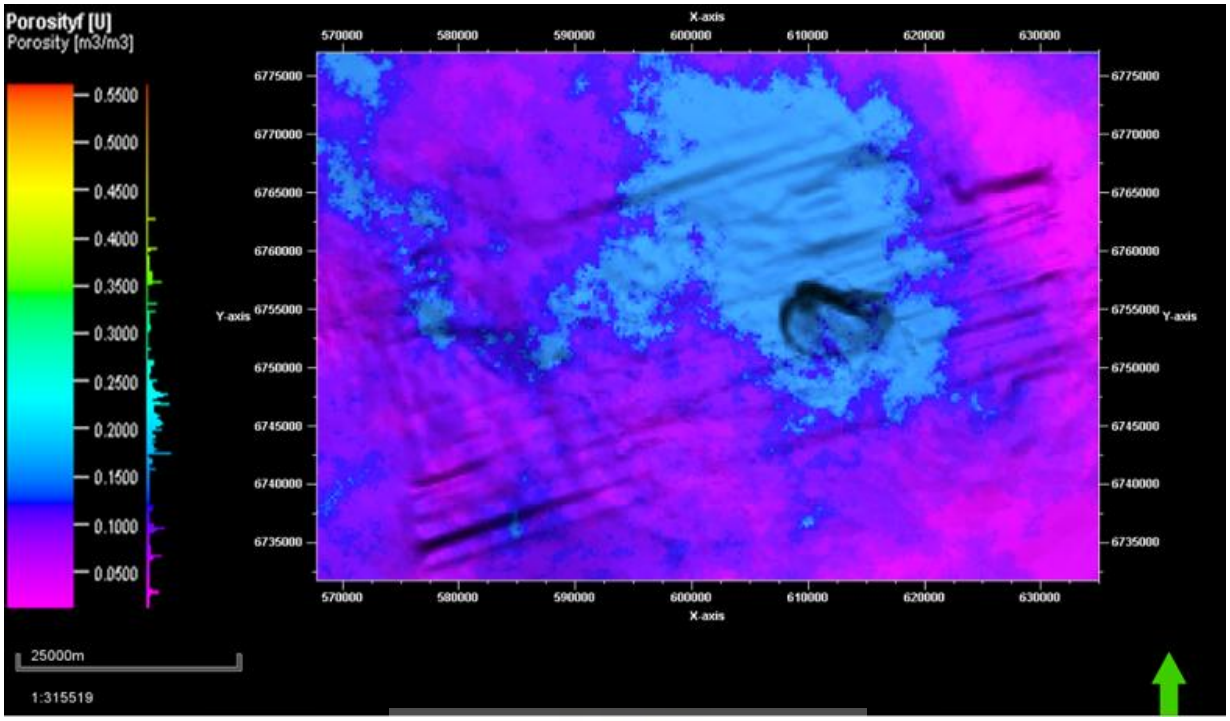

Figure 5-23: Porosity map for the Barremian - age sedimentary deposits. Porosity is within a uniform range but slightly higher in the North central section of the Barremian unit

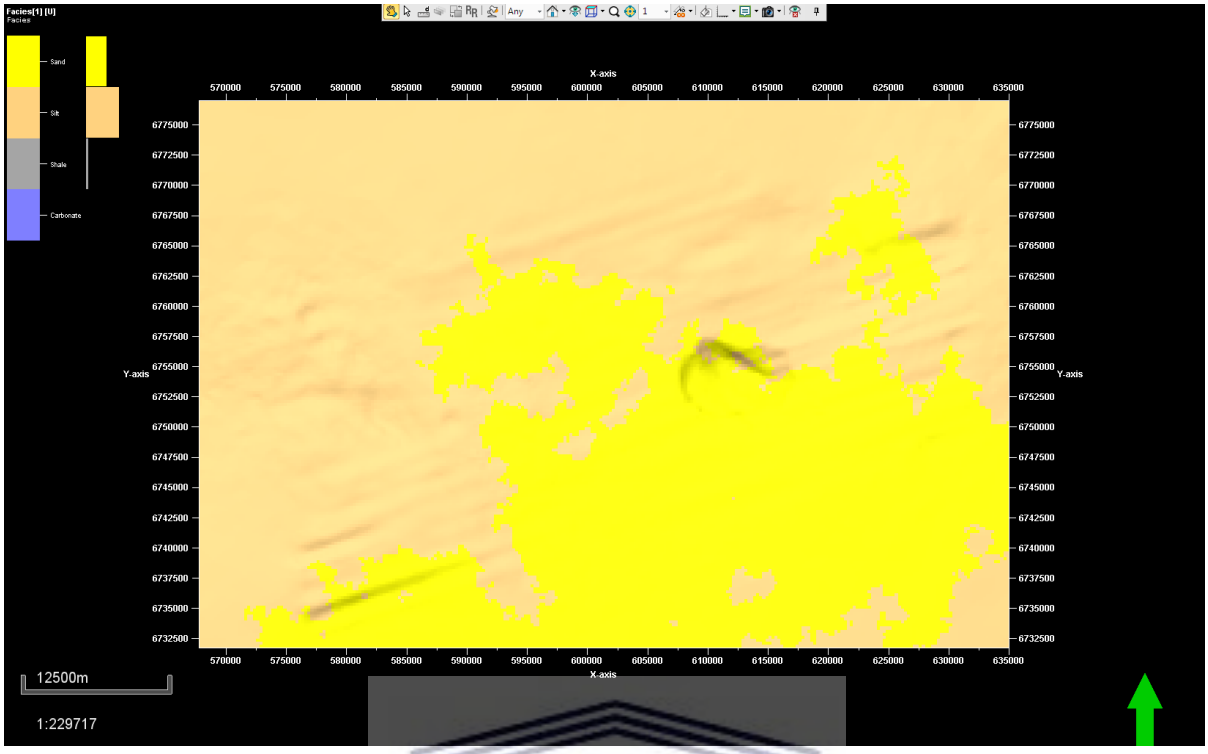

Figure 5-24: Facies distribution map for the Barremian- age sedimentary deposits. Siltstone deposits dominate the Southeastern section of the unit. (Dark grey-Shale, Yellow-Sandstones, Biege-Siltstone).

5.2.9 Porosity and Facies Model of Zone 9 (Hauterivianage).

Zone 9 map indicates a low porosity distribution throughout the unit with values ranging between 0.05 m^3/m^3 to 0.07 m^3/m^3as shown on the map (Figure 5-25). In a part of south east and south west, there are increased porosity values ranges of 0.14 m^3/m^3 to0.16 m^3/m^3. The facies distribution map indicates sedimentary deposits of sandstone, siltstone and shale. Siltstones deposits are more prominent while the sandstone deposits are localized to the north east, south east and western region of the unit(Figure 5-26). There are randomly localised deposits of shale within the unit.

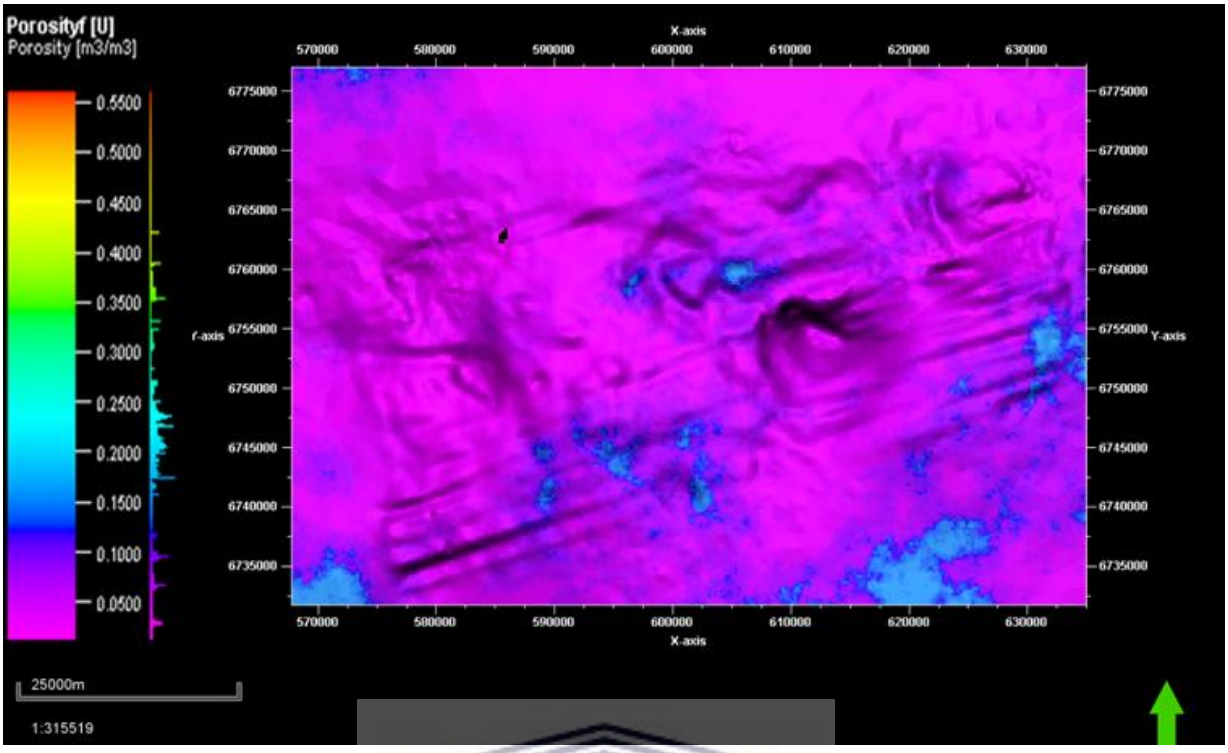

Figure 5-25: Porosity map for the Hauterivian - age sedimentary deposits. Porosity is within a uniform range but slightly higher in the Southwestern section of the Hauterivian unit.

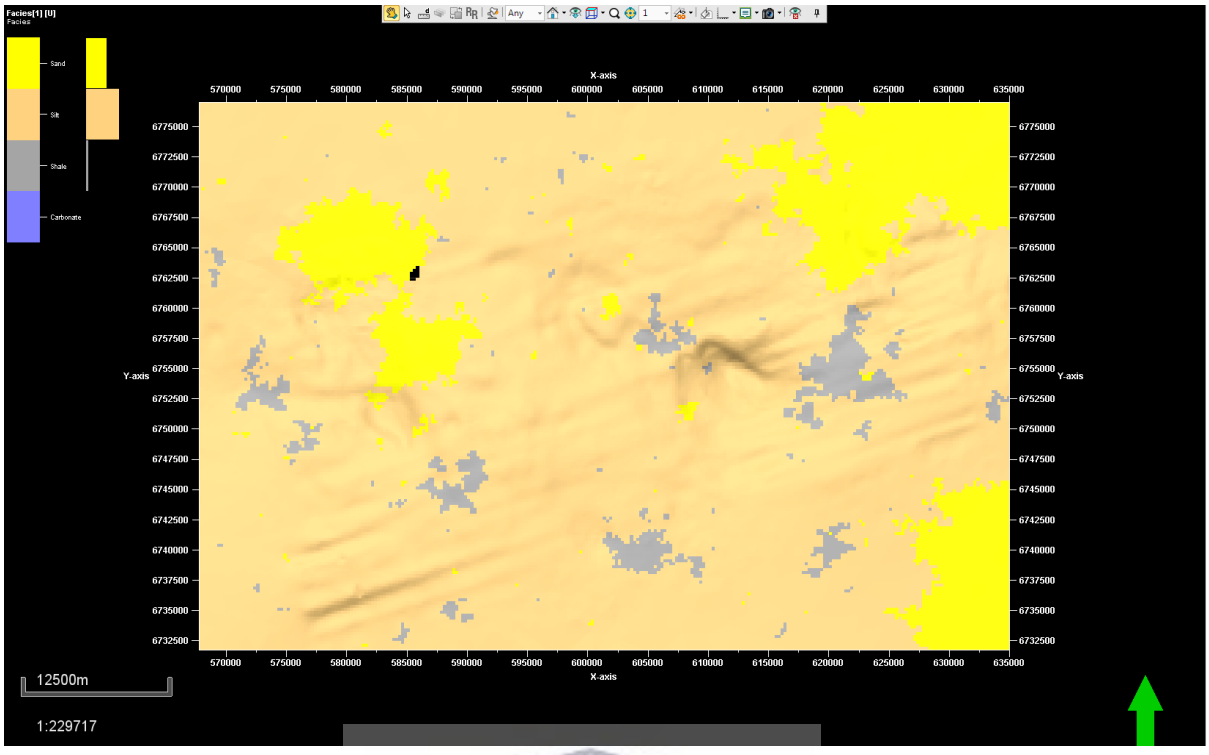

Figure 5-26: Facies distribution map for the Hauterivian- age sedimentary deposits. The shale is randomly deposited within the entire unit.(Dark grey-Shale, Yellow-Sandstones, Biege-Siltstone).

5.2.10 Summary of Geological Modelling Results

The facies modelling results revealed the dominance of Siltstones and Sandstones deposit as the main rock units across all ages. Sandstones deposit is extensive and prominent within the Cenozoic and Mastrichtian, while the Barremian Sandstones unit is identified as having the best potential for CO_2 storage considering that it is bounded at the top by the Aptian shale and below by the HauterivianSilstone and Shale unit. The porosity model result trend is expected to reduce with depth (from younger rock unit-older rock unit) because of post-deposition compaction and cementation mechanism as subsidence increases. However, within the Cenomanian unit, the porosity in the western section reduces drastically. This could indicate that the lithology (Silstone) in the western section is well consolidated as a result of severe cementation.

5.3 Carbon Injection Results

The relevance of carbon injection in this study is to assess the storage capacity of the samples taken at the laboratory scale.Samples1, 2, 3 and 4 were milled into powdery form in order to make it fit into the machine. The preparation of samples for carbon injection involved placing each sample into the carbon injection machine and subdued it to heating to 200 degrees Celsius for 120 minutes. This removes all water vapour and gases found within the pore spaces of the samples. Consequently, Nitrogen was forced into the empty pore spaces. Subsequently, the samples were allowed to cool from 200 degrees to 40 degrees. Subsequently the CO_2 was forced into the samples at a steady temperature of 40 degrees Celsius for 60 minutes. This process is called absorption.

The next process was the extraction of CO_2 from the pore spaces. This was done by extracting CO_2 from the pore spaces by heating the CO_2 saturated samples to a temperature of 200 degrees Celsius. This process is called desorption, and the amount of CO_2 desorbed can be used to estimate the storage capacity of the samples once the size of the bulk rock volume is known. The four samples analysed are discussed below.

5.3.1 Sample 1(1178m)

Sample 1 was tested for absorption and desorption capacity to evaluate the potential storage capacity. The absorption capacity is the rate at which the surface area' including Nano pores of the sample is saturated withCO_2, while desorption capacity indicate the amount of CO_2 that could take out of the saturated sample. The graph shows desorption capacity Delta Y; to be 0.852% (Figure 5-27). This indicates very low storage capacity for the sample, which could be due to the influence of diagenetic minerals which limits the permeation of CO_2 into the pore spaces.

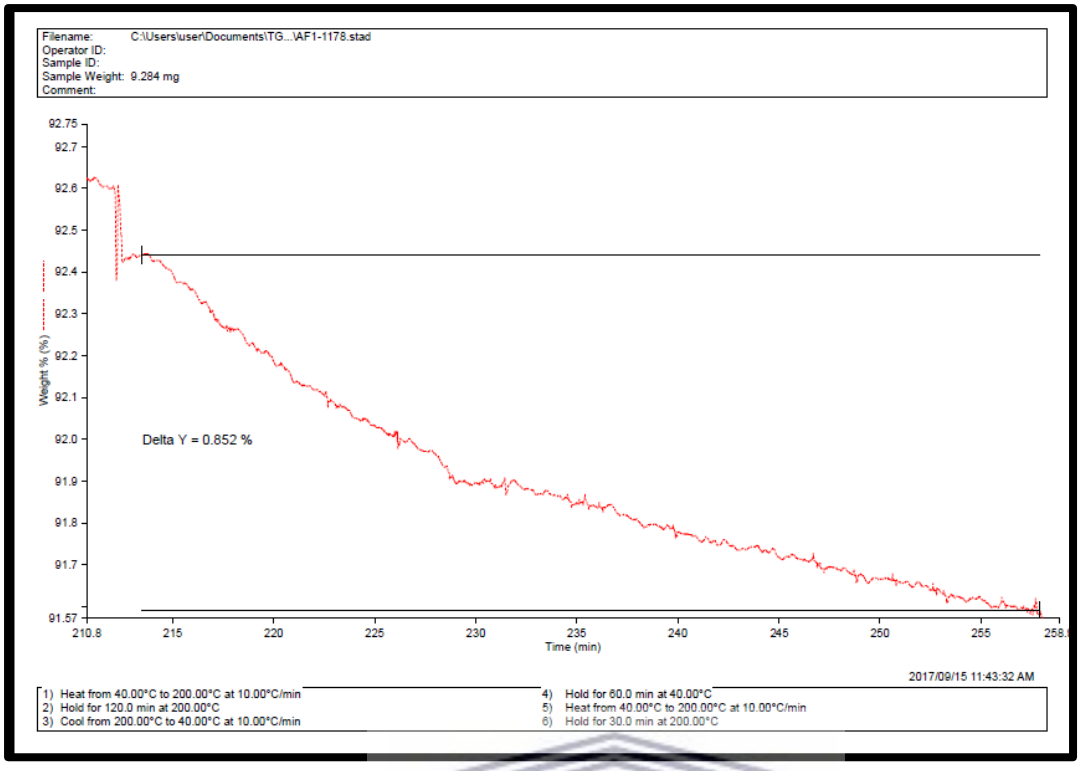

Figure 5-27: Desorption and Storage Capacity Test for sample1. The desorption Capacity is low considering a significant low value of 0.852%.

5.3.2 Sample 2 (2322m)

Sample 2 showed storage capacity value of 5.56% judging from the desorption test (Figure 5-28). This means the sample has sufficient Nano-pores with capacity to store significant CO_2 volume compared to sample1.

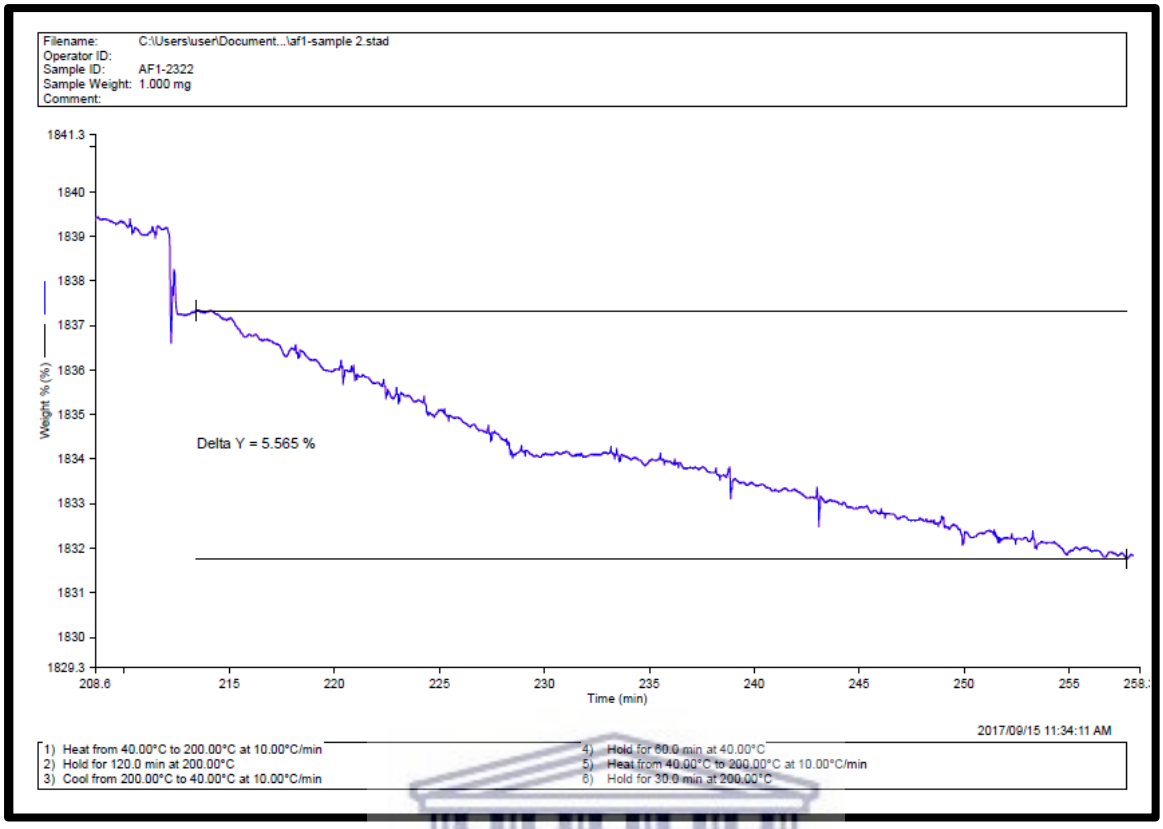

Figure 5-28: Desorption and Storage Capacity Test for sample 2. The desorption capacity is high at a value of 5.565%.

5.3.3 Sample 3(2542m)

Sample 3 shows storage capacity value of 5.91% judging from the desorption test performed on the sample(Figure 5-29). This means the sample has sufficient Nano pores spaces with capacity to store significant CO_2 volume compared to sample2.

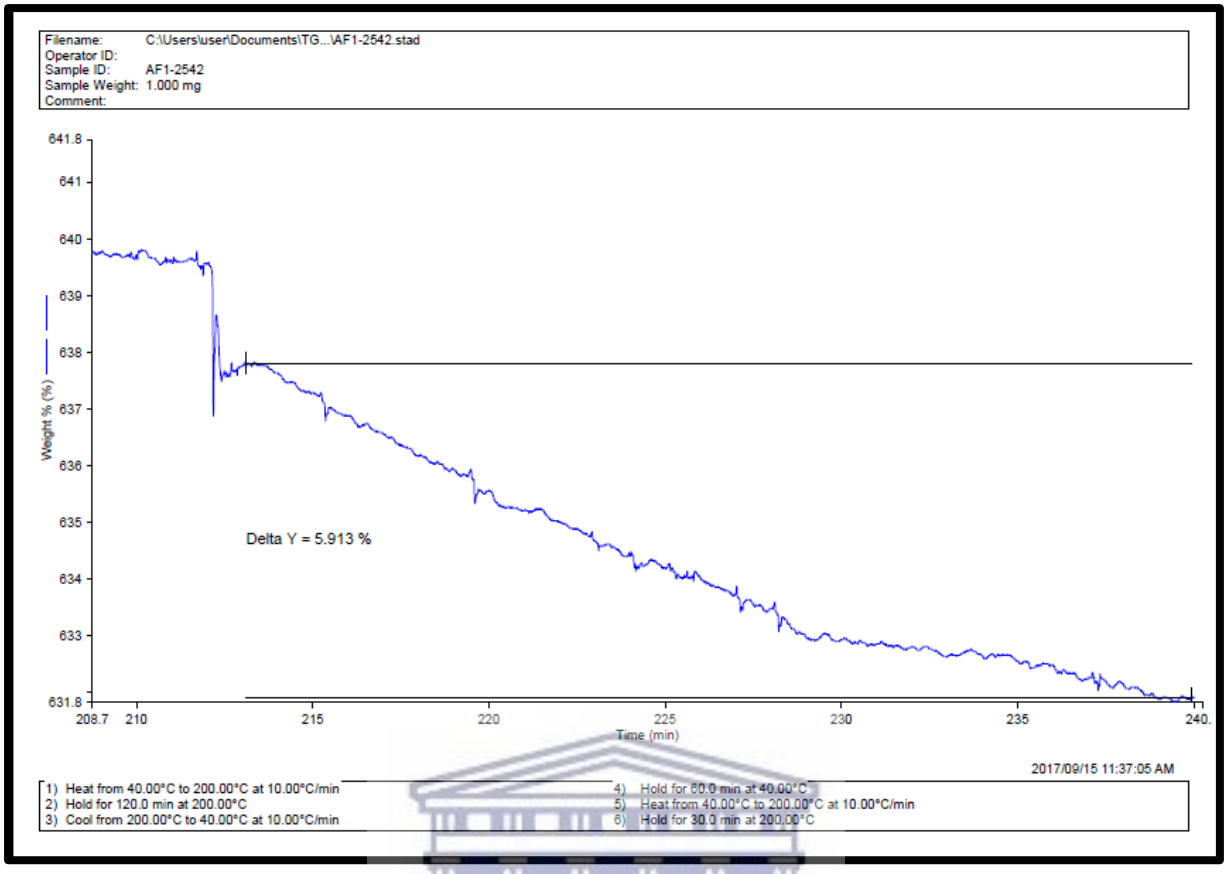

Figure 5-29: Desorption and Storage Capacity Test for sample 3. The desorption capacity is high at a valueof 5.913%.

5.3.4 Sample 4 (3190m)

Sample 4 shows storage capacity value of 5.06% judging from the desorption test (Figure 5-30). This means the sample could haveenough Nano pore spaces to store significant amount of CO_2 when compared to sample1 only.

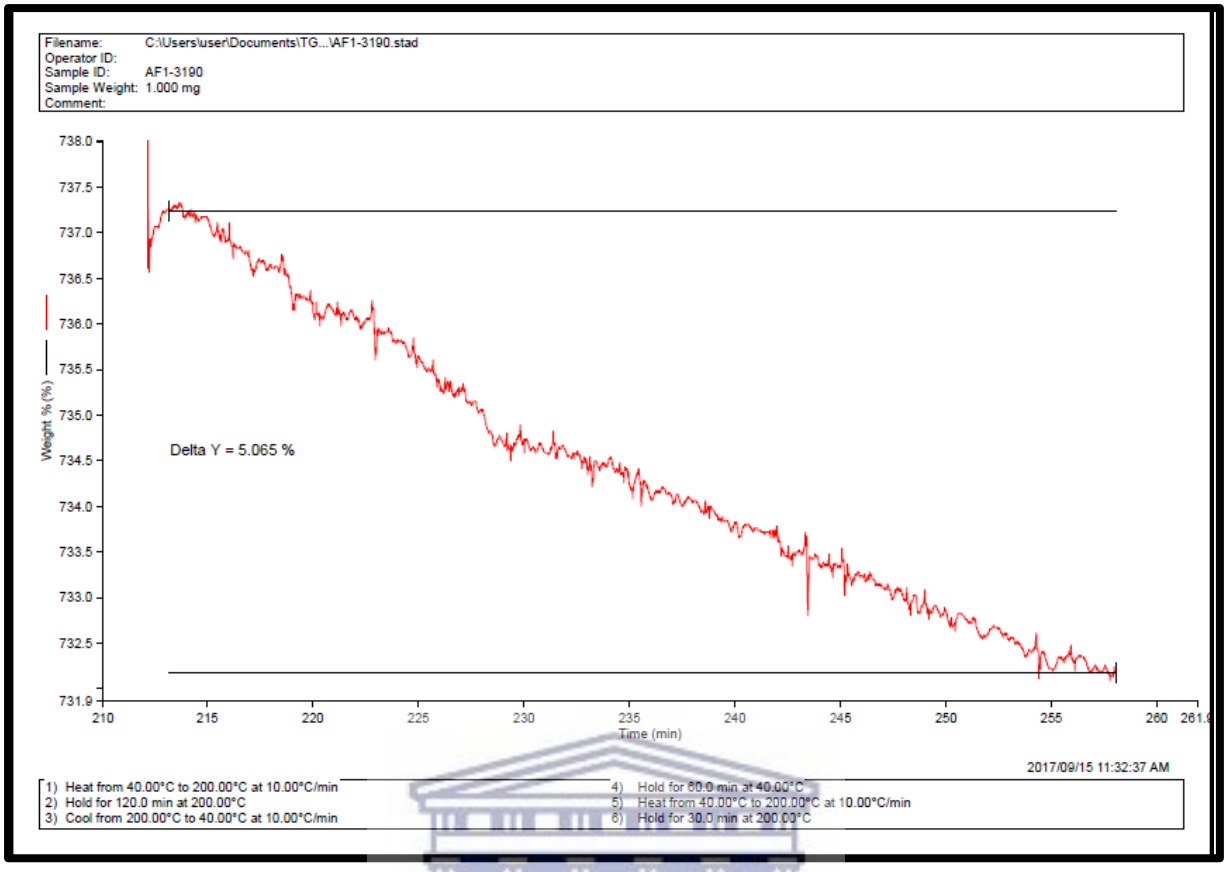

Figure 5-30: Desorption and Storage Capacity Test for sample 4. The desorption capacity is high at a value of 5.06% compared to sample1 only.

5.4 Empirical Storage Capacity Determination of the Barremian sandstone sequence

The Barremian sandstone which straddles the Aptian shale at the top and the Hauterivian Shale and Siltstone deposit at the bottom holds a good promise for potential CO_2 storage.

The Barremian sandstone in zone 8 displayed the thickest and most porous sandstone layer of all 9 zones, hence an estimated volume of CO_2 equation was used.

An estimated volume of CO_2 that could be stored in the reservoir of the Barremian sandstone in zone 8 is limited to the lateral seal of shale above the reservoir in zone 7 of the Aptian age.

The method used to determine the potential storage capacity of CO_2 was performed by Alexandros Tasianas and Nikolaos Koukouzas (2016). The Equation used to determine CO_2 storage capacity is: $mCO_2 = RV * Ø * Sg * \delta(CO_2)$.

Where:

mCO_2= mass of CO_2in kg

RV = total rock volume in m^3

Ø =average total effective porosity

Sg = gas saturation

$\delta(CO_2)$ = density of CO_2at pressure and temperature conditions at the particular depth where the reservoir is located in kg / m^3

The total rock volume calculated using the petrel software is 4.4652E+6m^3 with an average total porosity of 0.11 percent. Gas saturation of 1 and Density of CO_2 at the pressure and temperature conditions at the reservoir location was estimated to be 445.23 kg/m^3.

Thus,

mCO_2 (Barremian sandstone reservoir) = 4.4652+6m^3*0.11*1*445.2

= 2.18E+8 kg

=2.18E+5 tons

A maximum storage estimate of 218000 tonnes of CO_2 can be stored in the Barremian Sandstone reservoir.

5.5 Wireline Log Interpretations of Well AF-1

The wireline logs below shows a suite of logs comprising of Depth (Track1), Gamma Ray (Track 2), Facies (Track 3), Porosity (Track 4), Density(Track 5), Acoustic Impedance (Track 6), Sonic (Track7). The depth drilled for well AF-1 (25m Kelly bushing) terminated at 4000m. The gamma ray log was used to identify three potential reservoir intervals A,B,C and D encountered from starting depth 525m, 1110m 1350m and 2250m respectively (Figure 5.17). The potential reservoirs were identified by isolating sandstone lithology intervals that are bounded by Shale/Silt at the top and bottom. The density porosity expectedly decreases with depth, except for some anomaly increase at around 3000m. This might be attributed to secondary porosity likely caused by overburden pressure which induces micro-cracks and by

implication, porosity increase. Reservoir A, Band D have more potential to store supercritical CO_2 judging by the estimated thickness value of about 50m each respectively(Figure 5.17).

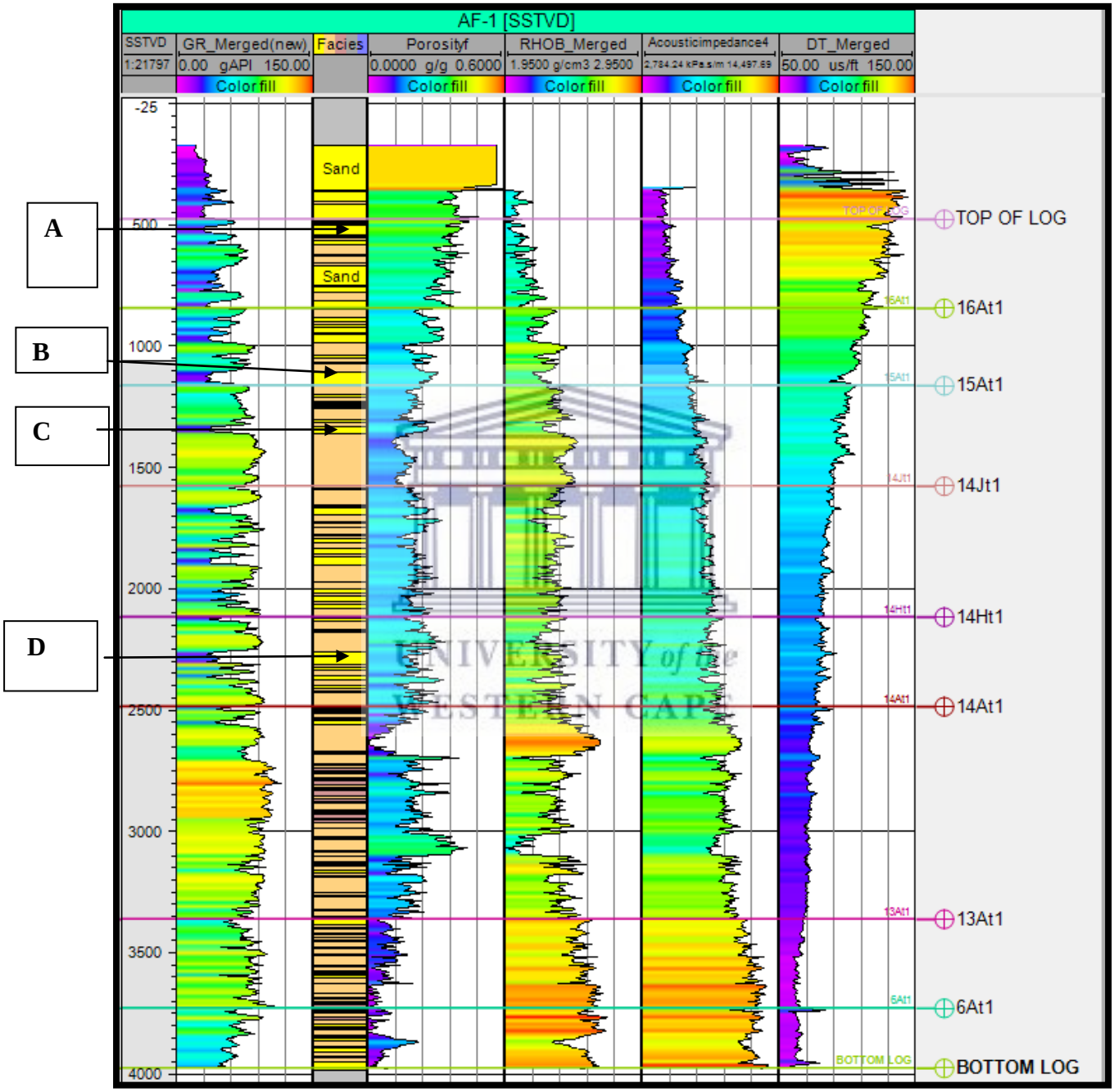

Figure 5-31: A suite of Geophysical logs consisting of Depth (Track1), Gamma Ray (Track 2), Facies (Track 3), Porosity (Track 4), Density (Track 5), Acoustic Impedance (Track 6), Sonic (Track7).

6 Chapter Six

6.1 Conclusions and Recommendation

Many studies on climate change mitigation in South Africa have focused more on carbon capturing using different technological methods (Osman et al., 2014; Surridge and Cloete, 2009).However, the identification of potential sites for long term storage of this captured gas has been challenging. Therefore, the South Africa Energy Development Institution is currently piloting concurrent projects in different basins in South Africa for the identification of potential sites for this purpose. Lesser previous studies have been done on the identification of storage sites in South Africa, most of which are limited to a dimensional profile type of investigation. For example,a study in the Karoo basin employed the use of Magnetotelluric geophysical tool to quantitatively investigate the Ecca group as a potential storage site, the resistivity data obtained from the study was used empirically as a variable in the Archie formula to estimate the porosity of the rock units.

The results from the study revealed variations in apparent resistivity along a dimensional survey profile, and the porosity estimate was done using the Porosity- Resistivity- Salinity nomogram (Khoza, 2012). The limitation of this study is the grid of investigation which is one dimensional. Another study in the Zululand basin, South Africa, revealed Aptian-aged Sandstones of the Makatini formation and upper Cenomanian to Turonian-aged sandstone along the contact betweenMzinene and St Lucia formation are potential sites for long term Carbon storage, however, the sites potential is limited by the lack of the laterally continuous cap rock around the study area (Chabangu et al., 2014).

Consequent upon the limitations of the above study, the current study employed a 3D Geostatistical modelling technique coupled with petrography study (thinsection and XRD) and carbon injection analyses to identify potential storage sites and predict the possible long

term mineralisation of CO_2 within the reservoir intervals. Results revealed a sample taken within the sandstones reservoir interval at 1178m for thin section analysis indicate an angular to rounded grain shape, poorly sorted and well consolidated rock unit. The presence of Albite as observed on the XRD (Figure 5.1B) predicts a possible mineralisation of CO_2 to form Dawsonite when reservoir is injected withCO_2. In addition, the presence of Kaolinite mineral within the reservoir interval suggests its wide surface area could make it an adsorbent for trapping CO_2.

Another sample taken within the reservoir interval at 2322m indicates the rock unit is generally angular-subrounded in shape, moderately-poorly sorted and poorly consolidated. For a good storage potential, unconsolidated reservoir has a better quality than a consolidated reservoir. This indicates a good storage potential at that depth. In addition, the presence of Calcite as seen on the thin section (Figure 5.2A), suggests probable precipitation of bicarbonate cement that could trap CO_2if stored there. The XRD result indicates similar diagenetic minerals observed in sample1 above(1178m) are present in sample 2(2322m). Therefore, mineralisation of CO_2 into Dawsonite is also predicted if CO_2 is injected at this depth. The geostatistical porosity and facies modelling results for the sedimentary deposits encountered within the study area indicates variations in porosity. Generally, the porosity for all rock units of different ages range from poor to good across all chronological units. However, the south central and south eastern section of the Barremian unit has widespread sandstones deposit (5.12B) which is capped by the widespread Aptian shale deposit unconformably overlaying the Barremian sandstones. The Barremian sandstone which straddles the Aptian shale at the top and the Hauterivian Shale and Siltsone deposit at the bottom holds a good promise for a potential CO_2 storage.

The carbon injection results indicate low storage capacity for sample 1 with desorption capacity of 0.8% (Figure 5.14) compared to other samples. Sample 2 and 3(Figures 5.15 and 5.16) have desorption capacities of 5.5% and 5.9% respectively. The latter has more storage capacity than all samples analysed. Well AF-1 falls within the seismic survey area of this study. The geophysical logs interpretations suggest there are four potential reservoir intervals within the AF-1 well (Figure 5.17). The intervals have an average porosity value of 0.24 m^3 /m^3, 0.2m^3 /m^3, 0.18m^3 /m^3 and 0.18m^3 /m^3. The porosity expectedly decrease with depth but was anomalously high at a depth of 3000m. This could be due to the influence of secondary porosity aided by micro-fracturing of the rock unit, possibly caused by overburden pressure.

Conclusively, the presence of Albite and Kaolinite in the main reservoir intervals suggests the likelihood of mineralisation of Carbon if the reservoir intervals are injected with CO_2. The Barremian-age Sandstone deposit of the South central and South eastern section remains the most ideal target for carbon storage, while reservoirs A B and D in well AF-1 remains the most qualitative intervals for carbon storage within the well. Finally, 3D Porosity and Facies models were constructed for the study area (Appendix page). These models can be used as an exploration tool to make extrapolation into the distal part of the Orange Basin and as a result aid future work. This study recommends that similar study should be carried out around all exploration wells drilled so far in the Orange Basin to increase the prospects of identification of storage sites for carbon sequestration purpose.

7 References

- Akinlua, A., Adekola, S. A., Swakamisa, O., Fadipe, O. A., &Akinyemi, S. A. (2010). Trace element characterisation of Cretaceous Orange Basin hydrocarbon source rocks. Applied Geochemistry, 25(10), 1587-1595.
- Bachu, S., Gunter, W.D., 2004. Acid gas injection in the Alberta Basin, Canada: a CO2 storage experience. In: Baines, S.J., Worden, R.H. (Eds.), Geological Storage of Carbon Dioxide for Emissions Reduction Technology. Geological Society Special Publication, Bath, UK, pp. 225–234
- Bachu, S., Nordbotten, J.M., Celia, M.A., 2005. Evaluation of the spread of acid-gas plumes injected in deep saline aquifers in Western Canada as an analogue for CO2 injection into continental sedimentary basins:. In: Proceedings of the 7th Intl. Conf. on Greenhouse Gas Control Technologies, September 2004, Vancou- ver, Canada, pp. 479–487.
- Bachu, S. (2000). Sequestration of CO 2 in geological media: criteria and approach for site selection in response to climate change. Energy conversion and management, 41(9), 953-970.(for deep aquifer storage)
- Barker, C. E. (1988).Geothermics of petroleum systems: Implications of the stabilization of kerogen thermal maturation after a geologically brief heating duration

at peak temperature. Petroleum systems of the United States: US Geological Survey Bulletin, 1870, 26-29.

- Beard, D. C., &Weyl, P. K. (1973). Influence of texture on porosity and permeability of unconsolidated sand. AAPG bulletin, 57(2), 349-369.
- Becquey, M., Lavergne, M., &Willm, C. (1979). Acoustic impedance logs computed from seismic traces. Geophysics, 44(9), 1485-1501.
- Berg, R. R. (1970). Method for determining permeability from reservoir rock properties.
- Bickle, M., Chadwick, A., Huppert, H. E., Hallworth, M., & Lyle, S. (2007). Modelling carbon dioxide accumulation at Sleipner: Implications for underground carbon storage. Earth and Planetary Science Letters, 255(1), 164-176.
- Biddle, K. T., &Wielchowsky, C. C. (1994). Hydrocarbon Traps: Chapter 13: Part III. Processes.
- Birkholzer, J. T., Zhou, Q., & Tsang, C. F. (2009). Large-scale impact of CO 2 storage in deep saline aquifers: a sensitivity study on pressure response in stratified systems. International Journal of Greenhouse Gas Control, 3(2), 181-194.(For deep aquifer storage.)
- Bleeker, W., & Davis, B. W. (2004, May). What is a craton? How many are there? How do they relate? And how did they form?.In AGU Spring Meeting Abstracts.
- Bloch, S., Lander, R. H., &Bonnell, L. (2002). Anomalously high porosity and permeability in deeply buried sandstone reservoirs: Origin and predictability. AAPG bulletin, 86(2), 301-328.
- Boden, T. A., Marland, G., & Andres, R. J. (2009).Global, regional, and national CO2 emissions.
- Bruant, R., Guswa, A., Celia, M., & Peters, C. (2002).Safe Storage of CO~ 2 in Deep Saline Aquifers.ENVIRONMENTAL SCIENCE AND TECHNOLOGY-WASHINGTON DC-, 36(11), 240A-245A.
- Busch, A., Gensterblum, Y., Krooss, B. M., &Littke, R. (2004). Methane and carbon dioxide adsorption–diffusion experiments on coal: upscaling and modeling. International Journal of Coal Geology, 60(2), 151-168.
- Celia, M. A., &Nordbotten, J. M. (2009). Practical modeling approaches for geological storage of carbon dioxide. Ground Water, 47(5), 627-638.
- Crain, E. R., &Eng, P. (2006). Crain's Petrophysical Pocket Pal. Ontario: ER Ross.

- Day, S., Duffy, G., Sakurovs, R., & Weir, S. (2008). Effect of coal properties on CO 2 sorption capacity under supercritical conditions. International Journal of Greenhouse Gas Control, 2(3), 342-352.
- Demaison, G., & Huizinga, B. J. (1991).Genetic classification of petroleum systems (1).AAPG bulletin, 75(10), 1626-1643.
- De Vera, J., Granado, P., &McClay, K. (2010).Structural evolution of the Orange Basin gravity-driven system, offshore Namibia.Marine and Petroleum Geology, 27(1), 223-237.
- Garnier, C., Finqueneisel, G., Zimny, T., Pokryszka, Z., Lafortune, S., Défossez, P. D. C., &Gaucher, E. C. (2011). Selection of coals of different maturities for CO 2 Storage by modelling of CH 4 and CO 2 adsorption isotherms. International Journal of Coal Geology, 87(2), 80-86.
- Gensterblum, Y., Van Hemert, P., Billemont, P., Busch, A., Charriere, D., Li, D., ...& Wolf, K. H. (2009). European inter-laboratory comparison of high pressure CO 2 sorption isotherms. I: Activated carbon. Carbon, 47(13), 2958-2969.
- Gomes, J. S., Ribeiro, M. T., Strohmenger, C. J., Naghban, S., &Kalam, M. Z. (2008, January). Carbonate reservoir rock typing-the link between geology and SCAL. In Abu Dhabi International Petroleum Exhibition and Conference.Society of Petroleum Engineers.
- Fraser, H. J. (1935). Experimental study of the porosity and permeability of clastic sediments. The Journal of Geology, 43(8, Part 1), 910-1010.
- Flett, M., Brantjes, J., Gurton, R., McKenna, J., Tankersley, T., &Trupp, M. (2009).Subsurface development of CO 2 disposal for the Gorgon Project.EnergyProcedia, 1(1), 3031-3038.
- Gibbins, J., & Chalmers, H. (2008).Carbon capture and storage.Energy Policy, 36(12), 4317-4322.
- Goldstein, R. H., & Reynolds, T. J. (1994).Fluid inclusion petrography.
- Haszeldine, R. S. (2009). Carbon capture and storage: how green can black be?.Science, 325(5948), 1647-1652.
- Hartwig, A., Anka, Z., & di Primio, R. (2012). Evidence of a widespread paleo-pockmarked field in the Orange Basin: an indication of an early Eocene massive fluid escape event offshore South Africa. Marine Geology, 332, 222-234.

- Hirsch, K. K., Scheck-Wenderoth, M., Paton, D. A., & Bauer, K. (2007).Crustal structure beneath the Orange Basin, South Africa. South African Journal of Geology, 110(2-3), 249-260.
- Hirsch, K. K., Scheck-Wenderoth, M., van Wees, J. D., Kuhlmann, G., & Paton, D. A. (2010). Tectonic subsidence history and thermal evolution of the Orange Basin.Marine and Petroleum Geology, 27(3), 565-584.
- Iding, M., &Ringrose, P. (2009).Evaluating the impact of fractures on the long-term performance of the In Salah CO 2 storage site.EnergyProcedia, 1(1), 2021-202.
- Katz, B. J., & Mello, M. R. (2000). AAPG Memoir 73, Chapter 1: Petroleum Systems of South Atlantic Marginal Basins--An Overview.
- Karacan, C. Ö., & Mitchell, G. D. (2003).Behavior and effect of different coal microlithotypes during gas transport for carbon dioxide sequestration into coal seams. International Journal of Coal Geology, 53(4), 201-217.
- Khoza, David. (2012). Quantifying South Africa's carbon storage potential using geophysics. *South African Journal of Science*, *108*(9-10), 1-2. Retrieved March 04, 2018
- Koide, H., Tazaki, Y., Noguchi, Y., Nakayama, S., Iijima, M., Ito, K., &Shindo, Y. (1992). Subterranean containment and long-term storage of carbon dioxide in unused aquifers and in depleted natural gas reservoirs.Energy Conversion and management, 33(5-8), 619-626.
- Koponen, A., Kataja, M., &Timonen, J. (1997).Permeability and effective porosity of porous media.Physical Review E, 56(3), 3319.
- Krooss, B. V., Van Bergen, F., Gensterblum, Y., Siemons, N., Pagnier, H. J. M., & David, P. (2002).High-pressure methane and carbon dioxide adsorption on dry and moisture-equilibrated Pennsylvanian coals. International Journal of Coal Geology, 51(2), 69-92.
- Kuhlmann, G., Adams, S., Campher, C., van der Spuy, D., di Primio, R., &Horsfield, B. (2010). Passive margin evolution and its controls on natural gas leakage in the southern Orange Basin, blocks 3/4, offshore South Africa. Marine and Petroleum Geology, 27(4), 973-992.
- Lemieux, J. M. (2011). Review: The potential impact of underground geological storage of carbon dioxide in deep saline aquifers on shallow groundwater resources. Hydrogeology Journal, 19(4), 757-778.

- Le Quéré, C., Rödenbeck, C., Buitenhuis, E. T., Conway, T. J., Langenfelds, R., Gomez, A., ...& Gillett, N. (2007). Saturation of the Southern Ocean CO2 sink due to recent climate change. science, 316(5832), 1735-1738.
- Levy, J. H., Day, S. J., &Killingley, J. S. (1997). Methane capacities of Bowen Basin coals related to coal properties. Fuel, 76(9), 813-819.
- Li, Z., Dong, M., Li, S., & Huang, S. (2006).CO 2 sequestration in depleted oil and gas reservoirs—caprock characterization and storage capacity.Energy Conversion and Management, 47(11), 1372-1382.
- Lucia, F. J. (1995). Rock-fabric/petrophysical classification of carbonate pore space for reservoir characterization.AAPG bulletin, 79(9), 1275-1300.
- Magoon, L. B., & Dow, W. G. (1994). The Petroleum System: Chapter 1: Part I. Introduction.
- Maldal, T., &Tappel, I. M. (2004).CO 2 underground storage for Snøhvit gas field development.Energy, 29(9), 1403-1411.
- Metz, B., Davidson, O., De Coninck, H., Loos, M., & Meyer, L. (2005).Carbon dioxide capture and storage.
- Michael, K., Golab, A., Shulakova, V., Ennis-King, J., Allinson, G., Sharma, S., & Aiken, T. (2010).Geological storage of CO 2 in saline aquifers—a review of the experience from existing storage operations.International Journal of Greenhouse Gas Control, 4(4), 659-667.
- Muntingh, A., & Brown Jr, L. F. (1993). Sequence Stratigraphy of Petroleum Plays, Post-Rift Cretaceous Rocks (Lower Aptian to Upper Maastrichtian), Orange Basin, Western Offshore, South Africa: Chapter 4: Recent Applications of Siliciclastic Sequence Stratigraphy.
- Nordbotten, J. M., Celia, M. A., &Bachu, S. (2005). Injection and storage of CO 2 in deep saline aquifers: analytical solution for CO 2 plume evolution during injection. Transport in Porous media, 58(3), 339-360.(For deep aquifer storage.)
- Oldenburg, C. M., Pruess, K., & Benson, S. M. (2001).Process modeling of CO2 injection into natural gas reservoirs for carbon sequestration and enhanced gas recovery.Energy& Fuels, 15(2), 293-298.
- Osman, Khalid, Coquelet, Christophe, &Ramjugernath, Deresh. (2014). Review of carbon dioxide capture and storage with relevance to the South African power sector. South African Journal of Science, 110(5-6), 01-12. Retrieved March 04, 2018

- Passey, Q. R., Creaney, S., Kulla, J. B., Moretti, F. J., & Stroud, J. D. (1990). A practical model for organic richness from porosity and resistivity logs.AAPG bulletin, 74(12), 1777-1794.
- Paton, D. A., Di Primio, R., Kuhlmann, G., Van Der Spuy, D., &Horsfield, B. (2007). Insights into the petroleum system evolution of the southern Orange Basin, South Africa.South African Journal of Geology, 110(2-3), 261-274.
- Pearson, P. N., & Palmer, M. R. (2000).Atmospheric carbon dioxide concentrations over the past 60 million years.Nature, 406(6797), 695-699.
- Perera, M. S. A., Ranjith, P. G., Choi, S. K., Bouazza, A., Kodikara, J., &Airey, D. (2011). A review of coal properties pertinent to carbon dioxide sequestration in coal seams: with special reference to Victorian brown coals. Environmental earth sciences, 64(1), 223-235.
- Perrodon, A., & Masse, P. (1984).Subsidence, sedimentation and petroleum systems. Journal of Petroleum Geology, 7(1), 5-25.
- Reid, R. P., Visscher, P. T., Decho, A. W., &Stolz, J. F. (2000).The role of microbes in accretion, lamination and early lithification of modern marine stromatolites.Nature, 406(6799), 989.
- Serra, O., (1984). Fundamentals of Well Log Interpretation (Vol. 1): The Acquisition of Logging Data: Dev. Pet. Sci., 15A: Amsterdam (Elsevier).
- Solomon, S., Plattner, G. K., Knutti, R., &Friedlingstein, P. (2009).Irreversible climate change due to carbon dioxide emissions.Proceedings of the national academy of sciences, pnas-0812721106.
- Special Report on Carbon Dioxide Capture and Storage: Prepared by Working Group III of the Intergovernmental Panel on Climate Change Cambridge University Press, Cambridge and New York (2005) 442 pp.
- Surridge, A.D., Cloete, M. (2009). Carbon capture and storage in South Africa. Carbon geological storage atlas.
- Tiab, D., & Donaldson, E. C. (2015).Petrophysics: theory and practice of measuring reservoir rock and fluid transport properties. Gulf professional publishing.
- Tissot, B. P., Pelet, R., &Ungerer, P. H. (1987).Thermal history of sedimentary basins, maturation indices, and kinetics of oil and gas generation.AAPG bulletin, 71(12), 1445-1466.

- Torp, T. A., & Gale, J. (2004).Demonstrating storage of CO 2 in geological reservoirs: the Sleipner and SACS projects.Energy, 29(9), 1361-1369.
- Vitousek, P. M., Mooney, H. A., Lubchenco, J., &Melillo, J. M. (1997).Human domination of Earth's ecosystems.Science, 277(5325), 494-499.
- Van der Meer, B. (2005). Carbon dioxide storage in natural gas reservoir.Oil& Gas Science and Technology, 60(3), 527-536.
- White, C. M., Smith, D. H., Jones, K. L., Goodman, A. L., Jikich, S. A., LaCount, R. B., ... & Schroeder, K. T. (2005). Sequestration of carbon dioxide in coal with enhanced coalbed methane recovery a review. Energy & Fuels, 19(3), 659-724.
- White, C. M., Strazisar, B. R., Granite, E. J., Hoffman, J. S., &Pennline, H. W. (2003). Separation and capture of CO2 from large stationary sources and sequestration in geological formations—coalbeds and deep saline aquifers.Journal of the Air & Waste Management Association, 53(6), 645-715.(For deep aquifer storage.)
- Xu, X., Chen, S., & Zhang, D. (2006).Convective stability analysis of the long-term storage of carbon dioxide in deep saline aquifers.Advances in water resources, 29(3), 397-407.
- Yoo, C. S., Cynn, H., Gygi, F., Galli, G., Iota, V., Nicol, M., ...&Mailhiot, C. (1999). Crystal structure of carbon dioxide at high pressure:"Superhard" polymeric carbon dioxide. Physical Review Letters, 83(26), 5527.

8 Appendix

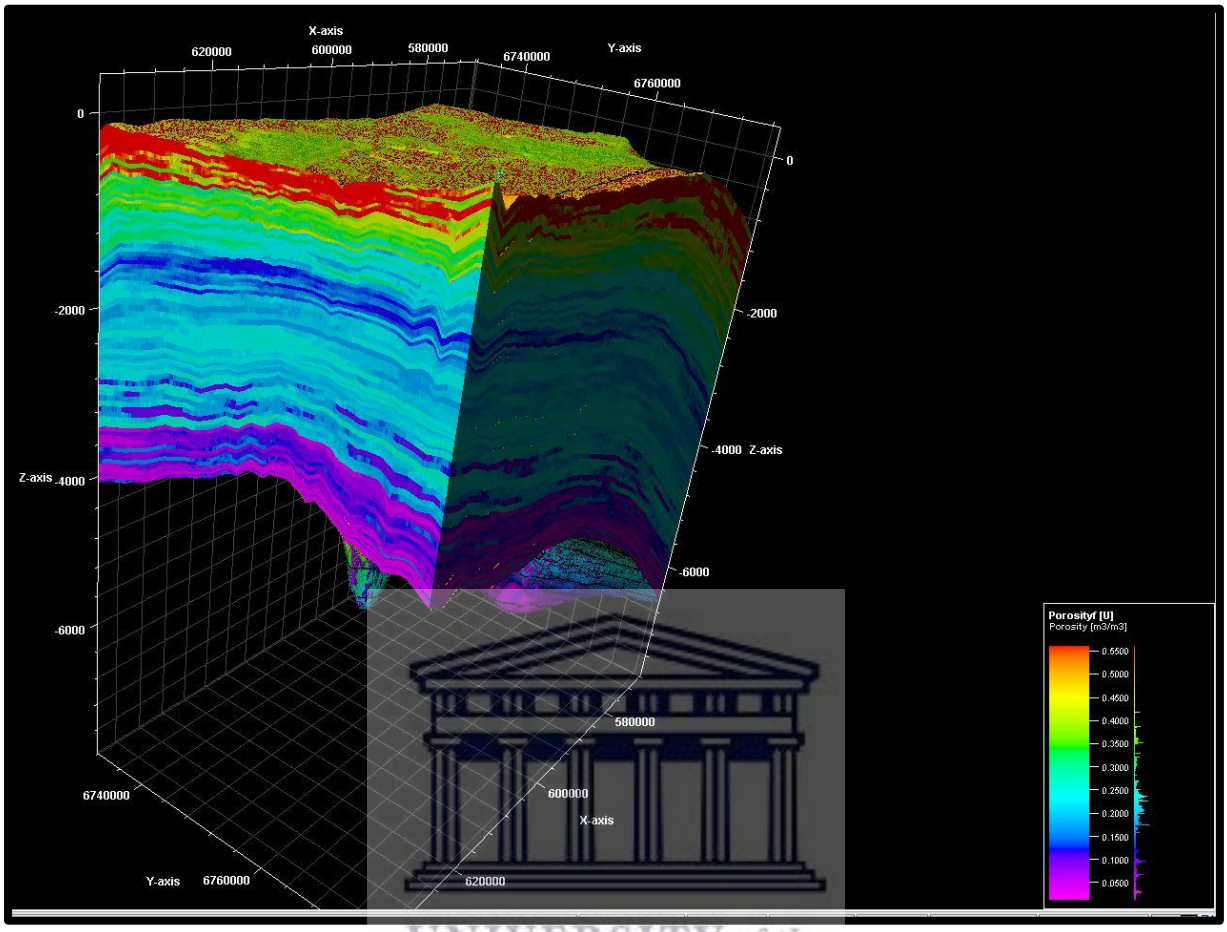

Figure 6-1: 3D Porosity Model of the Study Area. Each Layer represents geological age in chronological order.

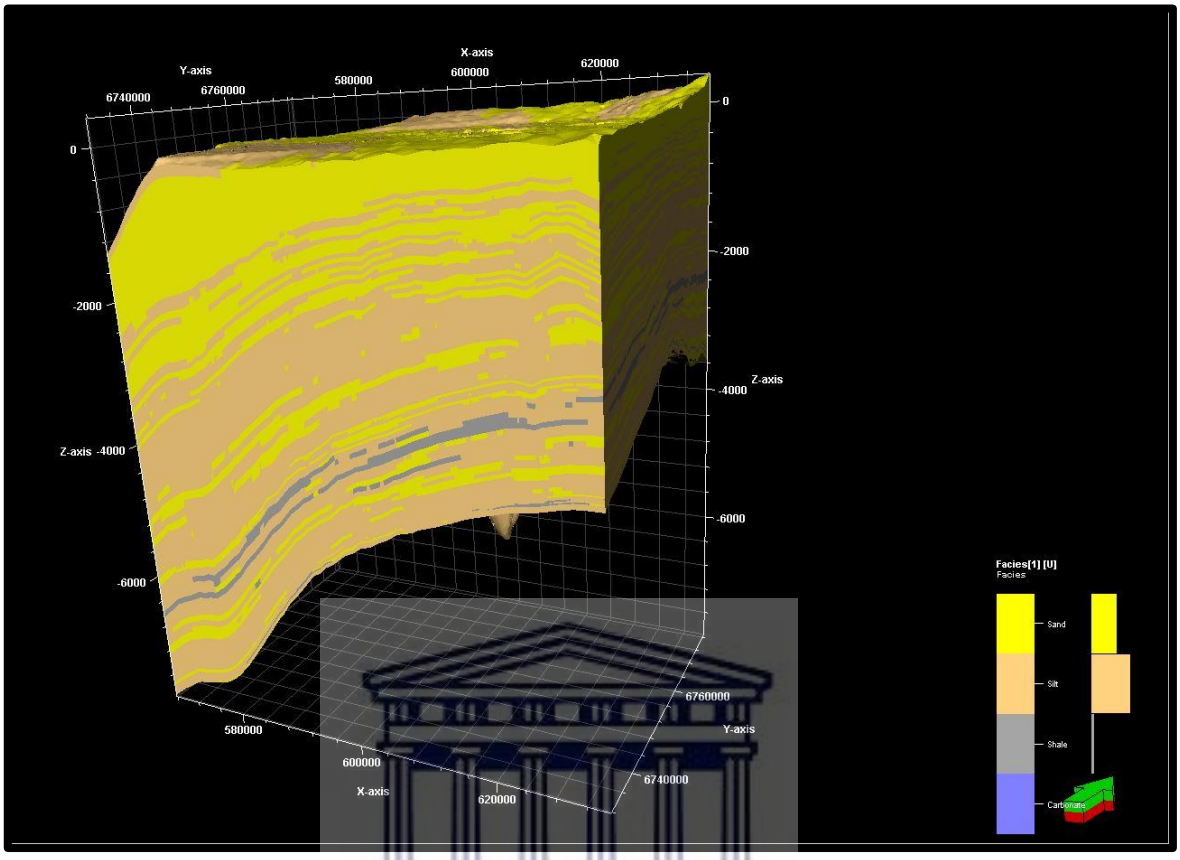

Figure 6-2: Facies Model of the study area. Three main clastic lithology groups of Sandstones, Siltstones and Shale were modelled for the study area.